

# Open Research Online

---

The Open University's repository of research publications and other research outputs

## Role of genes differentially expressed in thyroid carcinogenesis

### Thesis

#### How to cite:

Anania, Maria Chiara (2012). Role of genes differentially expressed in thyroid carcinogenesis. PhD thesis The Open University.

For guidance on citations see [FAQs](#).

© 2012 The Author

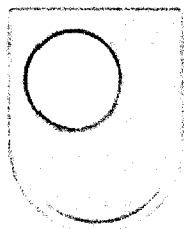
Version: Version of Record

---

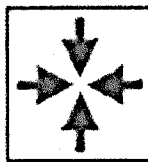
Copyright and Moral Rights for the articles on this site are retained by the individual authors and/or other copyright owners. For more information on Open Research Online's data [policy](#) on reuse of materials please consult the policies page.

---

[oro.open.ac.uk](http://oro.open.ac.uk)



The Open University



**FONDAZIONE IRCCS**  
**ISTITUTO NAZIONALE**  
**DEI TUMORI**

**Maria Chiara Anania**  
Degree in Biological Science

OU personal identifier A298071X

**ROLE OF GENES DIFFERENTIALLY EXPRESSED IN THYROID CARCINOGENESIS**

This thesis is presented to

The Open University for the Degree of Doctor of Philosophy

Discipline: Life and Biomolecular Sciences

Date of submission: 31<sup>st</sup> May 2012

Affiliated Research Centre:  
Fondazione IRCCS Istituto Nazionale dei Tumori, Milan (Italy)

Director of studies: Dr. Angela Greco  
External supervisor: Dr. Karen Pulford

**BEST COPY AVAILABLE.**

**VARIABLE PRINT QUALITY**

## NOTIFICATION OF REDACTION

**THESIS TITLE:**

Role of genes differentially expressed in thyroid carcinogenesis.

**AUTHOR:**

Maria Chiara Anania

**YEAR:**

2012

**CLASSMARK:**

616.99444 ANA

The following pages/sections have been redacted from this thesis:

Page No.	Item/section redacted
p.178 - End	PUBLICATIONS



# TABLE OF CONTENTS

<b>ABSTRACT</b>	5
<b>1. INTRODUCTION</b>	8
1.1 Thyroid cancer	9
1.2 Histological classification of follicular cell-derived thyroid tumors	11
1.2.1 Papillary thyroid carcinoma (PTC)	11
1.2.2 Follicular thyroid carcinoma (FTC)	12
1.2.3 Poorly Differentiated thyroid carcinoma (PDTC)	13
1.2.4 Anaplastic thyroid carcinoma (ATC)	13
1.3 Genetic alteration in thyroid cancer	14
1.3.1 v-Raf murine sarcoma viral oncogene homolog B1 (BRAF) oncogenes	14
1.3.2 REarranged during Transfection (RET) oncogenes	16
1.3.3 TRK oncogenes	18
1.3.4 RAS mutation	20
1.3.5 Paired box gene 8/Peroxisome proliferator-activate receptor (PAX8/PPAR $\gamma$ ) rearrangement	21
1.3.6 PI3K/AKT pathway mutations	22
1.3.7 Tumor protein 53 (TP53) mutation	23
1.3.8 Other alterations in thyroid cancer	24
1.4 Meccanisms of thyroid cancer aetiology	30
1.5 Therapy in thyroid cancer	33
1.5.1 Multikinase inhibitors as target therapy	33
1.5.2 Conclusions on therapeutic options	35
<b>2. EXPRESSION PROFILES IN THYROID CANCER</b>	37
2.1 Expression profiles in thyroid cancer	38
2.1.1 PTC signature	38
2.1.2 Post Chernobyl-PTC signature	41
2.1.3 FTC signature	42
2.1.4 PDTC and ATC signature	43
2.2 miRNA profiling in thyroid cancer	45
2.3 Gene silencing by promoter methylation in thyroid cancer	46
2.4 Conclusions of gene expression studies	50
<b>AIM OF THE THESIS</b>	51

<b>3. MATERIALS AND METHODS</b>	<b>52</b>
3.1 Microarray data sets and statistical analysis	53
3.2 Molecular biology	55
3.2.1 RNA extraction and RT-PCR	55
3.2.2 Real-time RT-PCR	55
3.2.3 Construction of expression vectors	55
3.3 Cell biology	58
3.3.1 Cell lines	58
3.3.2 Cell treatments	59
3.3.3 Cell transfection	60
3.3.4 <i>TIMP3</i> and <i>S100A11</i> silencing	60
3.3.5 Focus forming assay	61
3.3.6 Cell cycle analysis	61
3.3.7 Growth curves	62
3.3.8 Colony forming assay	62
3.3.9 Cell adhesion assay	62
3.3.10 Wound healing assay	63
3.3.11 Migration and invasion assay	63
3.3.12 Soft agar assay	64
3.4 Biochemical assay and studies	64
3.4.1 Western blot analysis	64
3.4.2 Dot blot analysis	65
3.4.3 TNF- $\alpha$ detection	66
3.5 In <i>vivo</i> studies	66
3.5.1 Immunohistological studies	66
<b>4. TIMP3 STUDIES</b>	<b>68</b>
4.1 Introduction	69
4.1.1 TIMP3	69
4.1.2 TIMP3 and thyroid cancer	72
4.2 Aims of the chapter	73
4.3 Results	74
4.3.1 Expression analysis of TIMP3 in PTC samples and thyroid tumour cell lines	74
4.3.2 Effect of TIMP3 restoration on cell growth	76
4.3.3 Effect of TIMP3 restoration on cell adhesion	81
4.3.4 Effect of TIMP3 restoration on cell migration and invasion	83

4.3.5	Effect of TIMP3 restoration on anchorage independent growth	85
4.3.6	Analysis of proteins mediating TIMP3 effects	86
4.3.7	Effect of TIMP3 restoration in mouse tumour xenografts	88
4.4	Discussion	92
<b>5.</b>	<b>S100A11 STUDIES</b>	<b>96</b>
5.1.	Introduction	97
5.1.1	S100A11	97
5.1.2	S100A11 and thyroid cancer	104
5.2	Aims of the chapter	105
5.3	Results	106
5.3.1	Expression analysis of S100A11 in PTC samples and PTC derived cell lines	106
5.3.2	Analysis of cellular localization of S100A11	109
5.3.3	Analysis of interaction between S100A11 and EGF/EGFR pathway	112
5.3.4	Effect of S100A11 silencing	114
5.3.4.1	Transient silencing of S100A11	114
5.3.4.2	Stable silencing of S100A11	116
5.3.4.3	Effect of stable S100A11 silencing in mouse tumour xenografts	120
5.3.5	Effect of S100A11 on the transforming potential of <i>TRK-T3</i> oncogene	122
5.3.5.1	S100A11 enhances “in vitro” TRK-T3 transforming activity	122
5.3.5.2	Biochemical and biological analysis of T3/S100 foci	123
5.3.5.3	Analysis of the tumorigenic capability of T3/S100 foci	127
5.4	Discussion	129
<b>6.</b>	<b>CITED 1 STUDIES</b>	<b>134</b>
6.1	Introduction	135
6.2	Preliminary results	136
<b>7.</b>	<b>IGFBP7 STUDIES</b>	<b>139</b>
<b>8.</b>	<b>GENERAL DISCUSSION AND FUTURE PLANS</b>	<b>142</b>
	<b>REFERENCES</b>	<b>148</b>
	<b>LIST OF ABBREVIATIONS</b>	<b>174</b>
	<b>LIST OF FIGURES</b>	<b>175</b>
	<b>LIST OF TABLES</b>	<b>176</b>
	<b>PUBLICATIONS</b>	<b>177</b>
	<b>ACKNOWLEDGEMENTS</b>	<b>178</b>

## ***Abstract***

Thyroid cancer represents the most common endocrine malignancy, and its incidence has increased significantly over the last few decades. Papillary thyroid carcinoma (PTC), the most frequent neoplasia originating from the thyroid epithelium, accounts for about 80% of all thyroid cancers. PTC is characterized by rearrangements of *RET* and *NTRK1* receptor tyrosine kinases, or by activating point mutations in the *BRAF* serine/threonine kinase or in the *RAS* genes. Even though the identification of PTC-associated oncogenes has provided a great contribution to the understanding of PTC pathogenesis, the molecular mechanisms underlying the development of this neoplasia, including the role of tumour suppressor genes, are still far from being completely elucidated.

Recently, global gene expression analyses have provided new findings contributing to the dissection of thyroid tumour pathogenesis, through the identification of genes discriminating among different histotypes, candidates as new therapeutic targets and possible tumour suppressor genes. Despite the numerous gene expression studies, there are few data addressing the role of differentially expressed genes in the pathogenesis of thyroid tumours. A microarray gene expression profile previously determined in our laboratory identified a list of genes differentially expressed in PTC versus normal thyroid; among those, we selected *TIMP3*, *S100A11* and *CITED1* genes for which a role in the pathogenesis of PTC was also suggested by recently published gene and protein expression data. In this PhD project, we performed functional studies in order to assess the role of *TIMP3*, *S100A11* and *CITED1* genes in thyroid carcinogenesis, with the aim of unveiling novel mechanisms and identifying novel therapeutic targets in thyroid tumours.

*TIMP3* (Tissue Inhibitor of Metalloproteinases-3) is a secreted protein able to inhibit extracellular matrix metalloproteinases. *TIMP3* gene promoter has been found hypermethylated in thyroid cancer and its downregulation was associated with several aggressive tumour features. To investigate the role of *TIMP3* in the pathogenesis of PTC

we used an integrated approach including analysis of several gene expression data sets and functional studies. TIMP3 was found to be downregulated in a consistent fraction in PTCs, with respect to normal thyroid. Restoration of TIMP3 in the PTC-derived NIM1 cell line had no effect on growth rate; however, it reduced migration, invasion and anchorage independent growth. The striking effect was observed *in vivo*, as TIMP3 reduced the tumourigenicity of NIM1 cells by repressing angiogenesis and macrophage infiltration. All these observations suggest a tumour suppressor role in thyroid carcinogenesis.

S100A11 (calgizzarin) is a member of the S100 Ca<sup>2+</sup>-binding protein family, which includes at least 20 proteins. Its role in tumour is not well known, and it appears to have distinct functions in different tumour types. Our microarray analysis showed that S100A11 is overexpressed in PTC compared to normal thyroid. In order to study the role of S100A11 in thyroid carcinogenesis, we performed functional *in vitro* and *in vivo* analysis. Analysis of cellular localization in PTC-derived K1 cell line, revealed that S100A11 was mainly cytoplasmic and was able to translocate into the nucleus after Ca<sup>2+</sup> and TGF- $\beta$  stimulation. We also found that this translocation did not increase p21 level, a negative regulator of cell growth. Moreover, we found that S100A11 did not alter the activation level of the EGF/EGFR pathway. We then investigated the effect of S100A11 silencing on tumourigenic properties of K1 cells. We found that S100A11 silencing did not affect cell proliferation, but it exerted a role on the anchorage-independent growth. Analysis of mouse tumour xenografts showed that S100A11 was not involved in the *in vivo* tumourigenicity of K1 cells. Concomitantly, we assessed the effect of *S100A11* gene modulation on the transforming potential of PTC-associated oncogenes. Cotransfection experiments in NIH3T3 cells, which represent a useful model for studying *in vitro* oncogene activity, showed that *S100A11* gene was able to enhance the transforming capability of the PTC-associated *TRK-T3* oncogene. Stable NIH3T3 foci expressing TRK-T3 and S100A11 concomitantly to TRK-T3 were produced. Functional studies showed that S100A11 was not involved in the regulation of cell proliferation, whereas it was able to promote

invasion, anchorage independent growth and *in vivo* tumourigenicity of these transformed foci.

CITED1 (CBP/p300-Interacting Transactivators with glutamic acid (E) and aspartic acid (D)-rich C-terminal domain 1) is part of a family of transcriptional cofactors that regulates diverse CBP/p300 transcriptional responses. In different microarray studies CITED1 was found overexpressed in PTC. It was also proposed as a highly sensitive and specific diagnostic marker, useful in differentiating PTC from benign and malignant thyroid tumours. For this reason, we are interested in the functional role of CITED1 in this histotype. Preliminary experiments involved the analysis of CITED1 expression in a collection of PTC-derived cell lines and the construction of *CITED1* cDNA expression vectors. Further analysis will involve the investigation of its effect on transforming activity of PTC-associated oncogenes and the effect of its gene silencing on the phenotype of a PTC-derived cellular model.



## ***1.Introduction***

### ***1.1.Thyroid cancer***

Thyroid cancer (TC) is the most common malignancy of endocrine organs (Parkin et al., 2005); it represents 1.7% of total estimated new cancer cases, and its incidence has been increasing and has almost tripled over the past 30 years in the US and other industrialized countries (Colonna et al., 2007). An high incidence of TC has also been reported in Italy, where it represents the second and the fifth most common cancer among women and men (below age 45 years), respectively. In particular, referring to 2001-2005 time period, the incidence rate was 18 per 100 000 women and 6 per 100 000 men, twofold higher than 1991-1995(Dal et al., 2011).

TCs could derive from epithelial follicular or parafollicular cells. The first, which are by far the most common, comprise papillary thyroid carcinoma (PTC) (about 80% of cases), follicular thyroid carcinoma (FTC) (10%), poorly differentiated thyroid carcinoma (PDTC) (4-6%), Hürthle cell (oxyphil) carcinoma (HCC) (3%) and anaplastic thyroid carcinoma (ATC) (2-5%). The second, originating from parafollicular cells, are known as medullary thyroid carcinomas (MTC) (5-10%). Papillary and follicular carcinoma and their variants are also defined differentiated thyroid cancers (DTCs). Follicular adenoma (FA) is a benign tumour that may represent a precursor for some follicular carcinomas. Less differentiated thyroid cancers, PDTC and ATC, could arise *de-novo* from thyrocyte or from de-differentiation of the differentiated papillary and follicular tumours (Figure 1.1)

The above reported increase in TC incidence is, in general, associated with increased access to high-resolution imaging and increased use of fine-needle aspiration (FNA) biopsy of small nodules, as well as progressively decreasing stringency of histopathological criteria applied to the diagnosis of papillary cancer over the past 10-15 years. No significant change has been observed in the incidence of the less common histological types: follicular, medullary and anaplastic carcinoma (Davies and Welch,



2006). However, in addition to the improvement in diagnostic tools, other factors could contribute to the increase of this incidence such as exposure to radiation during medical procedures (Mettler, Jr. et al., 2009), obesity (Kitahara et al., 2011) as well as the increase in pathological detection of incidental papillary thyroid cancer (Grodski et al., 2008).

At variance with the incidence rate, mortality rate is stable or decreasing both in the United States (Davies and Welch, 2006) and in Europe (La et al., 2010). Differentiated TCs and MTCs display a very good 10-year relative survival rate, ranging from 90% (Hundahl et al., 1998) to 74% , respectively; while it is dramatically short (less than 1 year) in the case of ATC which represents one of the most aggressive malignant tumours in humans. In at least the 20% of patients with differentiated TC, metastatic disease can occur (Durante et al., 2006), thus the 10-year survival rate decreases to 42% for metastatic differentiated TC patients (Haq and Harmer, 2005) and to 24% in the case of MTC. The prolonged survival of metastatic patients is a peculiar characteristic that distinguishes these particular cancers from the large majority of advanced malignant tumours.

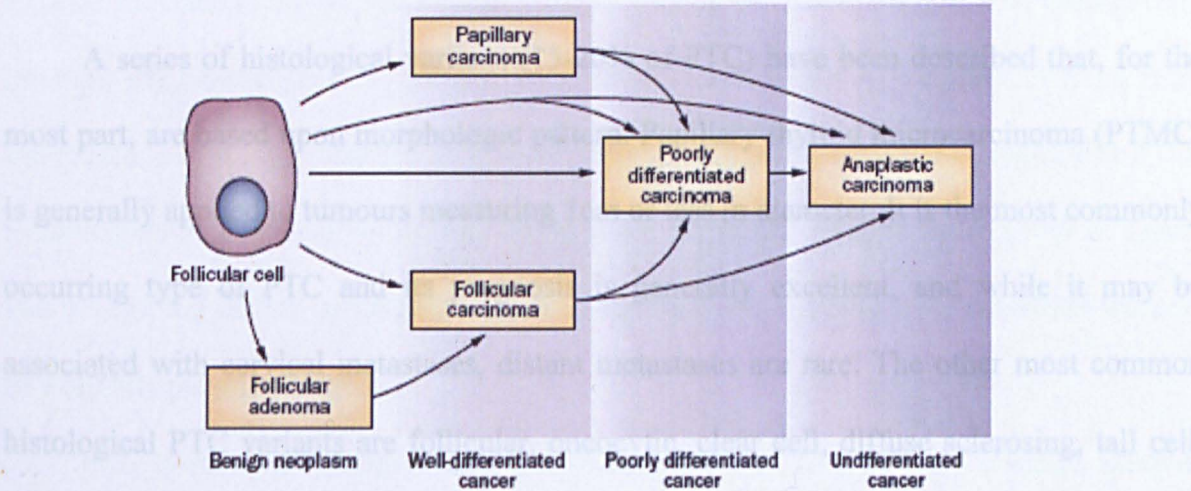


**Figure 1.1 Scheme of development of follicular cell-derived thyroid cancer** The most frequent type of thyroid cancers, papillary carcinoma, originates from thyroid follicular cell. Follicular carcinomas can develop either from pre-existing benign follicular adenomas or directly bypassing the stage of adenoma. Poorly differentiated and anaplastic carcinomas can arise *de novo* or from pre-existing well-differentiated papillary or follicular carcinomas (from (Nikiforov and Nikiforova, 2011))

## ***1.2 Histological classification of follicular cell-derived thyroid tumours***

### ***1.2.1 Papillary thyroid carcinoma (PTC)***

PTC, accounting for 80% of thyroid malignancies, affects females more frequently than males (4:1) and the mean age at diagnosis is 40 years (Sheils, 2005). Although PTC usually grows slowly and is clinically indolent, rare aggressive forms with local invasion or distant metastasis can occur. Lymphatic vessels are the main pathway of diffusion of PTC and cervical lymph node metastases are very frequent at the time of diagnosis. Distant metastasis is uncommon, but when present, is most commonly found in the lung and bone.

“Classical” PTC is microscopically characterized by a papillary architecture and a population of follicular cells with “ground glass” nuclei and irregularities of the nuclear contours, including grooves and nuclear pseudoinclusions. Psammoma bodies, which represent a typical PTC feature, are found in at least 50% of cases. They are relatively specific for papillary carcinoma and are thought to represent necrosis of tumour cells or tips of papillae. PTC cells express cytokeratins, thyroglobulin and thyroid transcription factor-1 (TTF-1).

A series of histological variants (15-20% of PTC) have been described that, for the most part, are based upon morphologic pattern. Papillary thyroid microcarcinoma (PTMC) is generally applied to tumours measuring 1cm or less in diameter. It is the most commonly occurring type of PTC and its prognosis is generally excellent, and while it may be associated with cervical metastases, distant metastases are rare. The other most common histological PTC variants are follicular, oncocytic, clear cell, diffuse sclerosing, tall cell, columnar cell, solid, and cribriform. Although the prognosis is similar to classic PTC for most of these variants, some histotypes, such as tall cell, columnar cell and solid variant, have a worse outcome. The tall cell variant, in particular, has a poorer prognosis than other variants. Extra-thyroid extension is common and there is a greater incidence of vascular invasion. The papillae are well formed and covered by cells that are at least twice as tall as

they are wide. Immunohistochemistry has shown that c-Met expression is significantly associated with tall cell histology, thus suggesting a role for its use in the early identification of patients with tall cell variant thyroid disease (Nardone et al., 2003).

### *1.2.2 Follicular thyroid carcinoma (FTC)*

FTC, accounting for approximately 10% of all thyroid malignancy, is more common in women over 50 years of age. It is rare in children, and more prevalent in iodine-deficient areas. It is characterized by follicular cell differentiation but lacking the above described nuclear features of PTC. Haematogenous diffusion is more frequent than lymphatic spread. At variance with PTC, cervical lymph node involvement is less common at diagnosis, while 20% of cases can present distant metastasis, mainly in the lung and bone sites. The risk of metastatic spread is higher in those cases with widespread vascular invasion. FTC cells commonly express thyroglobulin, TTF-1, and low molecular weight cytokeratin.

Hürthle cell carcinoma (HCC) or “oncocytic or oxyphilic” variant is a rare variant of FTC or (less commonly) of PTC. HCC are defined as tumours composed of 75% or more Hürthle cells and exhibiting complete capsular- and/or vascular- invasion. The tumour cells are typically characterized by an abundant granular, eosinophilic cytoplasm derived from the presence of a large number of mitochondria. HCCs differ from the conventional FTCs in biological and clinical behaviour, for example involving cervical nodes (30% of cases) and developing distant metastasis. For these reasons, some groups have classified them as as a distinct pathologic entity.

Fifty percent of patients with widely invasive FTC die of their disease, whereas patients with minimally invasive FTC have an expectancy of survival similar to that of a normal population when matched for age and sex.

### 1.2.3 Poorly differentiated thyroid carcinoma (PDTC)

PDTC is a rare and controversial entity (4-6% of TC), more commonly seen in women and patients over 50 years of age. These tumours appeared to confer a survival rate between that of differentiated thyroid cancers and ATC. The aetiology of PDTC is unknown. It can be the terminal stage of the de-differentiation process of PTC or FTC or can arise *de novo* (Pilotti et al., 1997). On presentation, it can appear as a unique thyroid mass, often rapidly growing, with or without cervical node involvement. Distant metastases can also be present. Three different histological patterns, insular, trabecular and solid, have been described (Sobrinho-Simoes et al., 2002). The infiltrative pattern of growth, necrosis, vascular invasion, along with the identification of the patterns described above should allow PDTC to be recognized. Expression of TTF-1 and thyroglobulin is common, although staining may be patchy and restricted to isolated tumour cells or poorly developed follicles.

### 1.2.4 Anaplastic thyroid carcinoma (ATC)

ATC is a relatively rare thyroid tumour (2-5% of TCs) with a mean age of 65 years at presentation. Like PDTC, it can be derived from DTC or can arise *de novo*. ATC is composed of undifferentiated cells that show the immunohistochemical features of epithelial differentiation. At the clinical level, ATC is characterized by a large thyroid mass, rapidly growing and infiltrating the surrounding tissues and muscles. The clinical course of the disease can be so rapid that surgical procedures, such as tracheotomy and gastrostomy, performed as supportive care, are often useless.

Microscopically, there are two main patterns. 1) Squamoid: these tumours are undifferentiated but, nonetheless, epithelial with occasional focal keratinisation; 2) The second pattern is comprised of large, pleomorphic giant cells resembling osteoclasts and spindle cells resembling sarcoma. Cytokeratins are frequently expressed while thyroglobulin and TTF-1 tend to be absent in the tumour cells. Overexpression of cell

cycle regulatory protein such as cyclin D1, along with decreased expression of p27 and mutations of p53 leading to increased staining patterns are frequent in undifferentiated carcinoma (Fagin et al., 1993; Pickett et al., 2005).

### **1.3 Genetic alterations in TC**

TC represents a type of neoplasia in which critical genes are frequently mutated via two distinct molecular mechanisms: point mutation or chromosomal rearrangement. A growing body of evidence suggests that these two distinct mutational mechanisms are associated with specific aetiological factors involved in thyroid carcinogenesis. In addition to these genetic variations, TC initiation and progression could also occur through accumulations of epigenetic alterations, including alterations in gene expression patterns, the presence of microRNAs, aberrant gene methylation and the dysregulation of oncogenic proteins. An outline summary of genetic abnormalities associated with TC is shown in Table 1.1 and in Figure 1.2. These will be discussed in more detail below.

#### **1.3.1 v-Raf murine sarcoma viral oncogene homolog B1 (BRAF) oncogene**

BRAF is a serine-threonine kinase that is translocated to the cell membrane after being bound and activated by RAS. This results in the phosphorylation and activation of mitogen-activated protein kinase (MAPK) and other downstream targets of the MAPK signalling pathway. *BRAF* is the commonest human oncogene, mutated in 7-9% of all malignant solid tumours, with the highest prevalence (60%) in melanoma. After melanoma, PTC is the second human malignancy where *BRAF* mutations are especially frequent, being found in 29-87% (with a mean frequency of about 45%) of cases (Kim et al., 2006).

Although more than 40 mutations have been identified in the *BRAF* gene, the most significant hot spot for mutation, accounting for over 90% of all *BRAF* mutations, is a



thymidine to adenine transversion at nucleotide 1799 (T1799A) in exon 15. This substitution leads to a valine to glutamate transversion at residue 600 near the catalytic centre of the protein (BRAFV600E) and is believed to produce a constitutively active kinase by disrupting hydrophobic interactions between residues in the ATP binding site (Wan et al., 2004). This is the most frequent mutation found in PTC, highly prevalent in PTC with classical histology and in tall cell variant. Other rare mechanisms, alternative to the *BRAFV600E* mutation, contribute to *BRAF* oncogenic mutation in PTC. The Lys601Glu point mutation and small in-frame insertions or deletions surrounding codon 600 have been reported (Hou et al., 2007b; Trovisco et al., 2004). The presence of an *AKAP9/BRAF* rearrangement has also been described (Ciampi et al., 2005). This rearrangement is a paracentric inversion of chromosome 7q that leads to the fusion between the portion of the *BRAF* gene that encodes the protein kinase domain and the *AKAP9* gene.

*BRAF* mutations are also present in PTMC, suggesting that they can occur early in tumour development (Adeniran et al., 2006). Transgenic mice with thyroid-specific expression of *BRAFV600E* developed PTC closely recapitulating those seen in human tumours (Knauf et al., 2005) and thus supporting the role of *BRAF* oncogene in tumour initiation and differentiation, as well as its correlation with tumour characteristics. *BRAF* mutations are not found exclusively in PTC, but also in ATC (20-26% of cases), supporting the notion that the latter may originate from PTC de-differentiation. (Nikiforova et al., 2003a; Smallridge et al., 2009).

Based on molecular results, numerous studies have investigated the clinical significance of *BRAF* mutation in PTC. The general tendency of the studies is to show an association of this mutation with factors related to poor prognosis, in particular advanced tumour stage on presentation, tumour recurrence and metastasis. *BRAFV600E* has been proposed as an independent predictor of tumour recurrence (Xing, 2007a). PTC carrying the *BRAFV600E* mutation exhibit decreased expression of genes involved in thyroid

hormone biosynthesis, including the sodium iodide symporter (NIS), the decreased ability to trap radioiodine and consequent treatment failure (Riesco-Eizaguirre et al., 2006; Xing et al., 2005).

### 1.3.2 *RE*arranged during Transfection (*RET*) oncogenes

RET is a transmembrane tyrosine kinase receptor, known to be the signalling component of a multimolecular complex that includes the glial cell line-derived neurotrophic factor (GDNF) a co-receptor  $\alpha$  (GFR $\alpha$  1-4). Upon interaction with one of the four GFR  $\alpha$  co-receptors, RET binds with high affinity to the GDNF family peptides including GDNF, neurturin, persephin and artemin (Airaksinen and Saarma, 2002). *RET* proto-oncogene, located at chromosome 10q11.2, is essential for development of the sympathetic, parasympathetic and enteric neurons, kidney and male germ cells (Arighi et al., 2005). The germ line loss of function mutations of *RET* cause impaired formation of the enteric nervous system and congenital aganglionosis of the colon (Hirschsprung's disease), while germ line activating point mutations are causally related to the hereditary forms of MTC, Multiple endocrine neoplasia type 2A and 2B (MEN2A, MEN2B) and Familial MTC ( FMTC) (Arighi et al., 2005).

Oncogenic rearrangements of *RET*, producing the RET/PTCs, were the first genetic lesion identified in PTC. RET/PTCs oncogenes, present in a significant fraction of PTC (20-30%), are chimeric oncoproteins containing the intracellular domain (including TK and C terminal tail) of RET fused in frame to the 5' end of different donor genes. The donor genes are responsible for: i ) the expression of chimeric *RET/PTC* oncogenes in thyrocytes; and, ii) constitutive, ligand-independent activation of RET/PTC oncoproteins leading to chronic stimulation of MAPK signalling which triggers tumourigenesis (Jhiang et al., 1996a; Santoro et al., 1992).

At least 12 different genes that are involved in the generation of *RET/PTC* oncogenes have been identified (Greco et al., 2009). Two of the most common rearrangement types

are *RET/PTC1* and *RET/PTC3*, in which *RET* is fused to either *CCDC6* (also known as H4) or *NCOA4* (also known as *ELE1* or *RFG*), respectively (Grieco et al., 1990; Santoro et al., 1994). Both of these rearrangements are paracentric intrachromosomal inversions, as all the fusion partners reside on the long arm of chromosome 10. By contrast, *RET/PTC2* and nine more recently discovered types of *RET/PTC* rearrangements are all interchromosomal (Bongarzone et al., 1993; Ciampi et al., 2007; Klugbauer et al., 1998; Klugbauer et al., 2000). The frequent occurrence of *RET/PTC* rearrangements in papillary microcarcinoma suggests that such rearrangements are an early event in thyroid carcinogenesis. Other reasons to support this are: 1) *RET/PTC* expression is present in microscopic and occult PTCs (Viglietto et al., 1995); 2) *RET/PTC1* expression is sufficient to cause PTC-diagnostic alteration in the nuclear envelope and chromatin structure of human normal primary thyrocytes (Fischer et al., 1998); 3) *RET/PTCs* induce morphological transformation of PC-C13 rat thyroid epithelial cells (Jhiang et al., 1996b). *RET/PTC* rearrangements are listed in Table 1.1.

*RET/PTC* is found on average in approximately 20% of adult sporadic papillary carcinomas, although its prevalence is highly variable between different observations due to either geographic variability or different sensitivity of the detection. *RET/PTC* is typically more common in tumours from patients with a history of radiation exposure (50-80%) and its prevalence is higher in young patients (40-70%) (Collins et al., 2002; Fenton et al., 2000). Radiation exposure after the Chernobyl accident particularly increased the frequency of PTC carrying *RET/PTC3* or *BRAF/AKAP9* rearrangement (Ciampi et al., 2005; Smida et al., 1999). In particular, in post-Chernobyl PTCs the presence of *RET/PTC3* is associated-with the solid/follicular variant, while the less frequent *RET/PTC1* rearrangement is associated with the classical and diffuse sclerosing variant (Nikiforov, 2006). The role of radiation exposure in the generation of *RET/PTC* is also supported by the experimental induction of *RET/PTC* by irradiating human cultured thyroid cells (Caudill et al., 2005; Ito et al., 1993).



### 1.3.3 *TRK* oncogenes

The neurotrophin tyrosine kinase receptor, type 1 (*NTRK1*) gene (also known as *TRKA*) located at chromosome 1, encodes the high affinity receptor for neural growth factor (NGF). It regulates growth, differentiation and apoptosis in the peripheral and central nervous system, and stimulates the proliferation of a number of non-neural cell types such as lymphocytes, keratinocytes and prostate cells.

In PTC *NTRK1* gene undergoes oncogenic rearrangements similar to those described above for *RET*. Several *TRK* oncogenes differing in the activating regions have been isolated from PTC. The most frequent oncogene is *TRK* (Butti et al., 1995) and is identical to that first isolated from colon carcinoma containing sequences from the non-muscle Tropomyosin gene (*TPM3*) on chromosome 1q22-23. *TRK-T1* and *TRK-T2* oncogenes both derive from a rearrangement between the *NTRK1* and Translocated Promoter Region (*TPR*) genes on chromosome 1q25, but each one displays a different structure. *TRK-T3* is activated by TRK Fused Gene (*TFG*), a novel gene on chromosome 3q11-12, first identified in this rearranged version (Greco et al., 2004). The *TRK* oncogenes are listed in Table 1.1.

Somatic rearrangements of the *NTRK1* gene in PTC are less common than those involving the *RET* gene and their frequency does not exceed 12%. The association of *NTRK1* rearrangements with radiation is not clearly defined since their frequency in PTC associated with therapeutic or accidental (Chernobyl) radiations was similar to that of sporadic tumours (Bounacer et al., 2000; Rabes et al., 2000).

Analysis of any correlation between *NTRK1* rearrangements with clinical and pathological features did not produce unequivocal data. This is related not only to the limited number of PTCs carrying *TRK* oncogenes so far identified, but also to the fact that in the majority of studies the genotyping of PTCs is restricted to *RET* rearrangements and *BRAF* mutation analyses.

Experimental evidence suggests that *TRK* oncogenes exert a direct role and represent an early event in the process of thyroid carcinogenesis. Transgenic mice carrying the *TRK-T1* oncogene under the control of the thyroglobulin promoter (Tg-*TRK-T1* mice) develop thyroid hyperplasia and PTC (Russell et al., 2000). Crossing of Tg-*TRK-T1* mice with *p27<sup>kip1</sup>*-deficient mice increased the penetrance of TC and shortened the latency period of tumour incidence, indicating that *TRK-T1* gene requires cooperation with oncosuppressor genes to transform thyroid epithelium (Fedele et al., 2009).

**Table 1.1 Fusion oncogenes in thyroid tumours**

ONCOGENE	DONOR GENE	CHROMOSOME LOCATION
<i>RET/PTC1</i>	<i>CCDC6</i> (coiled-coil domain containing 6)/ <i>H4/D10S170</i>	10q21
<i>RET/PTC2</i>	<i>PRKARIA</i> (protein kinase; cAMP-dependent, regulatory, type I, alpha)	17q23
<i>RET/PTC3</i>	<i>NCOA4</i> (Nuclear coactivator 4)/ <i>RFG/ELE1/ARA70</i>	10q11.2
<i>RET/PTC4</i>	<i>NCOA4</i> (Nuclear coactivator 4)/ <i>RFG/ELE1/ARA70</i>	10q11.2
<i>RET/PTC5</i>	<i>GOLGAS</i> (golgin subfamily a, 5)/ <i>RFG5/RET-II</i>	14q
<i>RET/PTC6</i>	<i>TRIM24</i> (tripartite motif-containing 24)/ <i>TIF1/TIF1A</i>	7q32-34
<i>RET/PTC7</i>	<i>TRIM33</i> (tripartite motif-containing 33)/ <i>RFG7/TIF1G</i>	1p13
<i>RET/PTC8</i>	<i>KTN1</i> (Kinetin 1)/ <i>CG1</i>	14q22.1
<i>RET/PTC9</i>	<i>RFG9</i>	18q21-22
<i>ELKS-RET</i>	<i>ELKS/ RAB6IP2/KIAA1081</i>	12p13.3
<i>PCMI-RET</i>	<i>PCMI</i> (pericentriolar material 1)	8p21-22
<i>RFP-RET</i>	<i>TRIM27</i> (tripartite motif-containing 27)/ <i>RFP</i>	6p21
<i>HOOK3-RET</i>	<i>HOOK3</i> ( <i>Homo sapiens</i> hook homolog 3)/ <i>HK3</i>	8p11.21
<i>TRK</i>	<i>TPM3</i> ( <i>Tropomyosin3</i> )	1q22-q23
<i>TRK-T1; TRK-T2</i>	<i>TPR</i> ( <i>Translocated promoter region</i> )	1q25
<i>TRK-T3</i>	<i>TFG</i> ( <i>Trk-fused gene</i> )	3q11-q12
<i>AKAP9-BRAF</i>	<i>AKAP9</i> ( <i>A-kinase anchor protein 9</i> )	7q21-q22

#### 1.3.4 *RAS* mutations

The human *HRAS*, *KRAS* and *NRAS* genes encode highly related G-proteins that reside in the inner surface of the cell membrane and transmit signals arising from cell-membrane receptor tyrosine kinases and G-protein-coupled receptors along the MAPK, phosphatidylinositol 3-kinase/protein kinase B (PI3K/AKT) and other signalling pathways.

Activating point mutations typically affect the codons 12, 13 and 61 of the *RAS* genes. In thyroid cancer, *NRAS* codon 61 and *HRAS* codon 61 mutations are most common. *RAS* mutations are found in a variety of thyroid tumours, including 10-20% of PTC, 40-50% of FTC and 10-40% of poorly differentiated and ATCs (Esapa et al., 1999; Ezzat et al., 1996; Motoi et al., 2000; Namba et al., 1990; Suarez et al., 1990). Among PTCs, tumours with *RAS* mutations forming neoplastic follicles, and not papillary structures, are diagnosed as the follicular variant of PTC. *RAS* mutations are also found in 20-40% of benign follicular adenomas, suggesting that the latter may serve as a precursor for *RAS*-positive FTC and the follicular variant of PTC (Adeniran et al., 2006; Zhu et al., 2003). Furthermore, *RAS* mutations may predispose well-differentiated cancers to dedifferentiation and anaplastic transformation (Garcia-Rostan et al., 2003). *RAS* activation by itself is not sufficient to induce malignant growth but may predispose cells to acquire further genetic or epigenetic alterations that lead to a fully transformed phenotype. This is consistent with the observation that *RAS* mutations may affect chromosomal stability *in vitro* (Saavedra et al., 2000).

A significant correlation between *RAS* mutations, metastases and poor prognosis has been found in patients (Garcia-Rostan et al., 2003). As *RAS* mutations are a marker for aggressive TC behaviour and poor outcome, surgical resection of *RAS*-positive adenomas might be proposed to prevent progression to carcinoma (Nikiforova and Nikiforov, 2008).

### 1.3.5 Paired box gene 8/ peroxisome proliferator-activated receptor (*PAX8/PPAR $\gamma$* ) rearrangement

The *PAX8/PPAR $\gamma$*  rearrangement results from the translocation (t(2;3)(q13;p25) between the *PAX8* gene, which encodes a paired domain transcriptional factor, and the *PPAR $\gamma$*  gene, expressed at low level in normal thyroid with unknown functions (Nikiforova and Nikiforov, 2008). The resulting fusion protein encodes a nearly full length *PPAR $\gamma$* , the expression of which is under the transcriptional regulation of the *PAX8* promoter (Kroll et al., 2000). The functional consequences of this rearrangement are not yet fully understood.

*PAX8/PPAR $\gamma$*  is a prototypic alteration found in FTC, where it occurs with a frequency of 30-35%. This rearrangement has also been found in some FA (2-13%) and in a small proportion (1-5%) of the follicular variant of PTC (Nikiforova et al., 2003b)

A novel *CREB3L2/PPAR $\gamma$*  fusion generated by t(3;7)(q34;p25) rearrangement has been detected in <3% of FTC (Lui et al., 2008). It has been reported that both of the *PAX8/PPAR $\gamma$*  and *CREB3L2/PPAR $\gamma$*  fusion proteins have oncogenic properties in normal human thyroid cells, but their mechanisms of action are still unclear (Lui et al., 2005).

With respect to the mechanisms activated by *PAX8/PPAR $\gamma$* , both gain and loss of function activities have been suggested. Specifically, deregulation of the normal functions of *PAX8* and *PPAR $\gamma$*  and the unique transcriptional activities of the fusion oncoprotein have been reported (Nikiforova and Nikiforov, 2008). It has been proposed that *PAX8/PPAR $\gamma$* -stimulated growth could depend at least in part on loss of *PPAR $\gamma$*  functions caused by the inhibition of wild-type protein (Nikiforova and Nikiforov, 2008). This is consistent with the concept that *PPAR $\gamma$*  down-regulation or inhibition may be a key event in thyroid carcinogenesis (Placzkowski et al., 2008), as also suggested by the evidence that *PPAR $\gamma$*  is downregulated in translocation-negative papillary or follicular thyroid tumours.

The *PAX8/PPAR $\gamma$*  rearrangement and *RAS* point mutations rarely overlap in the same tumour suggesting that they represent distinct pathogenetic pathways in the development of FTC. In keeping with this, analyses of gene expression profiles of *PAX8/PPAR $\gamma$*  positive FTCs have confirmed that these carcinomas have a distinct transcriptional signature (Nikiforova and Nikiforov, 2008). Although based on its presence in both benign and malignant lesions, the diagnostic and preoperative value of *PPAR $\gamma$*  rearrangement is subject to debate, it is plausible that benign nodules carrying the translocation may be considered at risk for progression.

### 1.3.6 *PI3K/AKT pathway mutations*

The PI3K/AKT pathway exerts an important role in many cellular events, including growth, proliferation and apoptosis. This pathway is particularly activated in many tumours, including thyroid tumours (Ringel et al., 2001; Vasko et al., 2004). In fact, FTC are characterized by high levels of AKT activation in comparison with normal tissue and PTC (Ringel et al., 2001; Vasko et al., 2004). The mechanisms underlying this activation could include mutations or amplification of the *PIK3CA* gene, encoding the catalytic subunit of PI3K (Wang et al., 2007), decreased expression or inactivation of its negative regulator phosphatase and tensin homologue (*PTEN*) (Paes and Ringel, 2008) and activation by constitutively active *RAS* oncogenes (Vasko et al., 2004). *PIK3CA* mutation, however, is not a common mechanism in the activation of this pathway in TC, but the amplification of this gene is more frequent. In PTC, the presence of rare mutations and more frequent amplification are detected in 15-53% of tumours (Abubaker et al., 2008; Hou et al., 2007a). Although *PIK3CA* amplification is also observed in FTC and even in FA (Hou et al., 2007a; Wu et al., 2005) it is most frequently observed in anaplastic TC. The occurrence of *PIK3CA* amplification and *RAS* mutation, even in follicular adenomas, has suggested that the PI3K/AKT pathway plays a role at an early stage of thyroid tumourigenesis. Of note, the mutual exclusivity of these genetic alterations has not been

observed in ATC, implying a role of the PI3K/AKT pathway in progression of FTC to ATC (Hou et al., 2007a).

PTEN is a dual-specific phosphatase, a negative regulator of the PI3K/AKT pathway by dephosphorylating phosphatidylinositol-3,4,5-triphosphate (PIP3), another protein that can also influence the MAPK pathway. *PTEN* acts as a tumour suppressor gene, its germline loss of function mutation predisposes to multiple tumours including FTC (Yeh et al., 1999). Single cases of a loss of function somatic mutation of *PTEN* have been described in FTC (7%), in ATC (12-50%) and rarely in PTC (2%) (Frisk et al., 2002; Garcia-Rostan et al., 2005; Hou et al., 2007a; Smallridge et al., 2009). A novel rearrangement involving in *PTEN* and the *H4* gene has been described in PTC (Puxeddu et al., 2005).

#### 1.3.7 Tumour protein 53 (*TP53*) mutation

*TP53* encodes the multifunctional nuclear protein p53 that is important for cell cycle arrest at DNA damage, senescence or apoptosis and it is one of the most commonly known tumour suppressor genes. Contrary to what is seen in many other cancers, *TP53* loss of function mutations occur late in thyroid tumourigenesis and are practically absent in differentiated TC (0-9%), while the prevalence reaches 17-38% in poorly differentiated and 55-88% in anaplastic cancers (Fagin and Mitsiades, 2008; Smallridge et al., 2009). Such mutations are associated with cell proliferation and loss of differentiation, as restoration of p53 function in ATC cell lines causes a reduction in the proliferation rate of the tumour cells, their re-expression of thyroid specific genes and responsiveness to TSH stimulation (Fagin et al., 1996; Moretti et al., 1997).

### 1.3.8 Other alterations in TC

#### *Loss of heterozygosity (LOH)*

TCs accumulate a number of alterations at the genomic level. Chromosome instability has been identified in follicular adenomas and carcinomas, which are frequently aneuploid with a high prevalence of LOH. This is in contrast to the diploid or near-diploid content of most papillary carcinomas, which generally show less frequent LOH (Castro et al., 2005; Sobrinho-Simoes et al., 2005).

The most frequently deleted chromosomal regions in FC and FA are on chromosome 2p, 3p, 9q, 10q, 11p, 15q and 17 p (Zedenius et al., 1995) (Ward et al., 1998) (Kitamura et al., 2001). The average rate of allelic loss of target regions is significantly higher in FC (30-50%) than in FA (6-15%) (Hunt et al., 2003; Ward et al., 1998). HCC usually reveal a comparable or even higher rate of LOH than conventional follicular tumours (Segev et al., 1998). Some studies have found a correlation between the frequency of LOH, tumour aggressiveness and outcome in patients with follicular carcinomas (Hunt et al., 2006).

#### *Mitochondrial defects*

Oncocytic tumours are characterized by the cytoplasmic accumulation of numerous mitochondria in Hurtle (oxyphil or oncocytic) cells that frequently show abnormal morphology. Mitochondrial abnormalities probably represent either a primary change associated with tumour initiation or a secondary change (Tallini et al., 1992).

Mutations of the gene *NADH* dehydrogenase [ubiquinone] 1 alpha subcomplex subunit 13 (*NDUFA13*) (also known as *GRIM-19*) have been identified in oncocytic thyroid tumours (Maximo et al., 2005). This gene encodes a protein that regulates cell death and promotes apoptosis and also affects mitochondrial metabolism by serving as an essential component of complex I of the respiratory chain (Angell et al., 2000). Somatic mis-sense mutations in *NDUFA13* were found in 10-20% of oncocytic follicular carcinomas and the oncocytic variant of papillary carcinoma (Maximo et al., 2005).

However, the role of *NDUFA13* mutations in carcinogenesis remains obscure although a lack of complex I has been proposed to prevent tumour cells from undergoing apoptosis.

### *Beta catenin ( $\beta$ -catenin)*

The  $\beta$ -catenin protein, when bound to E-cadherin (CDH1), mediates cell skeleton/adhesion interactions, and when not sequestered and not degraded, plays a role in gene transcription regulation of growth-promoting genes. It also belongs to the Wnt signalling pathway which is often associated with tumourigenesis. High levels of Wnt5a have been reported in the majority of PTCs and only in some cases of FTC (Kremenevskaja et al., 2005). Mutations in the  $\beta$ -catenin gene (*CTNNB1*) are most frequent in poorly differentiated and anaplastic cancers (Garcia-Rostan et al., 2001).

CDH1, is a calcium-dependent transmembrane glycoprotein, which functions as a cell-cell adhesion molecule and forms complexes with catenin proteins in the regulation of the Wnt pathway. CDH1 expression is reduced in thyroid carcinomas and has been associated with poor prognosis in PTC (von et al., 1997) and FTC (Brecelj et al., 2005), as well as the PTC-to-ATC transition (Wiseman et al., 2007). Expression of CDH1 in undifferentiated TC is extremely low (Brabant et al., 1993) probably due to promoter hypermethylation (Rocha et al., 2003; Soares et al., 1997).

### *Hepatocyte growth factor receptor (MET) oncogene*

The receptor-tyrosine kinase MET is the main signalling receptor for hepatocyte growth factor (HGF). HGF is a potent mitogen for epithelial cells and promotes cell motility and invasion. About 50% of cases of PTC are characterized by MET overexpression (Di Renzo et al., 1992) which is believed to be a sign of more aggressive disease (Mineo et al., 2004). *BRAF*-positive tumours were also associated with MET overexpression in aneuploid PTC (Rodrigues et al., 2007a). MET overexpression is, however, rare in other histological types of thyroid tumours (Ruco et al., 2001).



### *Epidermal growth factor receptor EGFR*

The EGFR family includes EGFR (also known ERBB1 and HER1), ERBB2 (HER2), ERBB3 (HER3) and ERBB4 (HER4). Multiple ligands bind to EGFR.

Thyroid tumours overexpress EGFRs and their ligands thus implicating EGFR signalling in thyroid tumourigenesis (Schiff et al., 2004). EGFR protein levels are increased in PTC in comparison to normal tissue and the high expression of EGFR has been suggested to be associated with worse outcome of PTC after thyroidectomy (Akslen and Varhaug, 1995; Ruan et al., 2008). HER2 could also be considered a predictor of metastasis in PTC (Kremser et al., 2003). A functional TGFA/EGFR autocrine signalling loop has been shown to sustain the proliferation of PTC cells, contributing to PI3K/AKT activation. TGFA/EGFR was common in PTC cells harbouring *BRAF* and *RET/PTC* mutations. Since other signal pathways have been demonstrated to function in tandem with EGFR pathway, the therapeutic targeting of EGFR only could be inadequate (Degl'Innocenti et al., 2010).

### *Mitogen-inducible gene 6 (MIG-6)*

*MIG-6* is an immediate early gene, the expression of which is induced by cellular stress, hormones or growth factors in many cells (Ferby et al., 2006). It exerts a negative role on EGFR signalling through a negative feedback loop, a process lost in cancer. In PTC, *MIG-6* inversely directly correlates with *EGFR* expression and its higher mRNA level was associated with better overall survival in PTC patients. *MIG-6* expression was found to be independently predictive of disease-free survival in *BRAF*-positive patients (Ruan et al., 2008).

VEGF overexpression is a characteristic feature of malignant tumours, including thyroid tumours (Wiseman et al., 2008). The quantitative evaluation of VEGF expression in PTC showed an association with the concomitant expression of other angiogenic factors in metastatic PTC (Klein et al., 2001). VEGF expression was closely correlated with tumour size, extrathyroidal invasion, lymph node metastasis and *BRAFV600E* mutation (Jo et al., 2006)

### *Cell cycle regulation*

The growth activity of well-differentiated TC is low compared with poorly differentiated and undifferentiated TC with MIB1 indexes of 1-3%, 6-7% and 14-52% respectively (Kato et al., 1995; Kjellman et al., 2003). The differences in proliferation are governed by altered cell-cycle regulators. Although the expression of cyclin D1 and cyclin E1 remain undetectable in normal thyroid follicular cells, cyclins D1 and E1 are observed in approximately 30% and 76% of PTC, respectively (Basolo et al., 2000; Brzezinski et al., 2004). Cyclin D1 overexpression correlates with metastatic spread in PTC and it is observed in undifferentiated carcinoma (Khoo et al., 2002; Wang et al., 2000). Although the copy number of the cyclin D1 (*CCND1*) gene is amplified in many tumours, neither major genetic alterations nor amplification of *CCND1* and cyclin E1 gene (*CCNE1*) have been found in TC (Khoo et al., 2002; Lazzereschi et al., 1998). The overexpression of cyclins is, therefore, probably a secondary effect induced by other genetic aberrations in thyroid tumours.

CDK inhibitors are commonly downregulated in TC. In fact, there is a progressive loss of p21<sup>CIP1</sup> (encoded by *CDKN1A* gene) with advancing tumour stage of PTCs, and 13% of PTC harbour *CDKN1A* deletions (Brzezinski et al., 2005). The expression of the cyclin-dependent kinase inhibitor p27<sup>KIP1</sup> (encoded by the *CDKN1B* gene) is significantly reduced in PTC, metastatic forms and undifferentiated carcinoma (Erickson et al., 2000).

Although point mutations of *CDKN2A* (which encodes p16<sup>INK4A</sup>) are rare in TC (Elisei et al., 1998; Yane et al., 1996), LOH in the region of *CDKN2A* is associated with FTC (27%) and undifferentiated TC (50%) (Tung et al., 1996). Hypermethylation of its promoter has also been detected in 30% of thyroid tumours (Elisei et al., 1998).

Lastly, Transcription factor (E2F1) is one of the main targets of Rb protein. It is upregulated in 35-89% of well-differentiated carcinoma and 67% of undifferentiated carcinomas (Onda et al., 2004; Volante et al., 2002).

### *Mucin (MUC1)*

MUC1 is a glycoprotein that is important for cell adhesion and is overexpressed in about 25% of PTC (Wreesmann et al., 2004). It has been demonstrated that MUC1 is able to promote an aggressive phenotype of PTC (Patel et al., 2005). MUC1 overexpression is frequent in tall cell variant of PTC known for its poor prognosis (Ghossein and LiVolsi, 2008).

### *Cytokines and inflammation*

In the last few years it has become evident that PTC represents an excellent model to study the link between inflammation and cancer. This connection is documented by two different types of evidence: 1) PTC-associated oncogenes trigger a pro-inflammatory programme in thyrocytes; 2) inflammatory cells, such as leukocytes and macrophages, are frequently found to infiltrate PTC.

Several inflammation related genes have been demonstrated to be convergent targets induced by all of the main known PTC-related oncogenes. *RET/PTC1* has been reported to induce an inflammatory programme directly in primary human thyrocytes (Borrello et al., 2005). *BRAF*, *RAS* and *RET/PTCs* were all shown to up regulate cytokines such as CXCL1 and CXCL10 and metalloproteases (Melillo et al., 2005).

The chemokine receptors interleukin 8 receptor  $\beta$  (CXCR2), CXCR3, CXCR4 and CXCR7 are expressed on PTC cells (Melillo et al., 2005) (Sancho et al., 2006). CXCR7 was reported to be associated with certain pathologic factors of PTC aggressiveness such as extra-thyroidal tumour extension, angio-lymphatic invasion and the presence of lymph node metastases (Wagner et al., 2008). CXCL14 was also described to be associated with metastatic PTC (Oler et al., 2008).

Osteopontin (SPP1) is a cytokine regulating cell trafficking within the immune system, binding a splice variant of CD44, that is not only overexpressed in PTC but contributes to mitogenesis (Figge et al., 1994), the survival and motility of PTC thyrocytes and their invasion potential (Guarino et al., 2005). In PTC, the gene expression level of *SPP1* was associated with metastasis and not with the *BRAF* status of the tumour (Oler et al., 2008).

#### 1.4 Mechanisms of thyroid cancer aetiology

Despite the high frequency of chromosomal rearrangements occurring in PTC, the molecular basis underlying the predisposition of thyrocytes to undergo chromosome rearrangements is not completely understood. A strong association exists between papillary thyroid cancer-specific chromosomal rearrangements and the exposure to ionizing radiation. As previously reported, *RET/PTC* rearrangements are found in up to 80% of papillary carcinomas in individuals exposed to either accidental radiation or therapeutic radiation (Bounacer et al., 1997; Rabes et al., 2000).

Although the exact molecular mechanisms involved in the formation of chromosomal rearrangements following radiation exposure are not well understood, several reports have proposed that the spatial proximity of translocation-prone gene loci may favour gene rearrangements (Nikiforova et al., 2000; Roccato et al., 2005). Spatial proximity may predispose the neighbouring genes to simultaneous damage by radiation and facilitate the mis-rejoining of free DNA ends located immediately adjacent to each other. In support of this, proximity between rearranging gene pairs such as *RET* and *H4*, and *NTRK1* and *TPR*, has been reported in interphase thyroid nuclei (Pierotti and Greco, 2006). Another possibility is that following DNA damage thyrocytes would be more prone to DNA repair than apoptosis, and this would increase the likelihood of gene rearrangements (Pierotti and Greco, 2006).

In addition to ionizing radiation, the induction of the *RET/PTC* rearrangement may also be associated with chromosome fragility. The 10q11.2 and 10q21 regions on chromosome 10 where the *RET* and *CCDC6 (RET/PTC1)* genes reside have been known to contain the fragile sites *FRAG10G* and *FRA10C* (Buttel et al., 2004; Richards, 2001). Chromosome fragility may be caused also by hypoxia, ethanol, endogenous and exogenous factors, and might therefore represent another mechanism of formation of the *RET/PTC* fusion gene in thyroid cells (Buttel et al., 2004; Richards, 2001).

In contrast to chromosomal rearrangements, point mutations are prevalent in thyroid cancers that lack any association with radiation exposure thus suggesting other aetiologic factors are involved. Many studies report a high prevalence of *BRAF* point mutations in PTC from several regions where there is a very high iodine intake by the population and exposure to certain specific chemical compounds such as boron, iron, vanadium and manganese (Lind et al., 1998; Pellegriti et al., 2009).

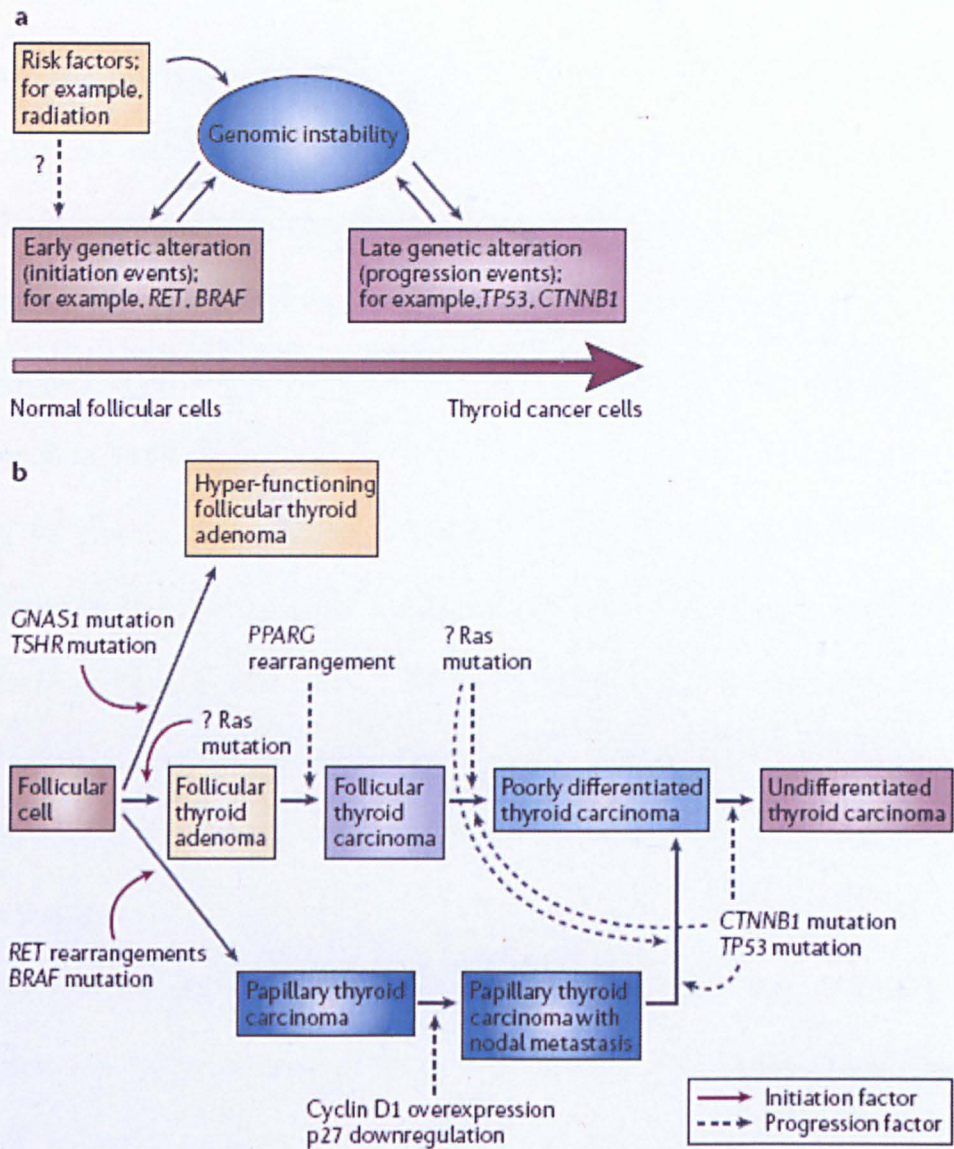


**Figure 1.2 Model of multistep carcinogenesis of thyroid neoplasia.** a) Risk factors promote genomic instability resulting in early genetic alterations involving the MAPK signalling pathway. This, in turn, induces genomic instability resulting in the induction of other late genetic alterations.; b) three distinct pathways are proposed for neoplastic proliferation of thyroid follicular cells: 1) hyper-functioning follicular thyroid adenoma; 2) follicular thyroid carcinoma and papillary thyroid carcinoma. In the figure frequent early and late alterations are reported. Poorly differentiated and undifferentiated thyroid carcinoma are considered to derive from pre-existing FTC and PTC through additional genetic events; however, even though not shown in the figure, they can arise *de novo* from follicular cells (from (Kondo et al., 2006)).

## **1.5 Therapy in thyroid cancer**

### **1.5.1 Multikinase inhibitors as target therapy**

Most thyroid cancers are effectively treated by surgical thyroidectomy and selective use of lymph-node dissection. In the case of differentiated thyroid cancers (PTC and FTC), thyroid-stimulating hormone (TSH) suppression and ablation of residual tissue using radioactive iodine 131 (RAI) are used. For the majority of patients the prognosis is excellent, with an overall survival rate of 85% at 10 years. Nevertheless, despite low mortality rates, local recurrence occurs in up to 20% of patients and distant metastasis in approximately 10% at 10 years (Eustatia-Rutten et al., 2006). Metastatic PTC and FTC poorly concentrate radioactive iodine as the disease becomes less differentiated (Dohan et al., 2003). In ATC surgery is not often technically feasible due to the local extension and invasion of the contiguous anatomic structures.

At present, RAI resistant thyroid carcinomas and ATC represent the most important challenges for therapy.

The molecular discovery described in the previous paragraphs has unveiled that the two most important pathways involved in TC pathogenesis progression are: the deregulation of TC genes such as *BRAF*, *RAS*, *RET* and angiogenesis. Since both signal through the MAPK and PI3K/Akt pathways a major therapeutic strategy is to block these intracellular signalling cascades. An important approach is through the use of Tyrosine kinase inhibitors (TKIs) which compete with ATP for the binding to the catalytic pocket of a TK. Several compounds belonging to this class have been developed and approved for treatment of different tumour types. Some of them are being used in advanced thyroid cancer and are listed in Table 1.2 (reviewed in (Gild et al., 2011)).

At present, only those patients with advanced TC unsuitable for surgery, showing evidence of progression disease and exhibiting RAI-refractoriness are candidates for TKI



therapy. Over the last year, the employment of multikinase inhibitor has achieved promising results in the management of advanced thyroid cancer.

**Table 1.2** Tyrosin kinase inhibitors in current trials and their targets

Drug	Targeted tyrosine kinase
Axitinib	VEGFR1–3, PDGFR, c-Kit
Cabozantinib (XL184)	HGFR, VEGFR2, RET
Lenvatinib (E7080)	VEGFR1–3, FGFR1–4, RET, c-Kit, PDGFR
Motesanib	VEGFR1–3, PDGFR, c-Kit, RET
Pazopanib	VEGFR, PDGFR, c-Kit
Sorafenib	VEGFR1–3, PDGFR, RET, RAF, c-Kit
Sunitinib	PDGFR, VEGFR1–3, c-Kit, RET, CSF1R, FLT3
Vandetanib (ZD6474)	VEGFR2–3, RET, EGFR

(adapted from Gild M L *et al.*, 2011)

Other therapeutic approaches consist of the use of compounds targeting molecules other than TKs. For example, demethylating and re-differentiating agents act by interfering with the epigenetic mechanisms involved in thyroid cancer pathogenesis, while other compounds exert their action through the inhibition of proteosome and angiogenesis.

The molecular targets for thyroid cancer therapy are reported in Figure 1.3

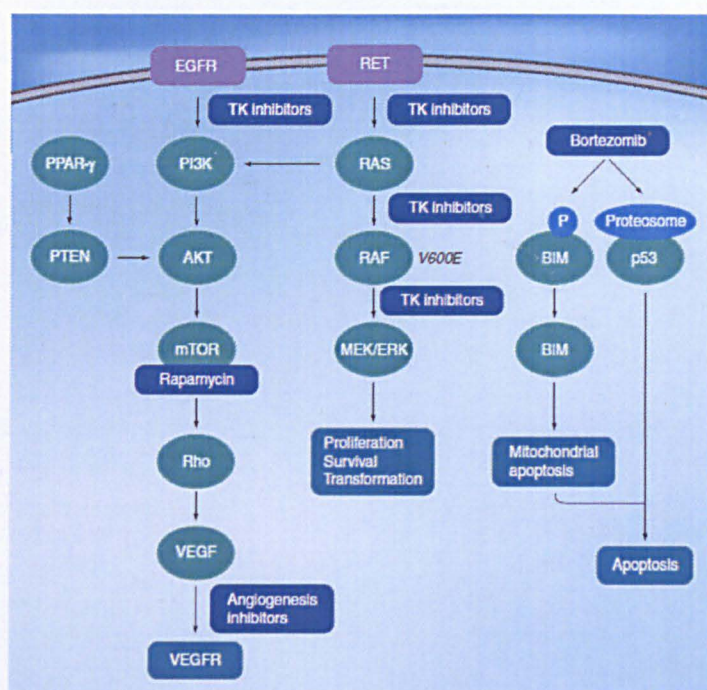


**Figure 1.3 Molecular pathways involved in thyroid tumourigenesis and molecular targets for new drugs** (from (Brilli and Pacini, 2011))

### 1.5.2. Conclusions on therapeutic options

The rationale for the employment of target therapy is to block off known aberrancies involved in TC pathogenesis, but until now none of the genetic defects have been identified as clearly linked to the activity of the experimental compounds. Possible explanations include the possibility of multiple redundancies in the oncogenic pathways so that more than one pathway could be activated in signal transduction in the tumour cells, in addition to the targeted molecules.

Success with single-agent therapies for TC has been modest. It is worth noting that translational studies looked for targets on the primary thyroid tumours which might have occurred several years before the appearance of metastases, which could include the acquisition or loss of genetic defects.



Improved anti-tumour efficacy might be achieved through the use of inhibitors with greater specificity for mutant kinases (e.g. vemurafenib for patients with *BRAFV600E* mutation) thus targeting a specific oncogenic mechanism. Alternatively through the use of inhibitors that target different kinase pathways known to be active within thyroid cancer thus avoiding pathway switching.

Several clinical issues regarding TKI therapy remain open. These include patient selection, the lack of predictive biomarkers of response and toxicity profile, the length of time and optimal sequence of TKI administration, the problems of drug resistance, the endpoints of clinical trials, overall survival (OS) versus progression-free survival (PFS).



## 2.1 Expression profiles in thyroid cancer

The majority of thyroid tumours are characterized by specific lesions such as rearrangements or mutations, alternative pathways relevant for thyroid carcinogenesis are not, as yet, completely understood. Larger scale studies analyzing gene expression profiles provide an important approach to the identification of other molecular mechanisms underlying thyroid carcinogenesis. An increasing number of studies have used microarray technology in order to understand the molecular aetiology of the tumour and to identify genetic markers that could improve differential diagnosis. Moreover, gene expression has demonstrated the potentiality of unveiling genes involved in the pathogenesis of thyroid tumours and possible new therapeutic targets. In fact, recent reports highlight the power of gene expression analysis as a tool for the identification of putative oncosuppressor and tumour promoter genes.

### 2.1.1 PTC signature

The first microarray-based study was performed by Huang *et al.* in 2001 (Huang *et al.*, 2001a). Expression profiles of eight PTC samples compared with paired normal tissue exhibited distinct clustered profiles. Differential expression occurred for numerous genes, already known to be involved in thyroid carcinogenesis, as well as for new identified genes. These genes grouped in functional categories such as cellular adhesion and extracellular matrix, cytoskeleton, growth factors and receptors, and signal transduction. Among genes underexpressed in PTC, several genes relating to specialized thyroid functions such as thyroid peroxidase (*TPO*), *DIO1*, *DIO2* and *SLC5A5* (also named *NIS*, encoding sodium iodide symporter) were found. These findings are consistent with the fact that most malignant thyroid tumours are hypofunctioning in trapping iodine and producing thyroid hormone. Other underexpressed genes were *GAS1*, *CDCL1* and *BCL2* and other involved in fatty-acid binding such as *FABP4*, *CRABP1* and *APOD*. Among the overexpressed genes, fibronectin 1 (*FNI*), *MET*, dipeptidylpeptidase IV (*DPP4*), alpha 1-

antitrypsin (*SERPINA1*), keratin 19 (*KRT19*), galectin-3 (*LGALS3*), previously associated with PTC, were found. Such analysis leads to identification of genes overexpressed and not previously associated, such as Cbp/p300-interacting transactivator 1 (*CITED1*), *ADORA1*, *SCEL*, *ODZ* and *DUSP6*. Other genes overexpressed in PTC encoded cell adhesion-associated proteins such as Tissue inhibitor of metalloproteinase 1 (*TIMP1*), midkine or neurite growth-promoting factor 2 (*MDK*) and *MUC1*, thus suggesting that the overexpression of adhesion-related genes is a characteristic feature of PTC (Huang et al., 2001a; Jarzab et al., 2005).

Jarzab *et al.* (Jarzab et al., 2005) confirmed the previous gene expression profile of PTC and proposed an optimal “20 best genes” to differentiate between PTC and normal tissue. This classifier gene set includes some genes with a very distinct change in expression signal (previously known to be up-regulated in PTC). The authors confirmed that the most frequent gene ontology class modulated in PTC referred to adhesion genes. Genes involved in signal transduction like *CITED1* or calcyclin (*S100A6*), the cell cycle regulators stratifin (*SFN*) and *CCND1*, the estrogen-responsive gene *EBAG9*, or *CD44* antigen constitute other examples of genes that were already identified in previous PTC studies. Signal transduction and apoptosis/cell cycle genes were moderately abundant (about 10%) in the gene set. Moreover, the authors also found upregulation of *MET*, which is a consistent feature found in nearly all of the PTC genomic studies (Huang et al., 2001a).

Vasko *et al.* (Vasko et al., 2007) performed a comparative gene expression profiling of the intratumoural invasive region of PTCs with the central region of the tumour. Genes found to be overexpressed were related to transcription, cell signalling (integrin/TFGbeta pathway), regulation of nuclear localization, small G protein and guanine nucleotide exchange factors. Genes underexpressed were related to cell-cell adhesion and communication processes. Authors concluded that genes differentially expressed in the invasive regions of PTCs are involved in the epithelial to mesenchymal transition process, a common feature of aggressive PTCs.

Several studies were devoted to assessing whether the various PTC-associated genetic lesions could generate different and specific gene expression patterns. In this respect, the first study was performed by Frattini *et al.* (Frattini et al., 2004). In this study, unsupervised hierarchical clustering showed that the PTC samples did not group according to their genetic lesion, but behaved as an homogenous group in terms of gene expression profiles, although triggered by different genetic lesions. Whereas the supervised analysis did not show any differences between PTC with unknown lesions and “*RTK*-rearranged” and “*BRAF*-mutated” PTCs, comparison between “*RTK* rearranged” and “*BRAF* mutated” PTCs identified 69 genes differentially expressed, all related to signal transduction pathway, tumour invasion, and angiogenesis. This finding suggested that although *RTK* and *BRAF* act along the same signal transduction pathways, they regulate different gene sets.

In 2005, Giordano *et al.* (Giordano et al., 2005) showed that the gene expression profile of the *BRAF*-associated PTC differs profoundly from the *RET/PTC* or *RAS*-associated PTC. In particular, over 3800 genes were found to be differentially expressed in PTC with *BRAF* mutation compared to those with *RET* alterations. The results were indicative that the tumour mutational status correlated with the gene expression profile. In contrast to Frattini *et al.*, these authors hypothesized that these mutations signalled through alternative pathways .

Gene expression profiling performed by Melillo *et al.* (Melillo et al., 2005) revealed that the ectopic expression of the three oncogenes *RET/PTC*, *RAS* and *BRAF* activate a common transcriptional program in thyroid cells. This included the upregulation of the *CXCL1* and *CXCL10* chemokines, which are involved in cell proliferation and invasion promotion.

Borrello *et al.* (Borrello et al., 2005) demonstrated that the *RET/PTC1* oncogene activates a proinflammatory program, and, in particular induces the expression of a large set of genes encoding chemokines (*CCL2*, *CCL20*, *CXCL8*, *CXCL12*), chemokine

receptors (*CXCR4*), cytokines (*IL1B*, *CSF-1*, *GM-CSF*, *G-CSF*), matrix degrading enzymes (*UPA*, *MMP9*) and adhesion molecules (L-selectin). All these molecules are involved in proliferation, survival, migration, invasion, metastasis, leukocyte recruitment, homing to lymph nodes.

### 2.1.2 Post Chernobyl -PTC signature

It is well known that there has been a considerable increase in the occurrence of PTCs after the Chernobyl power plant explosion, particularly in those patients who were children or adolescents at the time of exposure (Baverstock et al., 1992). Four transcriptomic studies comparing radiation-induced and sporadic thyroid cancer have been reported.

The first analysis of gene expression profiling compared sporadic and post-Chernobyl PTC, and autonomous adenomas were used as controls. Unsupervised clustering of this data did not distinguish between the post-Chernobyl and sporadic PTC, but separated both cancers from adenomas (Detours et al., 2005). A limit of this work was the low number of investigated genes (2400), thus the authors extended the study covering more genes and by studying more patients. In conclusion, also the latter analysis confirmed that post-Chernobyl and sporadic PTC had similar overall gene expression profiles, indicating that they both represent the same disease. However, subtle differences between these two groups in the expression of 118 genes, involved in response to H<sub>2</sub>O<sub>2</sub>, radiation and homologous recombination were observed. This suggests that different susceptibility profiles distinguish sporadic and radiation-induced PTC (Detours et al., 2007).

A third study by Port *et al.* (Port et al., 2007) found seven genes (*SFRP1*, *MMPI*, *ESM1*, *KRTAP2-1*, *COL13A1*, *BAALC* and *PAGE1*) completely discriminating post-Chernobyl from sporadic PTC. Moreover, six proteins (*NTRK1*, *MMPI*, *MMP9*, *MMP13*, *cathepsins W and X*) were found significantly overexpressed in post-Chernobyl PTCs. In the same samples, authors observed a marked down-regulation of the genes coding for



immunoglobulins suggesting the existence of a weakened immune defense (Port et al., 2007).

A recent study (Stein et al., 2010) investigated copy number and gene expression alteration in 10 post-Chernobyl PTCs and compared their results with sporadic PTC. They identified 141 gene expression changes that were specific to paediatric radiation-induced PTC, and these could be considered potential biomarkers of radiation exposure to the thyroid.

In conclusion, the existence of conflicting results from all these studies, might be attributed to differences in gene expression, complicated by the presence of factors such as age, ethnicity, differences in iodine uptake and heterogeneity of stage- and pathological variant-related factors.

### 2.1.3 FTC signature

The biology of FTC and its gene expression profile is much less known in comparison with PTC.

The majority of gene expression studies have concentrated on the search for gene signatures differentiating FTC from FA. Specific markers identified include *LGALS3*; haemoglobin  $\epsilon$  1(*HBE1*), *CK19* and *TPO*. The accurate classification of benign FA and malignant FTC was also achieved by using the combination of the, *CCND2*, *PCSK2* and *PLAB*, genes enabling a resulting sensitivity of 100% and 94% specificity (Weber et al., 2005). This combination was also able to distinguish the follicular variant of PTC.

Aldred *et al.* (Aldred et al., 2004) reported that PTC and FTC show distinctly different microarray expression profiles and can be distinguished by a minimum of the following 5 genes, *CITED1*, *CAV1*, *CAV2*, *IGFBP6* and *CLDN10*.

Borup *et al.* (Borup et al., 2010) performing global expression profiling of FTC found expression changes involved in DNA replication and mitosis, loss of growth arrest and proapoptotic factors.

Few studies were addressed to assessing whether the various FTC-associated genetic lesions could generate different and specific gene expression patterns.

FA and FTC are equally affected by *RAS* point mutations, for this reason, *RAS* mutations are considered an early event in follicular neoplasia. Few studies analysed the *RAS*-related signature of FTC. The impact of *RAS* mutation on the gene expression of thyroid cells derives from studies of FRTL-5 rat thyroid epithelial cells, infected with the Kirsten murine sarcoma virus carrying the *v-Ki-Ras* oncogene, and from a panel of thyroid cell lines (Visconti et al., 2007). From this study, *Annexin A2*, *RALA* (v-ral simian leukemia viral oncogene homolog A) were found upregulated, whereas dual-specificity phosphatase 1 (*DUSP1*) and small cell lung carcinoma cluster 4 antigen (*CD24*) were downregulated.

The gene signature of the *PAX8/PPAR $\gamma$*  rearrangement, the other genetic lesion associated with FTC, has also been studied. Lacroix *et al.* (Lacroix et al., 2005) revealed a pattern of 93 genes that discriminated FTCs, carrying or not this translocation (examples include *angiopoietin-like 4*, and *aquaporin 7*), but no differences in the expression of thyroid specific genes were noted.

Giordano *et al.* (Giordano et al., 2006) reported that the presence of this balanced translocation is associated with a specific gene expression signature composed of known PPAR target genes, involved in fatty acid and carbohydrate metabolism.

#### 2.1.4 PDTC and ATC signatures

As already reported, PDTC and ATC could arise *de-novo* from thyrocyte or from de-differentiation of DTC. It is agreed that PDTC represents an intermediated form between differentiated and undifferentiated tumours.

Fluge *et al.* (Fluge et al., 2006) analysed the gene expression profiles of PTC and PDTC, including tumours with extensive local invasion or distant metastases. *CITED1*, fibronectin, growth/differentiation factor 15, potassium inwardly rectifying channel

(*KCNJ2*), glutaminyl peptide cyclotransferase, *WNT7A* and dipeptidyl peptidase IV were found overexpressed in carcinomas of both the aggressive and classical PTC group. The growth factor homologue *Nel-like 2*, dual specificity phosphatase 5, the serine protease kallikrein 10, the tight junctions genes *claudin 1* and *16* were up regulated only in PTC, which may be consistent with altered cell polarity frequently found in the differentiated PTC. The aggressive, poorly differentiated PTC group was characterized by the up-regulation of genes involved in cell proliferation, e.g. *CDC2*, *CDC7* and topoisomerase II $\alpha$ , ubiquitin conjugating enzyme E2C, and by the up regulation of genes encoding extracellular matrix proteins such as seprase, extracellular matrix protein 1 and several collagens.

Montero-Conde *et al.* (Montero-Conde et al., 2008) compared the gene expression profiles of ATC and PDTC versus well-differentiated tumour samples. Transcriptome comparison of the differentiated and well differentiated tumours identified a large number of overexpressed genes, belonging to MAPK signalling and TGF- $\beta$  pathway, focal adhesion and cell motility, cell cycle and chemokines. They also found a prognosis signature that recognized ATC and PDTC, but also recurrent and metastatic well DTC.

Salvatore *et al.* (Salvatore et al., 2007) presented a gene expression signature of ATC characterized by the upregulation of genes involved in cell cycle progression and chromosome segregation. They stressed the importance of the Polo-like kinase 1 (PLK1) protein for ATC cell proliferation and cell survival in contrast to normal thyroid cells.

Ito *et al.* (Ito et al., 2009) reported high expression of the S100 calcium-binding protein S100A8 and S100A9 in ATC but a lack of these proteins in well differentiated thyroid tumors. ATC are also characterized by the loss of the pleomorphic adenoma gene-like 1 (*PLAGL1*) (Rodrigues et al., 2007b) and by the downregulation of epithelial cell adhesion molecule (EpCAM), which, on the contrary, are expressed in well DTC and PDTC (Ensinger et al., 2006).

## 2.2 miRNA profiling in thyroid cancer

MiRNAs are small non-coding RNAs of approximately 21-25 nucleotides that negatively regulate gene expression at both the transcriptional and post-translational levels. Several studies have shown the deregulation of miRNAs expression in human TC and functional studies support a critical role of miRNAs in thyroid carcinoma development.

A study analysing the miRNA genome-wide expression profile in human PTC has reported an aberrant miRNAs expression profile that clearly separates PTC from normal tissue (He et al., 2005; Pallante et al., 2006). In particular, a set of seven miRNAs (*miR-221*, *-222*, *-146*, *-21*, *-155*, *-181a* and *181b*) was identified.

He *et al.* (He et al., 2005) observed the overexpression of a small set of miRNAs (*miR221*, *222*, *147b*) in PTC compared to normal thyroid tissue that acted efficiently as class predictors. Interestingly, *miR-221* expression was not only up-regulated in PTC tumours, but also showed a clear-cut variation in the unaffected thyroid tissue of the same patients, suggesting that the unaffected normal thyroid tissue adjacent to tumours may harbour genetic changes before the appearance of morphological malignancy. Overexpression of *miR221* and *miR222* was also identified by Pallante *et al.* in fine needle aspiration biopsies (FNAs) of PTC. Further functional studies have determined that *miR221* and *miR222* negatively regulate *p27kip1*, an inhibitor of cell cycle progression and *p27kip1* (Visone et al., 2007b), and *c-KIT* (He et al., 2005). Other studies have shown that *miR-221* can also target *CDKN1C/p57*, a gene that has a critical role in the cell cycle control (Fornari et al., 2008). This evidence suggests that the upregulation of *miR221/222* significantly modifies the cell cycle of thyroid cells, and, when associated with a genetic lesion affecting the MAPK pathway, could lead to the malignant phenotype.

*MiR146* represents one of the most upregulated miRNAs in PTCs. Jazdzewski *et al.* (Jazdzewski et al., 2008) showed that a common polymorphism in *pre-miR-146a*, affecting the amount of mature miRNAs, also contributes to the genetic predisposition to PTC, and plays a role in tumorigenesis through somatic mutation. Preliminary evidence suggests that

these effects are mediated through target genes whose expression is affected by the SNP status, such as NF- $\kappa$ B dependent genes. Moreover, *miR146b* was proposed as a potential marker for diagnosis since it is overexpressed in PTC but not in FTC, FA and hyperplasia (HP). (Chen et al., 2008)

Even though most of the studies conducted on miR expression in thyroid cancer have focused on PTC, recently several papers have also reported miR deregulations in FTC. Nikiforova *et al.* (Nikiforova et al., 2008) found a different signature associated with FA and FTC both in conventional variants and in oncocytic tumours. The most upregulated miRNAs in FTC were *miR-187*, *-224*, *-155*, *-222* and *-221*, whereas the most highly upregulated in conventional FA were *miR-339*, *-224*, *-205*, *-210*, *-190*, *-328* and *-342*. It has also been shown that oncocytic tumours display a peculiar set of upregulated miRNAs that are distinct from other follicular tumours. In particular the authors showed that a set of 7 miRNAs can be used to distinguish hyperplastic nodules from thyroid tumours in thyroid FNA samples (Nikiforova et al., 2008). Weber *et al.* (Weber et al., 2006) compared the miRNA expression of FTC and FA cases and identified overexpression in FTC of a small set of miR involved in cell proliferation and apoptosis.

With respect to ATC, a significant downregulation of *miR-30d*, *-125b*, *-26a* and *-30a-5p* has been described (Visone et al., 2007a). Recent results report a role of *miR-30a* in regulating *Beclin 1*, a key autophagy-promoting gene (Zhu et al., 2009). Another study revealed that *miR-21*, *-146b*, *-221* and *-222* were overexpressed in ATC. *miR-26a*, *-138*, *-219* and *-34* were found to be downregulated (Mitomo et al., 2008). These results suggest that the loss of *miR-138* expression may partially contribute to the gain of hTERT protein expression in ATC cells (Mitomo et al., 2008).

### ***2.3 Gene silencing by promoter methylation in thyroid cancer***

As shown in other human cancers, methylation-mediated gene silencing is an important mechanism in thyroid tumourigenesis (Xing, 2007b). Aberrant methylation of a

large number of tumour suppressor and thyroid-specific genes in TCs has been detected by several groups. Methylation of tumour suppressor genes, including those for tissue inhibitor of metalloproteinase-3 (*TIMP3*), death-associated protein kinase (*DAPK*), *SLC5A8*, and retinoid acid receptor-beta-2 (*RARβ2*), was found to be linked with tumour aggressiveness and *BRAF* mutation in PTC (Hu et al., 2006).

An association of aberrant methylation of DNA repair genes, particularly the *hMLH1* gene, with *BRAF* mutation and aggressiveness of PTC was recently demonstrated, suggesting a role for *hMLH1* silencing in *BRAF* mutation-promoted thyroid tumourigenesis (Guan et al., 2008).

Another gene silenced through this epigenetic mechanism is *PTEN*, a negative regulator of the PI3K/AKT pathway, which was found to be progressively increased from benign thyroid FA to FTC and to aggressive ATC (Hou et al., 2008).

The expression of thyroid-specific molecules, such as TSHR, NIS, TPO, Tg, and pendrin, is often lost in TC resulting in the impairment or loss of the ability of TC cells to concentrate radioiodine. Aberrant methylation of these thyroid specific genes provides an explanation for their commonly seen silencing in TC. In particular, the *TSHR* gene was silenced through the *BRAF* mutation promoted MAPK pathway signalling, as this event was partially reversible by MAPK inhibitors (Xing, 2007c). This suggests that the functional disruption of this important gene through epigenetic methylation can be directly linked to the aberrant activation of a major signalling pathway in TC.

The following tables summarize the most important gene expression studies in the thyroid cancer field. In particular, signatures related to the different histotypes and differentially expressed genes as potential prognostic and diagnostic biomarkers are reported.

Table 2.1 Gene expression profiles in PTC compared with normal thyroid tissues

	GENES UP-REGULATED	GENES DOWN-REGULATED	PUTATIVE MARKERS	REMARKS
<i>Gene expression signatures</i>				
	coding for cell cycle, adhesion and extracellular matrix proteins (i.e. <i>FN1, MET, DPP4, SERPINA1, KRT19, LGALS3, CITED1, ADORA1, SCEL, ODZ, DUSP6, TIMP1, LAMB3, MDK, MUC1</i> )	coding for tumour suppressors, thyroid function-related proteins, fatty-acid binding proteins: (i.e. <i>TPO, DIO1, DIO2, NIS, GAS1, CDCL1, BCL2, FABP4, CRABP1, APOD</i> )	<i>MET, LGALS3, FN1, CITED1 (D)</i>	D: diagnostic; P: prognostic
Huang et al., 2001 <sup>1</sup>				
Finley et al., 2004 <sup>2</sup>	<i>Adrenomedullin, TROP-2, MET, NRP2</i>	<i>Trefoil factor</i>		
Wreesmann et al., 2004 <sup>3</sup>			<i>MUC1 (P)</i>	comparative analysis of indolent conventional cPTC and tall-cell variant PT (aggressive morphological variant)
Jarzab et al., 2005 <sup>4</sup>	<i>DPP4, GJB3, ST14, SERPINA1, LRP4, MET, EVA1, SPURVE, LGALS3, HBB, MKRN2, MRC2, IGSF1, KIAA0830, RXRG, P4HA2, CDH3, IL13RA1, MTMR4</i>			
Vasko et al., 2007 <sup>5</sup>	genes related to EMT-process, TGF-beta, NFkB and integrin pathway, small G protein regulators and <i>CDC42, Vimentin, RUNX2</i>			comparative analysis between the invasive and central front of PTC
<i>Gene expression profiles in relation to mutational status</i>				
Frattini et al., 2004 <sup>6</sup>	69 genes differentially expressed, all related to signal transduction pathway, tumour invasion, and angiogenesis			comparison between <i>BRAF</i> -positive and <i>RET</i> -rearranged PTC
Giordano et al., 2005 <sup>7</sup>	genes related to immune response (i.e. <i>TM7SF4, CLECSF2, STAT1, LY75</i> )			similarities in the gene expression profiles of PTC with various mutations <i>BRAF</i> -associated vs <i>RET</i> /PTC associated PTC: 3800 genes differentially expressed
Borrello et al., 2005 <sup>8</sup>	genes involved in inflammation, tumour invasion (chemokines, matrix degrading enzymes and adhesion molecules chemokines (i.e. <i>CCL2, CCL20, CXCL8, CXCL12, CXCR4, IL1B, CSF-1, GM-CSF, G-CSF, UPA, MMP9, L-selectin</i> )			ectopic expression of <i>RET</i> /PTC oncogene in human primary thyrocytes
Melillo et al., 2005 <sup>9</sup>	genes involved in cell proliferation and invasion promotion (i.e. <i>CXCL1, CXCL10</i> )			ectopic expression of <i>RAS, BRAF, RET</i> /PTC oncogenes in thyroid cells
<i>Post- Chernobyl PTC vs sporadic PTC</i>				
Detours et al., 2007, 2008 <sup>10</sup>				118 genes differentially expressed, involved in the differential response to H2O2, gamma-radiation and homologous recombination
Port et al., 2007 <sup>11</sup>	646 genes (some ones related to oxidoreductases, G-proteins and growth factors)	677 genes (some ones coding for immunoglobulin)	<i>SFRP1, MMP1, ESM1, KRTAP2-1, COL13A1, BAALC, PAGE1 (D)</i>	
Stein L et al., 2010 <sup>12</sup>	<i>TESC, PDZRN4, TRAA/TRDa, GABBR2, CA12</i>	<i>PAPSS2, PDLIM3, BEX1, ANK2, SORBS2, PPARGCIA</i>	<i>CAMK2N1, AK1, DHRS3, PDE9A (D)</i>	
<i>miRNA profiles</i>				
He at al., 2005 <sup>13</sup>	<i>miR-221, miR-222, miR-146, miR-21, and miR-181a</i>		<i>miR-221, miR-222, miR-146, miR-21, and miR-181a (D)</i>	
Nikiforova et al., 2008 <sup>14</sup>	<i>miR-187, -221, -222, -224, -146b, -155, -197</i>		<i>miR-187, -221, -222, -224, -146b, -155, -197 (D)</i>	
Pallante et al., 2010 <sup>15</sup>	<i>miR-221, -222, -146, -21, -155, -181a, -181b</i>	<i>miR-1, -191, -486, -451</i>	<i>miR-221, -222, -181b (D)</i>	
Yip et al., 2011 <sup>16</sup>	<i>miR-146b, miR-221, miR-222, miR-155, miR-31</i>	<i>miR-1, miR-34b, miR-130b, miR-138</i>	<i>miR-146b (targeting MET) in BRAF-positive tumours (P)</i>	comparison between aggressive and non aggressive PTC
<i>DNA methylation signatures</i>				
Hu et al., 2006 <sup>17</sup>				Genes frequently hypermethylated
Smith et al., 2007 <sup>18</sup>				<i>TIMP3, DAPK, SLCSA8, RARb2, TSHR, ECAD, NIS-L, ATM, DAPK</i>
Guan et al., 2008 <sup>19</sup>				DNA repair genes (i.e. <i>hMLH1</i> gene)

1(Huang et al., 2001a); 2 (Finley et al., 2004a); 3 (Wreesmann et al., 2004); 4 (Jarzab et al., 2005); 5 (Vasko et al., 2007); 6 (Frattini et al., 2004); 7 (Giordano et al., 2005); 8 (Borrello et al., 2005); 9 (Melillo et al., 2005); 10 (Detours et al., 2007; Detours et al., 2008); 11 (Port et al., 2007); 12 (Stein et al., 2010); 13 (He et al., 2005); 14 (Nikiforova et al., 2008); 15 (Pallante et al., 2010); 16 (Yip et al., 2011); 17 (Hu et al., 2006); 18 (Smith et al., 2007); 19 (Guan et al., 2008)

Table 2.2 Gene expression profiles in PTC compared with FTC tumours

	GENES UP-REGULATED	GENES DOWN-REGULATED	PUTATIVE MARKERS	REMARKS
Aldred et al., 2004 <sup>20</sup>	CITED1, CLDN10, IGFBP6		D: diagnostic; P: prognostic CITED1, CAV1, CAV2, IGFBP6, CLDN10 (D)	

20 (Aldred et al., 2004)

Table 2.3 Gene expression profiles in FTC compared with normal thyroid tissues

	GENES UP-REGULATED	GENES DOWN-REGULATED	PUTATIVE MARKERS	REMARKS
Barden et al., 2003 <sup>21</sup>	ADM, GPC1, TGFA, MET, IGFBP3	DIO1, CREM, FBLN5, MT1	D: diagnostic; P: prognostic	
Cerutti et al., 2004 <sup>22</sup>			DDIT3, ARG2, ITM1, C1orf24 (D)	
Weber et al., 2005 <sup>23</sup>			CCND2, PCSK2, PLAB (D)	
Foukakis et al., 2007 <sup>24</sup>	TERT, TFF3, PPARG, CITED1, EGR2		TERT, TFF3 (P)	
Visconti et al., 2007 <sup>25</sup>	Annexin A2, RALA	DUSP1, CD24		Ras-related signature
Lacroix et al., 2005 <sup>26</sup>	angiotensin-like 4, aquaporin 7			PAX8/PPARgamma-related signature
Giordano et al., 2006 <sup>27</sup>	genes involved in fatty acid metabolism, amino acid and carbohydrate metabolism, miR-101, miR-30A-3P, miR-200A, miR-199A			PAX8/PPARgamma-related signature

21 (Barden et al., 2003); 22 (Cerutti et al., 2004); 23(Weber et al., 2005); 24 (Foukakis et al., 2007); 25 (Visconti et al., 2007); 26 (Lacroix et al., 2005); 27 (Giordano et al., 2006).

Table 2.4 Gene expression profiles in ATC compared with normal thyroid tissues

	GENES UP-REGULATED	GENES DOWN-REGULATED	PUTATIVE MARKERS	REMARKS
Salvatore et al., 2007 <sup>28</sup>	genes involved in the regulation of cell cycle progression and chromosome segregation		D: diagnostic; P: prognostic	
Montero-Conde et al., 2008 <sup>29</sup>	genes belonging to MAPKinase and TGFbeta signalling pathway, focal adhesion and cell motility, activation of actin polymerization and cell cycle		23 genes (I.e. ANLN, BIRC5, RRM2, PDK2, PPAP2B) (P)	

28 (Salvatore et al., 2007); 29 (Montero-Conde et al., 2008).



Table 2.5 Overview of the most relevant gene expression studies of malignant thyroid tumours

	Contribution of the study to the identification of:
Mazzanti et al., 2004 <sup>30</sup>	10 and 6 gene model as diagnostic tool for thyroid tumours
Finley et al., 2004 <sup>31</sup>	gene expression profiles capable of differentiating aggressive thyroid carcinomas from non-aggressive ones
Zou et al., 2004 <sup>32</sup>	metastasis-associated genes ( <i>MET, ezrin, integrin, motility related protein 1, cadherin P, NEDD5, S100A4</i> )
Kebebew et al., 2005, <sup>33</sup>	cell cycle regulatory and angiogenesis-modulating genes (i.e. <i>ANGPT2, TIMP1, ECM1, TMPRSS4</i> ) as diagnostic and prognostic markers
Griffith et al., 2006 <sup>34</sup>	<i>MET, TFF3, SERPINA1, TIMP1, FN1 and TPO, TGFA, QPCT, CRABP1, FCGBP, EP58, PROS1</i> as diagnostic and prognostic markers
Prasad et al., 2008 <sup>35</sup>	overexpressed genes ( <i>HMG2, LRRK2, PLG1, DPP4, CDH3, CEACAM6, PRSS3, SPOCK1, PDE5A</i> )
Nikolova et al., 2008 <sup>36</sup>	<i>RGS4</i> gene as diagnostic tumour marker and putative therapeutic target
Ducena et al., 2011 <sup>37</sup>	multiplex biomarker and diagnostic model based on 6 genes ( <i>LGLS3, BIRC5, TFF3, CCND1, MET, CITED1</i> )
Vriens MR et al., 2011 <sup>38</sup>	4 miRs ( <i>miR-100, miR125b, miR-138, and miR-768-3b</i> ) as markers for diagnosing thyroid cancer

30 (Mazzanti et al., 2004); 31 (Finley et al., 2004b); 32 (Zou et al., 2004); 33 (Kebebew et al., 2005a; Kebebew et al., 2005b); 34 (Griffith et al., 2006); 36 (Nikolova et al., 2008); 37 (Ducena et al., 2011); 38 (Vriens et al., 2012).

2.4 Conclusions of gene expression studies

Microarray technology has become a powerful tool to analyze the gene expression of tens of thousands of genes simultaneously. In general, microarray investigations in TC are focused on two main aims: first, understanding of the molecular aetiology of thyroid neoplasia and second, identification of genetic markers that could improve pre-operative differential diagnosis. These studies have been performed in order to bypass the current limitations in the histological and molecular classification of thyroid tumours.

An additional level of complexity in gene expression profiling is related to the fact that thyroid tumours consist of neoplastic cells intermingled irregularly with normal (e.g. epithelial cells, connective tissue and endothelium) and reactive cells (e.g. stromal and immune) cells. All these components might represent possible bias for gene expression profiles. Despite this, many studies identified promising classifiers that are able to differentiate between benign and malignant tumours in microarray analysis.

Although there are several problems that still remain to be resolved (e.g. investigations on larger numbers of tumours and the development of technology to enable accurate analyses from FNA samples), gene expression profiling represents a potentially invaluable means to develop panels of informative robust biomarkers to facilitate diagnosis, prognosis and disease management of TC.

## *Aim of the thesis*

Global gene expression analyses have contributed to the dissection of thyroid tumour pathogenesis and to the identification of tumour suppressor genes and new candidate therapeutic targets. Despite the numerous gene expression studies, there are few data addressing the role of differentially expressed genes in the pathogenesis of thyroid tumours.

Using the cDNA microarray platform, our laboratory has previously determined the gene expression profile of four different histotypes (PTC, FTC, follicular adenomas, normal thyroid tissues) and levels were compared with each other by means of a class comparison analysis. This study allowed us to identify 393 genes regulated in the PTC versus normal thyroid. Among the genes differentially expressed in PTC detected by our analysis, we selected *Tissue Inhibitor of Metalloproteases-3 (TIMP-3)*, *S100/calgizzarin* and *CITED1(CBP/p300-Interacting Transactivators with glutamic acid (E) and aspartic acid (D) rich C-terminal domain 1)* genes for which a role in the pathogenesis of PTC was also suggested by recently published gene and protein expression data.

The aim of this thesis was the dissection of the role of these selected genes whose expression was found differentially regulated in PTC with respect to normal thyroid. The strategy involved meta-analysis of public gene expression data, as well as functional studies, based on PTC-derived cell lines, aimed at the dissection of the effect of their expression modulation on tumour cell phenotype.

A large part of the work was devoted to studying TIMP3 and S100A11. These sections have been well developed, whereas CITED1 studies were presented at an early stage. The thesis also includes a brief report of a study on *Insulin-like growth factor-binding protein 7 (IGFBP7)*, another gene found downregulated in PTC, in which the candidate collaborated.



### 3.1 Microarray data sets and statistical analysis

The expression of *TIMP3* and *S100A11* was examined on microarray data sets containing normal thyroid tissue and PTC. One data set, generated in our laboratory, contains the expression profile data of 59 thyroid samples collected at the Department of Pathology of our Institute. All the patients gave their written informed consent. Sample collection includes: 9 normal thyroid tissues and 32 PTC. The PTC case collection consists of 25 classical variant and 7 tall cell (TC) variants; 12 samples carry the *BRAFV600E* mutation, 7 samples carry *RET/PTC* rearrangements, 2 samples carry *TRK* rearrangements; for the remaining 11 samples none of the above genetic lesions was detected. The *cDNA* microarray used in this study contains 4451 unique clones selected from the Human sequence verified I.M.A.G.E. clone collection (Research Genetics/Invitrogen, Carlsbad, CA, USA) along with plant genes, printing controls (water/DMSO) and spike genes (Amersham Bioscience, Amersham, UK) added as internal controls. Each *cDNA* fragment was PCR-amplified and spotted in triplicate on type 7 star slides (Amersham Bioscience, Amersham, UK). The procedures of RNA isolation, probe labelling, sample hybridization and scanning were performed as described by De Cecco *et al.* (De Cecco *et al.*, 2004). Supervised analysis (class comparison and hierarchical clustering) was performed using BRB ArrayTool v.3.3\_Beta1 (<http://linus.nci.nih.gov/BRB-ArrayTools.html>).

The expression levels of *TIMP3*, *S100A11* and *CITED1* genes in all the tissue samples hybridized on the array were measured as log ratio between the expression level of the specimens and that of the reference (a total of 10 human cell lines of different origins). Genes showing a positive log ratio value (i.e. more expressed in the thyroid sample than in the reference) are called up-regulated; those with a negative log ratio value are called down-regulated.

The other data sets are publicly available and are all derived from experiments using HG-U133 series microarrays (Affymetrix, Santa Clara, CA, USA). These data derive from:

- a) 51 PTC samples including 26 classical types, 10 TC and 4 normal thyroid tissues. Of the tumour samples, 26 carried the *BRAFV600E* mutation, 9 *RET/PTC* rearrangements, 5 *RAS* mutation, 10 were negative for these alterations and 1 was not investigated (HG-U133A) (Giordano et al., 2005));
- b) Paired PTC and unaffected thyroid tissue samples from 9 patients (HG U133 Plus 2.0) (He et al., 2005);
- c) Paired PTC and contralateral thyroid tissue samples from 16 patients (HG U133 Plus 2.0) (Jarzab et al., 2005);
- d) Paired PTC and contralateral thyroid tissue samples from 7 patients (HG U133 Plus 2.0) (Reyes et al., 2006);
- e) Paired PTC and contralateral thyroid tissue samples from 8 patients (HG-U95Av2) (Huang et al., 2001b);
- f) Paired central and invasive region of PTC and normal tissue from 4 patients (HG U133 Plus 2.0) (Vasko et al., 2007).

RMA normalized data were extracted from the NCBI Gene Expression Omnibus database (GSE3467 for the He dataset and GSE6004 for the Vasko dataset) or from the author's website (Giordano and Jarzab dataset). The mean RMA log2 intensity values of the four probesets specific for TIMP3 (201147\_s\_at; 201148\_s\_at; 201149\_s\_at and 201150\_s\_at in HGU133-A and HG-U133Plus2 platforms) was considered. For S100A11 the following probesets 200660\_at in HG-U133Plus2 platforms and 38138\_at in Affymetrix HG-U95Av2 platform were considered.

Statistical analysis and graphs were generated using GraphPad Prism version 5.0. Comparison between two groups was performed, for unmatched samples, by the non parametric Mann-Whitney and for matched samples by Wilcoxon signed pairs test. When three or more groups were considered, ANOVA followed by post tests was performed.  $p < 0.05$  was considered significant.

3.2 Molecular biology

3.2.1 RNA extraction and RT-PCR

RNA extraction was performed using TRIZOL reagent (Invitrogen, Carlsbad, CA, USA). One µg of RNA was retro-transcribed using SuperscriptIII (Invitrogen, Carlsbad, CA, USA). Details of RT-PCR conditions are reported in table 3.1.

PCR products were separated on 2% agarose gels, stained with ethidium bromide and visualized under UV transillumination.

Table: 3.1 Details of RT-PCR conditions for *TIMP3*, *S100A11*, *CITED1* and *GAPDH* genes

Template	Primers	Fragment lenght	PCR condition
<i>TIMP3</i>	5'-CTGACAGGTCGCGTCTATGA-3' 5'-GGCGTAGTGTTTGGACTGGT-3'	240 bp	95° 7' + ( 95° 1' + 56° 30" + 72° 30") x 38 + 72° 5'
<i>S100A11</i>	5'-GTCCTGATTGCTGTCTTCC-3' 5'-ACCAGGGTCCTTCTGGTTCT-3'	130 bp	95° 7' + ( 95° 1' + 56° 30" + 72° 30") x 33 + 72° 5'
<i>CITED1</i>	5'-TCACTTGCTGGCTAGTATGCAG-3' 5'-TGGGTCCGAATCGATGATAGCAG-3'	190 bp	95° 7' + ( 95° 1' + 56° 40" + 72° 40") x 33 + 72° 5'
<i>GAPDH</i>	5'-ACCATCTTCCCAGGAGCGAGAT-3' 5'-GGCAGAGATGATGACCCTTT-3'	142 bp	94° 2' + ( 94° 1' + 54° 1' + 72° 1' ) x 35 + 72° 2'

3.2.3 Real-Time RT-PCR

For each sample, 20 ng of retrotranscribed RNA were amplified in PCR reactions carried out in triplicate on an ABI PRISM 7900 using TaqMan gene expression assays (Applied Biosystem, Foster City, CA). Hs00271612\_A1 was used for S100A11 expression; human HPRT (HPRT-Hs99999909\_A1) was used as housekeeping gene for the normalization among samples. Data analysis was performed using the SDS (Sequence Detection System) 2.2.2 software.

3.2.4 Construction of expression vectors

*TIMP3* vector:

The *TIMP3* cDNA was isolated by RT-PCR from a human placenta cDNA library using the following primers: 5'-CCGGA TTCGGCGGCAGCGGCAATGA-3' and 5'-CGCGGATCCGGGGTCTGTGGCATTGATGATGCTT-3', containing the *EcoRI* and the

*Bam*HI restriction sites (bold), respectively. The 650 nucleotides PCR product was digested with *Eco*RI and *Bam*HI endonucleases and inserted into the pcDNA3.1/mycHis(-) A vector (Invitrogen, Carlsbad, USA) carrying compatible ends. The resulting construct carries the *TIMP3* cDNA in the sense orientation with respect to the CMV promoter present in the vector and encodes the TIMP3-myc fusion protein. This construct was used for NIM1 cells transfection.

#### *S100A11* vectors:

**pcDNA3-S100A11myc:** *S100A11* cDNA was isolated by RT-PCR from a human placenta cDNA library using the following primers: 5'-CCGGAATTCCAAGCTCCAACATGGCAAAAATCTCC-3' and 5'-CGCGGATCCGGTCCGCTTCTGGGAAGGGACAGC-3' containing the *Eco*RI and the *Bam*HI restriction sites (bold), respectively. The 325 nucleotides PCR product was digested with *Eco*RI and *Bam*HI endonucleases and inserted into the pcDNA3.1/mycHis(-)A vector carrying compatible ends. The resulting construct carries the *S100A11* cDNA in the sense orientation with respect to the CMV promoter present in the vector and encodes the S100A11-myc fusion protein. This construct was used for K1 cells transfection.

**pIRESneo-S100A11myc:** *S100A11* cDNA was amplified from pcDNA3-S100A11myc using primers 5'-GGAATCGATATCCAAGCTCCAACATGGCAAAAATCTCC-3' and 5'-GGAATCGATATCTAGAAGGCACAGTCGAGG-3' containing the *Eco*RV restriction sites (bold). The 500 bp PCR product (containing *S100A11* cDNA in frame with myc/hys epitope derived from pcDNA3.myc) was inserted into pIRESneo vector (Clontech Laboratories, Mountain View, CA, USA) (digested with *Eco*RV) that allows high level expression of the gene of interest and the neomycin resistance gene from the same bicistronic mRNA transcript. Sense orientation with respect to the CMV promoter present in the vector was verified by *Bam*HI digestion. This construct was used for transfection experiments in NIH3T3 cells (Focus Forming Assay).

### CITED1-vectors:

**pcDNA3-CITED1myc:** *CITED1* cDNA was isolated by RT-PCR from a human placenta cDNA library using the following primers: 5'-CCGGAATTCTGCCAAGGCTCTGAAATG-3' and 5'-CGCGGATCCGCAGCTAGATGGAAAGTCCGCAGT-3' containing the *EcoRI* and the *BamHI* restriction sites (bold), respectively. The 600 bp nucleotides PCR product was digested with *EcoRI* and *BamHI* endonucleases and inserted into the pcDNA3.1/mycHis(-)A vector carrying compatible ends. The resulting construct carries the *CITED1* cDNA in the sense orientation with respect to the CMV promoter present in the vector and encodes the CITED1-myc fusion protein.

**pIRESneo-CITED1myc:** *CITED1* cDNA was amplified from pcDNA3-CITED1myc using primers 5'-GGAATCGATATCTGCCAAGGCTCTGAAATGCCA-3' and 5'-GGAATCGATATCTAGAAGGCACAGTCGAGG-3' containing the *EcoRV* restriction site (bold). The 750 bp PCR product (containing *CITED1* cDNA in frame with myc/hys epitope derived from pcDNA3.myc) was inserted into pIRES neo vector (digested with *EcoRV*) that allows high level expression of the gene of interest and the Neomycin resistance gene from the same bicistronic mRNA transcript. Sense orientation with respect to the CMV promoter present in the vector was verified by *BamHI* digestion.

Both of these constructs were used for HEK293T cells transfection.

### TRK-T3 vector

*TRK-T3* cDNA was released from pCRT3 plasmid (Greco et al., 1995) by digestion with *BamHI* and *NotI* restriction enzymes and inserted into pIREShygro carrying compatible ends. This construct was used for transfection experiments in NIH3T3 cells (Focus Forming Assay).



### 3.3 Cell biology

#### 3.3.1 Cell lines

TPC1, NIM1, BCPAP and K1 cell lines, derived from PTC; WRO82-1 cell line, derived from FTC; FRO81-2, FB1, BHT101, 8505C cell lines, derived from ATC and the Human Embryonic Kidney (HEK) 293T cells were cultured at 37°C in a 5% CO<sub>2</sub> humidified atmosphere. With the exception of K1 cell line, grown in DMEM:HAM'S F12:MCDB 105 (2:1:1) containing 2mM glutamine and 10% fetal calf serum (FCS), and Nthy-ori 3-1, grown in RPMI medium (Lonza, Basel, Switzerland), the other cell lines were maintained in DMEM medium containing 10% FCS, 2mM glutamine and 100U/ml penicillin/streptomycin. Primary thyrocyte cultures were established and maintained in nutrient mixture Ham's F12 medium (custom made by Invitrogen, Paisley, UK) containing 5% calf serum and bovine hypothalamus and pituitary extracts, as previously described (Curcio et al., 1994). Information regarding mutational status and *in vivo* tumourigenicity of thyroid cell lines is provided in table 3.2 .

Mouse NIH3T3 fibroblasts were cultured in DMEM with 10% of calf serum (Colorado Company, CO) in a 10% CO<sub>2</sub> humidified atmosphere.

Conditioned media were obtained by incubating subconfluent cultures in serum free medium for 24h.

Table 3.2 Mutational status of thyroid cell lines

Cell line	Hystological type	mutational status*				
		RET	HRAS	BRAF	PI3K	TP53
NThy-ori 3-1	normal human thyrocytes**					
TPC1	PTC	RET/PTC1	His27His	WT		
K1	PTC	WT	His27His	V600E/WT	Glu542Lys	Arg213Arg
NIM1	PTC			V600E/WT***		
BCPAP	PTC	WT		V600E		Asp259Tyr
WRO82-1	FTC			V600E/WT		Pro23Leu
8505C	ATC	WT	His27His	V600E		Arg248Gln
BHT101	ATC					
FB1	ATC					
FRO81-2	ATC	WT		V600E/WT		

(\* from Pilli *et al.* 2009, \*\* SV40 Large T antigene, \*\*\*our unpublished results)

*In vivo* tumourigenicity of thyroid cell line

cell line	Tumourigenicity	Reference
TPC1	no	our unpublished results
K1	yes	Ferrario et al, Laboratory Investigation, 2008, 88(5):474-81
NIM1	yes	Vizioli et al, Oncogene, 2010, 29(26):3835-44
BCPAP	yes	Fabien et al Cancer, 1994, 73(8):2206-12)
WRO82-1	yes	Estour et al Virchows Arch B Cell Pathol Incl Mol Pathol 1989 57(3):167-74
8505C	yes	Nucera et al Thyroid, 2009, 19 (10): 1077-84
BHT101	yes	Palyi et al Virchows Arch B Cell Pathol Incl Mol Pathol, 1993, 63(4):263-9
FB1	yes	Fiore et al, J. Clin. Endocrinol. Metab., 1997, 82: 4094-4100

3.3.2 Cell treatments

- The recombinant TIMP3 protein (R&D Systems, Minneapolis, MN, USA) (50 nM) was applied to NIM1 cells;
- 5'-Aza-2'-deoxycytidine (Sigma Aldrich, St. Louis, MO, USA) ( 5 µM) was applied to NIM1 cells for four days,
- PMA (Sigma Aldrich, St. Louis, MO, USA) (100 ng/ml) was applied to NIM1 cells 5 hours;
- TRAIL (Alexis, San Diego CA, USA) (50ng/ml) was applied to NIM1 cells for 5 hours;
- Ca<sup>2+</sup> (1.5 mM and 10 mM) was applied to K1 cells for 1, 6, 16 and 24 hours;

- Recombinant EGF protein (PeproTech, London, UK) (20 ng/ml) was applied to K1 cells for 20 minutes, 8 and 24 hours;
- Recombinant TGF- $\beta$  (Peprotech, London, UK) (10ng/ml) was applied to K1 cells for 1 and 8 hours.

### 3.3.3 Cell transfection

- For TIMP3 studies, transient and stable transfections of NIM1 cells were performed using Lipofectamine LTX (Invitrogen, Carlsbad, CA). Cells ( $4 \times 10^5$ ) were seeded in 60mm dishes and transfected with 2  $\mu$ g of plasmid DNA and 5  $\mu$ l of LTX the following day. After 48 hours transfected cells were either harvested and processed, or subjected to G418 (Lifetechnologies, Invitrogen, Carlsbad, CA, USA) selection (400  $\mu$ g/ml). G418-resistant colonies were isolated and propagated in G418-containing medium two weeks later.
- For S100A11 studies, transient transfection in K1 cells was performed using FuGene6 (Roche, Mannheim, Germany) following manufacturer's instructions. Cells ( $1.5 \times 10^5$ ) were seeded in 60mm dishes and transfected with 2  $\mu$ g of plasmid DNA and 5  $\mu$ l of FuGene6 the following day. After 72 hours transfected cells were harvested and processed,
- For CITED1 studies, transient transfection in HEK293T cells was performed with Lipofectamine2000 (Invitrogen, Carlsbad, CA) according to manufacturer's instruction. Cells ( $3 \times 10^5$ ) were seeded in 60mm dishes and transfected with 2  $\mu$ g of plasmid DNA and 5  $\mu$ l of Lipofectamine2000 (Invitrogen, Carlsbad, CA) the following day. After 48 hours transfected cells were harvested and processed.

### 3.3.4 TIMP3 and S100A11 silencing

Transient knock-down of TIMP3 and S100A11 in K1 cells was performed by transfection with ON-TARGET plus SMART pool for human TIMP3 or NON-TARGET

siRNA control (ThermoScientific, Dharmacon Inc, Chicago, IL.) using Lipofectamine RNAiMax (Invitrogen, Carlsbad, CA) following manufacturer's instruction.

Stable S100A11 silencing in K1 cells was performed by transfection of S100-specific shRNA expression pRS vector (OriGene, Rockville, MD, USA). Scrambled shRNA expression pRS vector was used as control. The transfection was carried out using FuGene6 (Roche, Mannheim, Germany) following manufacturer's instructions. After 72 hours, transfected cells were either harvested and processed, or subjected to puromycin (Lifetechnologies, Invitrogen, Carlsbad, CA, USA) selection ( 1  $\mu$ g/ml). Puromycin-resistant colonies were isolated and propagated in Puromycin-containing medium two weeks later.

### 3.3.5 Focus forming assay

The NIH3T3 cells ( $2.5 \times 10^4$ ) were plated in 100mm Petri dishes. The day after cells were transfected by the  $\text{CaPO}_4$  method using 1  $\mu$ g of expression plasmid DNA together with 30  $\mu$ g of mouse carrier DNA. NIH3T3 cells were transfected with: *S100A11* cDNA, cloned into pIRES vector containing the G418-resistant gene and producing a *myc*-tagged protein; *TRK-T3* cDNA, cloned into pIRES vector containing hygromycin-resistant gene. The expression plasmids were transfected alone or in combination. Transfected cells were selected in DMEM supplemented with 10% serum in the presence of antibiotics G418 (500 $\mu$ g/ml), Hygromycin (50  $\mu$ g/ml) (Roche Diagnostics, Indianapolis, IN, USA) to determine the transfection efficiency, and in medium containing 5% serum to determine the transforming activity. After 20 days, G418<sup>R</sup>, Hygro<sup>R</sup>, G418<sup>R</sup>/Hygro<sup>R</sup> foci or colonies were either fixed and Giemsa stained or isolated and propagated for further studies.

### 3.3.6 Cell cycle analysis

Flow cytometry analysis was carried out using FACS Calibur (Becton Dickinson, San Jose, CA, USA). Both adherent and floating cells were harvested, washed twice with

PBS and fixed in cold ethanol (70%) for 24 hours. After two washes with PBS, cells were incubated in PBS containing 1 µg/ml RNase and 50 µg/ml propidium iodide at room temperature for 30 min in the dark. Data were analysed by using Cell Quest software (Becton Dickinson, San Jose, CA, USA).

### *3.3.7 Growth curves*

Growth curves were determined by alamarBlueAssay (Biosource, Nivelles, Belgium). Cells were plated in 96-multiwell (400 cells per well). After adhesion of cells, the alamarBlue reagent was added to the medium at 10% v/v. The fluorescence at  $\lambda = 590$  and 535nm was detected every 24hrs for different days, using a microplate reader (TecanUltra Tecan Trading AG, Switzerland). Data were normalized for values detected at day 1.

### *3.3.8 Colony forming assay*

Cells were plated at different densities (200 cells in 60 mm<sup>2</sup> culture dish for TIMP3 experiment, 2000 cells in 60 mm<sup>2</sup> culture dish for S100A11 experiment) and cultured for different days. Where required, conditioned media were used. Colonies were fixed with methanol and stained with Giemsa (Sigma-Aldrich, St.Louis, MO USA).

### *3.3.9 Cell adhesion assay*

After 24 hours incubation with appropriated conditioned medium, cells ( $3 \times 10^4$  cells/well) were seeded in sextuple in a 96-well plate pre-treated with 30 µg/ml Type IV Collagen (BD Biosciences, Bedford, MA, USA). After 1hr of incubation, non-attached cells were removed by gently washing twice with 100 µl PBS. Attached cells were fixed with 10% buffered formalin solution for 20 minutes at room temperature, followed by staining in 0.2% (w/v) crystal violet for 10 minutes. Stained cells were lysed in 1% SDS

and the intensity of stain was quantified by a spectrometer at the absorbance of 595 nm (TecanUltra Tecan Trading AG, Switzerland).

### *3.3.10 Wound healing assay*

Cells were seeded in 60 mm dishes. At confluence, a scratch was applied with a tip. Plates were washed with PBS, reseeded with complete medium, and returned to the incubator. Pictures were taken at 0, 8 and 24 hours at 10X magnification by using a digital camera system coupled with a microscope (LEICA, DMIRB).

### *3.3.11 Migration and Invasion Assay*

In TIMP3 migration assay, cells were seeded in the upper chamber ( $1.2 \times 10^5$  cells per well) of 24-well Transwell plates equipped with polycarbonate filters (Costar; Corning Incorporated, NY, USA), in serum-free medium. Conditioned media were added to the lower chamber as chemoattractant. After 5 hours incubation at 37°C, filters were cleaned on the upper side with a cotton swab, fixed with 99% ethanol and stained with a 0.4% sulforhodamine B/1% acetic acid solution. Migrated cells were counted under an inverted microscope in six randomly chosen fields. The same procedure was used for invasion assay, except that cells were seeded at  $2.4 \times 10^5$  cells per well in Transwell chambers coated with 12.5 µg of Matrigel /well (BD Biosciences, Bedford, MA, USA), and samples processed after 24 hours incubation. All samples were performed in duplicate.

For NIH3T3 transformed foci, the invasion assay was performed using the QCM™ Cell Invasion Assay (Millipore, Billerica, MA USA) according to manufacturer's instructions. Briefly,  $2 \times 10^5$  cells were allowed to invade through a coated transwell toward 10% FBS for 48 hours. Invaded cells on the bottom of the insert membrane were dissociated from the membrane, subsequently lysed and detected by CyQuant GR® dye. The fluorescence at  $\lambda = 590$  and 535nm was detected using a microplate reader (TecanUltra Tecan Trading AG, Switzerland).

### ***3.3.12 Soft agar assay***

Cells were suspended in 1.5 ml of DMEM medium containing 0.33% agar and 10% FCS, added into a layer of medium containing 0.5% agar and 10% FCS in 60mm dishes, and incubated for 3 weeks. For NIH3T3 cells 5% FCS was used. After staining with p-iodonitrotetrazolium chloride (Sigma Aldrich, St Louis, Mo, USA) the plates were analysed for colony number and size. Pictures were taken at 4X or 10X magnification by using a digital camera system coupled with a microscope (LEICA, DMIRB).

## ***3.4 Biochemical assays and studies***

### ***3.4.1 Western blot analysis***

Proteins were extracted in RIPA modified buffer (20mM Tris-HCl, pH 7.4, 150mM NaCl, 5mM EDTA, 1% NonidetP-40) supplemented with Complete Mini EDTA-free protease Inhibitor Cocktail (Roche, Mannheim, Germany), 1mM Na<sub>3</sub>VO<sub>4</sub> and 1mM PMSF. Cell fractionation was performed using the ProteoExtract Subcellular Proteome Extraction (S-PEK) Kit (Calbiochem, San Diego, CA) according to manufacturer's instructions. Protein and conditioned medium samples were boiled in NuPAGE LDS sample buffer (Invitrogen, Carlsbad, CA, USA) and separated on 4-12% or 10% NuPAGE Novex Gel (Invitrogen, Carlsbad, CA) in MES or MOPS running buffer, respectively. Proteins were transferred into nitrocellulose filters and immunoblotted with the appropriated antibodies listed in Table 3.3. The immunoreactive bands were visualized using horseradish peroxidase-conjugated secondary antibodies followed by enhanced chemiluminescence (GE, Bio-Rad Hercules, CA, USA). The membranes were scanned using the Chemidoc XRS and densitometric analysis was performed by using Quantitative One software (Bio-Rad Hercules, CA, USA).

### 3.4.2 Dot blot analysis

For dot blot, conditioned media were harvested, concentrated by centrifugation at 4000 rpm using AgilentSpin Concentrators (Agilent Technologies Inc, Wilmington, DE, USA), and applied to a nitrocellulose membrane (Hybond™-C Super, GE Healthcare) under vacuum in an immunodot apparatus (Millipore, Bellerica, MA USA). The membrane was blocked for 1 hour with 5% BSA in TBS-0.05% Tween and incubated overnight at 4°C with the appropriated antibodies listed in Table 3.3 .

**Table 3.3:** List of antibodies used for western and dot blot analysis

Akt	Cell Signaling Technology (Beverly MA, USA)
ALCAM	Novocastra (Newcastle, UK)
beta-actin	Sigma-Aldrich (St Louis, Mo, USA);
beta-tubulin	Sigma-Aldrich (St Louis, Mo, USA);
Cleaved PARP	Cell Signaling Technology (Beverly MA, USA)
C-myc (9E10)	Roche (Indianapolis, IN, USA);
Cytokeratin 8/18	Novocastra (Newcastle, UK)
E-cadherin (H-108: sc 7870)	Santa Cruz Biotechnology (Santa Cruz, CA, USA)
EGFR	Cell Signaling Technology (Beverly MA, USA)
ERK 1/2	Sigma-Aldrich (St Louis, Mo, USA);
NBS1	Novus Biologicals (Littleton, CO, USA)
Nucleolin	MBL Medical & Biological Laboratories Co. (Naka-ku Nagoya, Japan)
p21 (C-19)-G	Santa Cruz Biotechnology (Santa Cruz, CA, USA)
pAKT	Cell Signaling Technology (Beverly MA, USA)
phospho-EGFR	NanoTools (Teningen, Germany)
phospho-ERK1/2	Sigma-Aldrich (St Louis, Mo, USA);
phospho-SMAD2	Cell Signaling Technology (Beverly MA, USA)
S100A11 (FL-105)	Santa Cruz Biotechnology (Santa Cruz, CA, USA)
SMAD2/3	Cell Signaling Technology (Beverly MA, USA)
Syndecan-4 5G9	Santa Cruz Biotechnology (Santa Cruz, CA, USA)
TIMP3	Abcam (Cambridge, UK);
TRK (C-14)	Santa Cruz Biotechnology (Santa Cruz, CA, USA)
Vimentin	Novocastra (Newcastle, UK)
Vinculin	Sigma-Aldrich (St Louis, Mo, USA);



### 3.4.3 *TNF- $\alpha$ detection*

TNF- $\alpha$  concentration in conditioned media, produced as described above, was evaluated by a fluorescent bead immunoassay (FlowCytomix™ Kit, Bender MedSystems, Vienna, Austria), according to manufacturer's instructions. The limit of detection of the assay for the TNF- $\alpha$  analyte is 3.2 pg/ml.

## 3.5 *In vivo studies*

Animal studies were reviewed and approved by the Ethics Committee for Animal Experimentation of the Fondazione IRCCS Istituto Nazionale dei Tumori and are in accordance with the guidelines of the UK Coordinating Committee for Cancer Research (U.K.Coordinating Committee on Cancer Research, 1988). Female CD-1 nu/nu mice (8- to 9-weeks old) (Charles River, Calco, Italy) were injected subcutaneously into the left flank. Tumour growth was assessed by evaluating tumour latency, ie days to reach 0.1 g, and by monitoring tumour weight (TW) twice a week. TW was estimated by the formula  $TW(g)=d^2 \times D/2$  where d and D are the shortest and the longest diameters of the tumor, respectively, measured in cm.

### 3.5.1 *Immunohistological studies*

Representative portions of excised tumour xenografts were fixed in 10% neutral buffered formalin, routinely processed and embedded in paraffin blocks. Four  $\mu$ m-thick sections were stained with hematoxylin and eosin (HE) and evaluated under a light microscope to assess the pattern of tumour growth. To establish the extent of tumour angiogenesis, serial sections were immunostained with a primary rat monoclonal antibody against CD31 antigen (clone SZ31, DIA 310 M, Dianova) and positive endothelial outlines identified within the tumour stroma and/or capsule were counted in four randomly selected 200x microscopic fields. To establish the number of histiocytes associated with the tumour

growth, additional serial sections were immunostained with a primary rat monoclonal antibody against F4/80 antigen (clone Cl: A3-1, MCA497G, AbD Serotec) and positive cells were counted in five 400x microscopic fields randomly selected along the tumour edge. Both the immunostains were performed using a standard immunoperoxidase protocol (Vectastain Elite ABC kit, PK-6100, Vector Lab) followed by diaminobenzidine chromogen reaction (Peroxidase substrate kit, DAB, SK-4100, Vector Lab).



## 4.1. Introduction

### 4.1.1. *TIMP3*

The *Tissue Inhibitor of Metalloproteinase-3 (TIMP3)* gene encodes a member of TIMP family molecules that inhibit the proteolytic activity of matrix metalloproteinases (MMPs). TIMP3 is a secreted protein and, unlike other TIMP family members, which after secretion become freely diffusible within the cell microenvironment, binds tightly to the ECM. In addition, TIMP-3 exhibits direct inhibitory activity against several ADAMs including TNF- $\alpha$  convertase (TACE, ADAM-17) (Fata et al., 2001), and this inhibition is crucial for controlling TNF-mediated inflammation (Mohammed et al., 2004). TIMP-3 also inhibits cell shedding of several molecules (L-selectin, syndecans-1 and -4, IL-6 receptor, c-MET) and cleavage of IGF binding proteins-3 and 5 (Fata et al., 2001). TIMP3 also regulates ADAM-mediated activation of the EGF receptor ligands, TGF- $\alpha$ , EGF, amphiregulin and heregulin (Gschwind et al., 2003) and it is able to block MMP-mediated cleavage of laminin-5 (Schenk et al., 2003).

TIMP3 differs from the other MMPs as point mutations in its gene have been linked to Sorsby's fundus dystrophy (SFD), an autosomal dominant inherited retinal degenerative disease that leads to blindness (Yeow et al., 2002).

*TIMP3* silencing through promoter hypermethylation has been associated with poor prognosis in a range of human cancers, and this evidence points to a role of TIMP3 as a tumour suppressor. TIMP3 is frequently hypermethylated in kidney, brain, colon cancer (Bachman et al., 1999), non small cell lung carcinoma (Zochbauer-Muller et al., 2001), pancreatic carcinoma (Ueki et al., 2000) and hepatocellular carcinoma (Yuan et al., 2006). In esophageal and gastric carcinoma *TIMP3* was also found frequently methylated, and the loss or reduction of resulting TIMP3 expression was associated to shorter survival (Gu et al., 2008). Furthermore a recent study by Barski *et al.* (Barski et al., 2010) reported that *TIMP3* downregulation by promoter methylation is associated with a more aggressive, high grade meningioma phenotype.

Conversely, recent studies showed that over expression of *TACE* and *TIMP3* mRNA in head and neck cancer (HNSCC) is associated with tumour development and progression, suggesting that *TIMP3* overexpression is a compensatory mechanism to counterbalance the pathologic increase in TACE sheddase activity (Kornfeld et al., 2011).

Loss of *TIMP3* expression, through loss of heterozygosity on chromosome 22q, is also frequently observed in various cancers, such as secondary glioblastoma (Nakamura et al., 2005) and clear renal cell carcinomas (Masson et al., 2010).

Evidence is emerging that the downregulation of *TIMP3* expression in tumours can be achieved also through deregulation of microRNAs. In fact, *TIMP3* is a target of several microRNAs upregulated in human tumours: 1) *miR21*, involved in glioma invasion (Gabriely et al., 2008) and in ductal adenocarcinoma (Nagao et al., 2012); 2) *miR181b*, induced by TGFbeta and involved in hepatocarcinogenesis (Wang et al., 2010); 3) *HsamiR-191* can target *TIMP3* mRNA and suppress *TIMP3* protein expression in hepatocellular carcinoma (He et al., 2011); 4) *miR221* and *222*, controlled by MET, targeting also *PTEN* and involved in NSCLC and HCC (Gabriely et al., 2008; Garofalo et al., 2009; Wang et al., 2010). A reciprocal relationship between *TIMP3* and *miR-221/222/181b* expression was also observed in primary human breast carcinomas. These miRNAs facilitate growth factor signalling in tamoxifen resistant breast cancer by downregulating *TIMP3* (Lu et al., 2011).

The tumour suppressor role of *TIMP3* is also documented by a large body of data showing its capability to inhibit growth, invasion and metastasis of several cancers (Anand-Apte et al., 1996; Qi et al., 2003). Treatment of human melanoma, lung, prostate and breast cancer cells and xenografts with recombinant *TIMP3* protein reduced cell proliferation, induced caspase-mediated apoptosis, sensitized cells to paclitaxel, reduced tumour growth and metastasis (Mahller et al., 2008). In melanoma cells *TIMP3* is involved in the stabilization of death receptors TNF-RI, FAS and TRAIL-RI on the surface of cells, sensitizing them to apoptosis induced by their ligands (Ahonen et al., 2003). *TIMP3*

promotes apoptosis in non adherent small cell lung carcinoma cells lacking functional death receptor pathway (Kallio et al., 2011).

Anti-tumoural effects of TIMP3 are also ascribed to its anti-angiogenic properties which are based on its ability to block the binding of VEGF to its receptor (Qi et al., 2003). Restoration of TIMP3 expression by different approaches also resulted in the reduction of neovascularization in tumour xenografts of melanoma, neuroblastoma and malignant peripheral nerve sheath tumours (MPNST) (Ahonen et al., 2003; Mahller et al., 2008).

A summary of TIMP3 activities is shown in Figure 4.1.

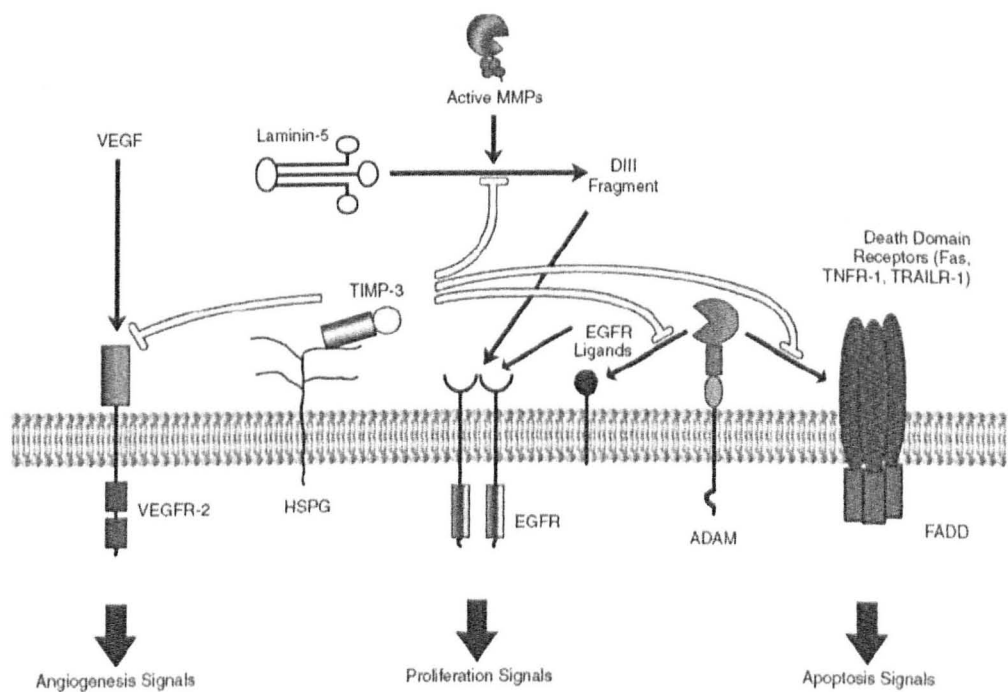


**Figure 4.1 Mechanisms involved in TIMP3 effects on apoptosis, angiogenesis, cell proliferation and migration.** TIMP3 promotes apoptosis by blocking the MMP-mediated shedding of death receptors; it inhibits angiogenesis blocking of VEGF to its receptor; it inhibits migration blocking the MMP-mediated cleavage of laminin-5, and proliferation by inhibiting ADAM-mediated release of EGF receptor ligands (from Edwards, 2004)

#### 4.1.2. *TIMP3* and thyroid cancer

Thyroid tumours show hypermethylation of the *TIMP3* gene (Hoque et al., 2005). In addition, *TIMP3* was identified within a group of tumour suppressor genes (also including *SLC5A8*, *DAPK*, *RARβ2*) which were hypermethylated in a consistent fraction (53%) of PTCs in association with tumour aggressiveness and the presence of a *BRAF* mutation (Hu et al., 2006). In particular, methylation of *TIMP3* was significantly associated with several aggressive features of PTC, including extrathyroidal invasion, lymph node metastasis, multifocality and advanced tumour stages. Methylation of *TIMP3* was also associated with *BRAF* mutation and occurred more frequently in the more aggressive classical and tall-cell PTC subtypes than in the less aggressive follicular-variant PTC, with the latter known to infrequently harbour the *BRAF* mutation. (Hu et al., 2006). Moreover, the *TIMP3* gene was found to be downregulated in primary thyrocytes infected with RET/PTC1 retroviral vector with respect to uninfected cells (Borrello et al., 2005).

## 4.2 Aims of the chapter

At variance with other tumours, there are no studies regarding the functional role of TIMP3 in thyroid tumour biology. To investigate the role of TIMP3 in the pathogenesis of PTC, we used an integrated approach including analysis of several gene expression data sets and functional studies.

The aims of this chapter are: to analyze *TIMP3* expression in PTC samples using publicly available microarray data sets; to investigate the effect of TIMP3 restoration in NIM1 cells, a PTC-derived cell line, on:

- Cell growth and apoptosis;
- Adhesion, migration and invasion;
- Anchorage-independent growth;
- *In vivo* tumourigenicity.



### 4.3. Results

#### 4.3.1. Expression analysis of *TIMP3* in PTC samples and thyroid tumour cell lines

Hypermethylation of the *TIMP3* promoter has been detected in a high proportion (53%) of PTCs and associated with aggressiveness and *BRAF* mutation (Hu et al., 2006). Based on the evidence that *TIMP3* can also be regulated at post-transcriptional level by microRNAs, it was believed that gene expression analysis could represent the most accurate method for the assessment of *TIMP3* downregulation in PTC. Several microarray datasets of tumour and normal thyroid tissues were therefore analysed. cDNA microarray analysis previously produced in our laboratory (Ferrario et al., 2008) showed that *TIMP3* gene expression was downregulated in both the classical histotype as well as in the tall cell (TC) variant ( $p < 0.01$ ) compared with normal thyroid (Figure 4.2a). Frequent downregulation of *TIMP3* compared with normal samples was also observed when a number of independent data sets of microarray gene expression data of PTC samples, publicly available and all obtained using Affymetrix HG-U133 series platforms were considered. As shown in Figure 4.2b, in the Giordano data set a significantly reduced expression of *TIMP3* ( $p < 0.05$ ) was observed in the TC series (10 out of 26) though not in the classical histotype of PTC when compared with normal thyroid (Giordano et al., 2005). In both the He and Jarzab data sets (He et al., 2005; Jarzab et al., 2005), a statistically significant reduced ( $p < 0.01$ ) *TIMP3* expression was displayed by PTC when compared with unaffected thyroid tissues from the same patients (Figure 4.2c and d). Although not statistically significant, in the Vasko data set (Vasko et al., 2007), both microscopically dissected central and invasive region of PTC of three out of four patients displayed a reduced expression of *TIMP3* transcript in comparison with the corresponding normal region (Figure 4.2e).

Overall this meta analysis suggests that *TIMP3* downregulation was a general event in PTC carcinogenesis.

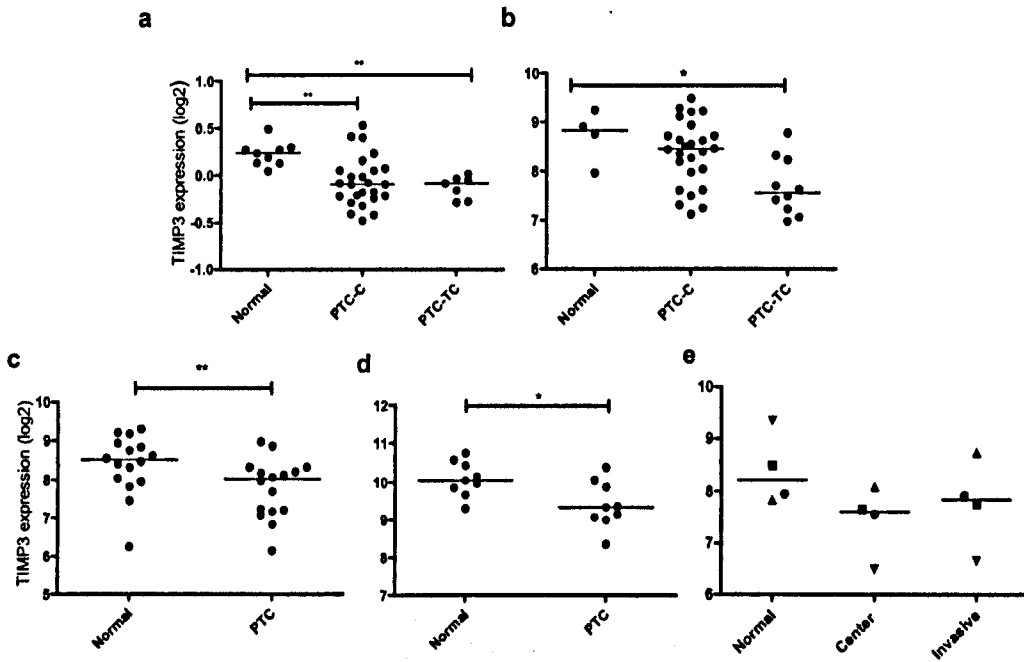


**Figure 4.2 Meta-analysis of *TIMP3* gene expression levels in PTC in five different data sets.** Data are reported as scatter plots of log2 values and median is recorded. **a)** Our data set: *TIMP3* downregulation was significant in both classical (C) and tall cell (TC) variants of PTC (\*\* $p < 0.01$  by Kruskal-Wallis followed by Dunns multiple comparisons post-test); *TIMP3* relative expression values were measured as log2 ratio between expression level of the specimen and that of the reference. **b)** Giordano data set: in comparison to normal samples, *TIMP3* downregulation was significant in TC variants of PTC (\* $p < 0.05$  by Kruskal-Wallis followed by Dunns multiple comparisons post-test.). **c** and **d)** Jarzab and He data sets included normal and PTC samples taken from the same patient: in each data set PTC samples displayed decreased expression of *TIMP3* when compared to the normal thyroid in paired tissue samples (\*\* $p < 0.01$  or \* $p < 0.05$  by Wilcoxon paired test). **E)** Vasko data set: central and invasive region of PTC and corresponding normal region have different symbols for each patient; three out of four patients displayed reduced expression of *TIMP3* transcripts in their tumoural area.

The expression of *TIMP3* by RT-PCR in a panel of thyroid tumour cell lines including PTC-derived (TPC1, NIM1, BCPAP and K1), FTC-derived (WRO82-1) and ATC-derived (FRO81-2, FB1, BHT101 and 8505C) cell lines and the human HEK293T cell line (known to express *TIMP3* protein) was performed. With the exception of the TPC1 (which carries the *RET/PTC1* oncogene) and BHT101 (no genetic lesion is known), all the other thyroid tumour derived cell lines harbour the *BRAFV600E* mutation

(Schweppe et al., 2008). (Details of the mutational status of these cells lines are reported in Table 3.2 of materials and methods section). The experiment reported in Figure 4.3a showed that although TIMP3 expression was undetectable in the TPC1 and NIM1 cell lines, treatment with the demethylating agent 5-Aza-2'-deoxy-cytidine (5-Aza-dC) restored the TIMP3 mRNA expression (Figure 4.3b). This suggests that aberrant promoter hypermethylation silences the TIMP3 gene in TPC1 and NIM1 cells

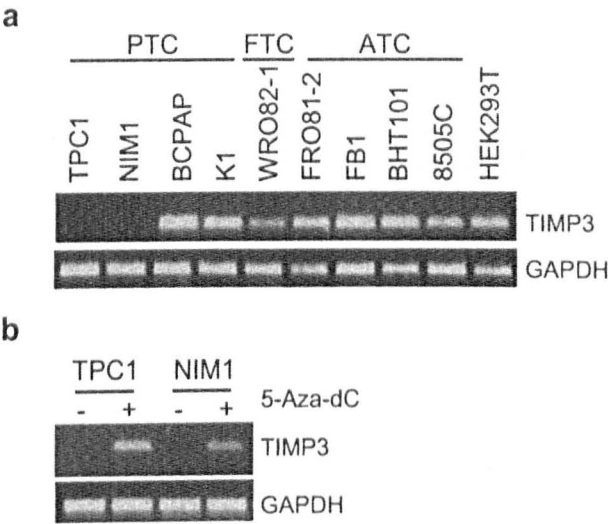


**Figure 4.3 TIMP3 mRNA expression by RT-PCR** a) Analysis of a panel of thyroid tumour derived cell lines; GAPDH gene expression was used as loading control. b) Effect of 5-Aza-2'-deoxy-cytidine (5-Aza-dC) treatment on TIMP3 expression in NIM1 and TPC1 cell lines.

#### 4.3.2. Effect of TIMP3 restoration on cell growth

We produced an *in vitro* model based on the restoration of TIMP3 expression in NIM1, a PTC-derived cell line harbouring the BRAFV600E mutation, derived from a metastasis and tumourigenic in nude mice (Zeki et al., 1993). The TIMP3-myc expression plasmid carrying the TIMP3 cDNA fused in frame with the myc epitope was constructed. This produced a 27 kDa TIMP3-myc protein reacting with both anti-myc (Figure 4.4.a) and anti-TIMP3 antibodies, as assessed by western blot analysis of transiently transfected

NIM1 cells. The *TIMP3-myc* expression construct was used to generate stable NIM1 clones expressing the exogenous TIMP3-myc protein, following transfection and selection in geneticin. Western blot analysis identified 11 out of 27 independent clones expressing variable levels of TIMP3-myc protein. Three NIM1-TIMP3 clones, named NIM1-T11, NIM1-T14 and NIM1-T23 were further characterized. The exogenous TIMP3-myc protein was detectable both in the cell extracts and in the conditioned media, as shown in Figure 4.4b.

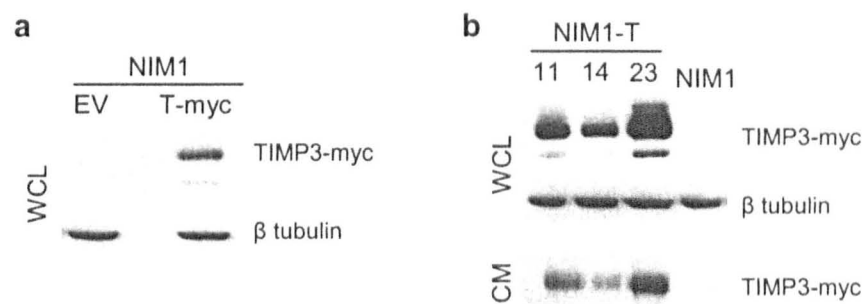


**Figure 4.4 Restoration of TIMP3 expression in NIM1 cell line.** Detection of TIMP3-myc protein by western blot using anti-myc antibody in: **a)** NIM1 cell line transiently transfected with empty (EV) or TIMP3-myc (T-myc) vector, and **b)** in whole cell lysates (WCL) (top) and conditioned medium (CM) (bottom) of stably TIMP3 transfected clones.  $\beta$ -tubulin was used as loading control for whole cell lysates; conditioned media were normalized for cell number

TIMP3 inhibits, among others, TACE/ADAM17, a convertase involved in the production of soluble TNF- $\alpha$  (Fata et al., 2001). Thus, the cleavage of TNF- $\alpha$  represents a read-out of TIMP3 activity. The TNF- $\alpha$  present in conditioned media of NIM1-TIMP3 clones was determined by flow cytometric analysis. NIM1 clones transfected with empty vector (NIM1-EV) were used as controls. As shown in Figure 4.5, the amount of soluble TNF- $\alpha$  in the NIM1-TIMP3 clones was drastically reduced with respect to NIM1-EV clones, thus demonstrating the activity of TIMP3-myc protein. Further evidence was provided by the reduction of syndecan-4 and ALCAM in the NIM1-TIMP3 clones conditioned media. The shedding of both of these proteins is mediated by TACE/ADAM17 (Fata et al., 2001; Rosso et al., 2007), and will be shown later.

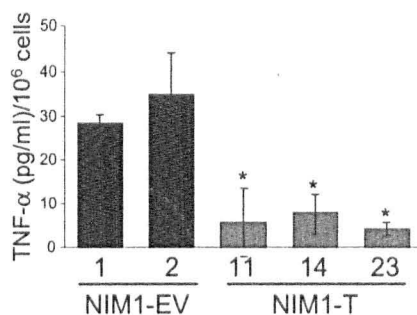


**Figure 4.5 Detection of TNF- $\alpha$  protein in the conditioned media of NIM1-EV and NIM1-T clones.** Cells were treated with PMA (100ng/ml, 2h) and the amount of released TNF- $\alpha$  in the conditioned media was analysed by flow cytometry. Values are expressed as mean  $\pm$  SD of duplicate samples. The asterisk indicates differences significant by the Student's t-test ( $p < 0.05$ ).

A large body of published data shows that TIMP3 is able to inhibit cell growth and to promote apoptosis in several tumour types such as melanoma and non adherent small cell lung carcinoma (Anand-Apte et al., 1996; Kallio et al., 2011). The effect of TIMP3 on NIM1 growth rate was investigated using a variety of approaches. In cells exposed to conditioned medium containing (CM+) or lacking (CM-) TIMP3 protein (derived from NIM1-T23 or untransfected NIM1 cells, respectively ), no differences in growth rate were observed (Figure 4.6).

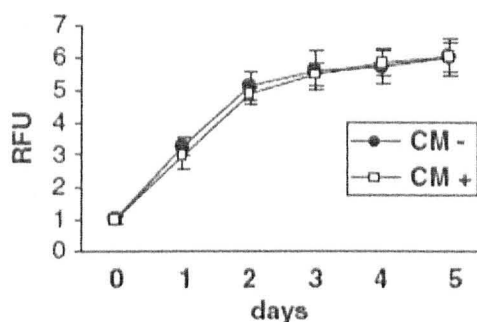


**Figure 4.6. Cell proliferation analysis of NIM1 treated with conditioned media.** Proliferation of NIM1 cells in the presence of TIMP3-containing (CM+) or control (CM-) medium determined by the alamarBlue Assay. The experiment was conducted in the presence of FCS; at the indicated time points the Relative Fluorescence Unit (RFU) was determined and data were normalized for values at day 1.

In keeping with these results, flow cytometric analyses showed the NIM1-TIMP3 clones and the control NIM1-EV clones display comparable cell cycle dynamics (Figure 4.7a).

TIMP3 is able to sensitize melanoma cells to undergo apoptosis induced by death receptors ligands (Ahonen et al., 2003). We investigated whether TIMP3, alone or in combination with the pro-apoptotic agent TRAIL effective in NIM1 cells, was capable to induce apoptosis in our system. NIM1 cells were treated for 24h and 48h with CM+ or CM- and the levels of cleaved PARP were detected by Western blot analysis. The results are shown in Figure 4.7b. In CM- treated cells we observed basal levels of cleaved PARP, not affected by treatment with CM+ medium. As positive control, the induction of PARP cleavage by treatment of TRAIL is shown (Figure 4.7b, top left panel). When TRAIL was administered to cells pre-treated with the CM+, no difference in PARP cleavage with respect to the control was observed (Figure 4.7b, top right panel). Similar results were observed by analyzing the NIM1-TIMP3 clones, which showed levels of cleaved PARP similar to those of NIM1-EV clones and untransfected NIM1 cells (Figure 4.7b, bottom panel).

These data indicate that TIMP3 is neither able to promote apoptosis in NIM1 cells, as also suggested by FACS analysis (Figure 4.7a), nor to sensitize them to TRAIL-induced apoptosis.

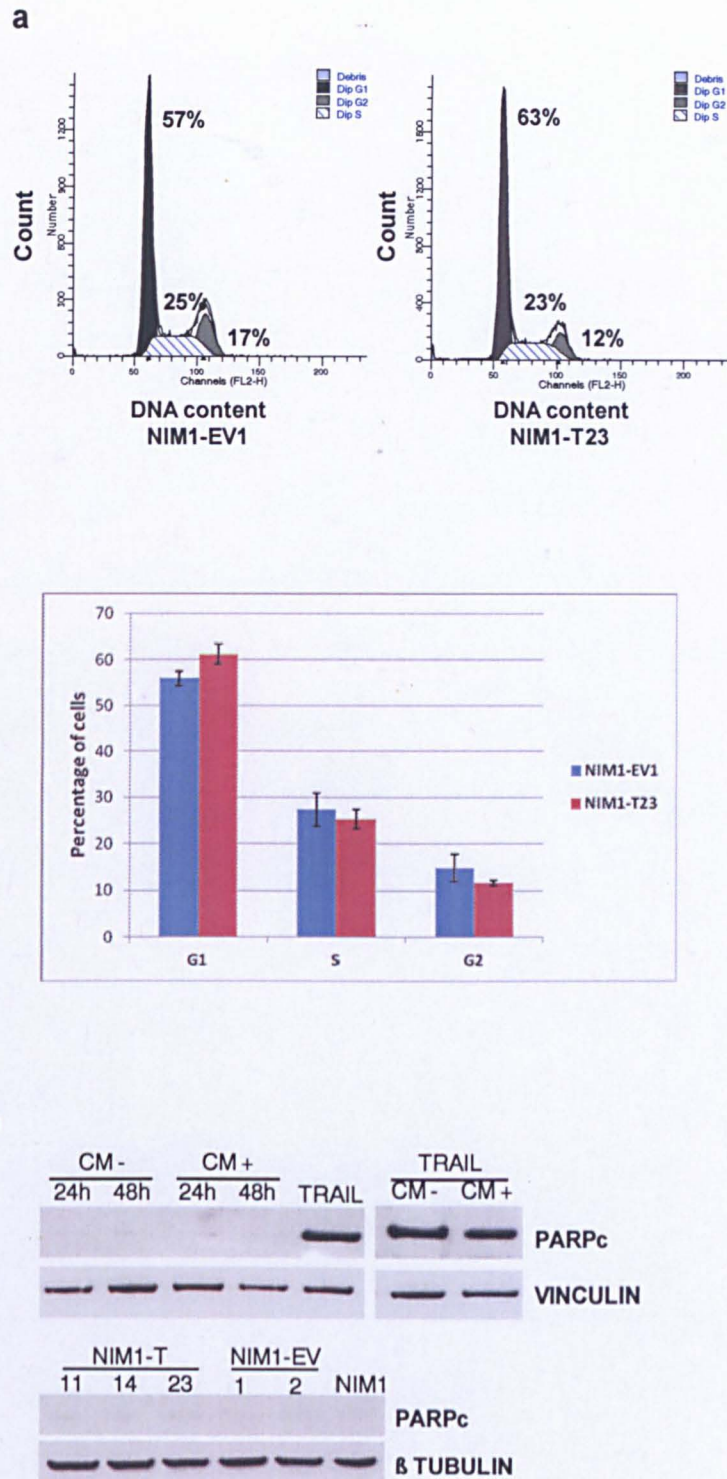


**Figure 4.7 Effect of TIMP3 re-expression on NIM1 cell cycle and apoptosis.** a) top: flow cytometric analysis of NIM1 clones transfected with empty vector (NIM1-EV1) or TIMP3-myc construct (NIM1-T23); percentage of cell cycle distribution is shown; bottom: the data represent the percentage average of cells in different stages of the cell cycle of three independent experiments; b) Western blot detection of cleaved PARP protein. Top: NIM1 cells treated with CM+ or CM- medium (left panel), or treated with TRAIL (50 ng/ml for 5h) following 24 h pre-incubation with CM+ or CM- (right panel); vinculin was used as loading control. Bottom: NIM1-T and NIM1-EV clones;  $\beta$ -tubulin was used as loading control.

#### *4.3.3. Effect of TIMP3 restoration on cell adhesion*

When NIM1 cells were plated at low density in CM+ or CM-, no differences in colony numbers or dimensions were observed at days 10 and 17 (data not shown), a result in keeping with the lack of effect of TIMP3 on growth rate described above. Interestingly, a difference was observed at day 24 where the NIM1 colonies grown in CM+ were more compact and dense than those in CM-, which underwent cell detachment (Figure 4.8a), suggesting an effect of TIMP3 on cell adhesion. To further dissect this issue we performed an adhesion assay in which NIM1 cells were pretreated with CM+ or CM- for 24 h and seeded in a 96 plate coated with type IV collagen (a component of ECM, known to interact with cell-surface heparin sulfate proteoglycans (Khoshnoodi et al., 2008), whose shedding is inhibited by TIMP3 (Fitzgerald et al., 2000) in the presence of the same media. The number of cells attached to the substrate 1h after seeding was measured. As shown in Figure 4.8b, treatment with CM+ increases the adhesion of NIM1 cells by 1.4 fold. Similar results were obtained in the presence of recombinant TIMP3 protein, which caused a 1.8 fold increase in NIM1 cell adhesion (Figure 4.8c), thus ruling out the possibility of ascribing the above reported results to the presence in the CM+ of secreted factors other than TIMP3. The adhesion assay was also applied to the NIM1-TIMP3 clones and all showed a 2 to 3 fold increase in adhesion with respect to the NIM1-EV control clones (Figure 4.8d). Collectively these data indicate the involvement of TIMP3 in the regulation of NIM1 cell adhesion.



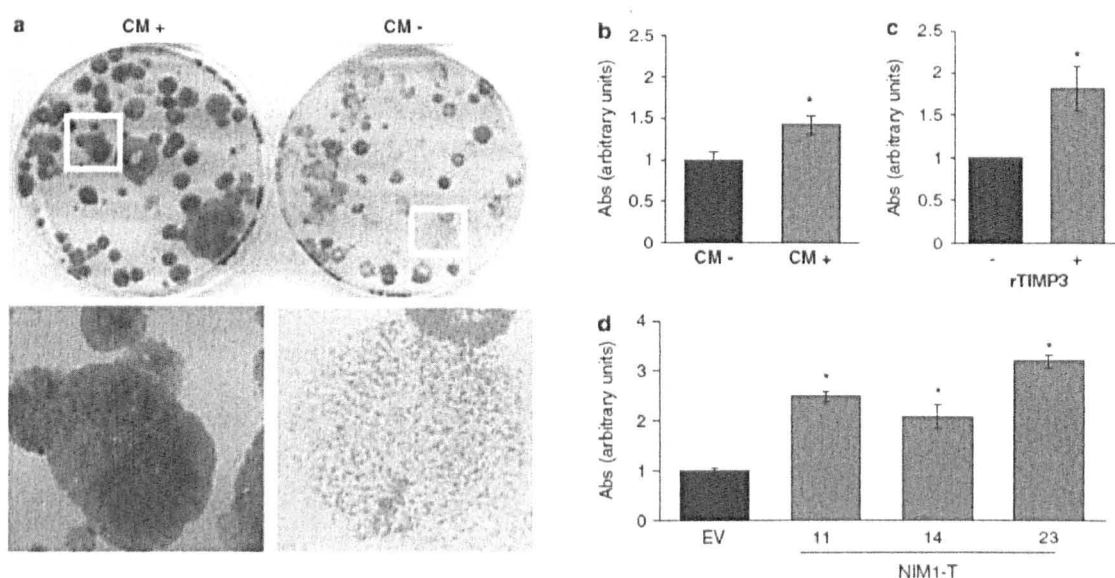


**Figure 4.8 Effect of TIMP3 expression on NIM1 cell adhesion.** a) Colonies formed by NIM1 cells in the presence of TIMP3-containing (CM+) or control medium (CM-). Two hundred cells were plated into 100 mm<sup>2</sup> Petri dishes; colonies were fixed and stained after 24 days; representative pictures of colonies at a higher magnification are shown. b) Adhesion of NIM1 cells to ECM in the presence of CM+ and CM-. Cells that adhered to the plate after 1 hour incubation were fixed and stained with crystal violet. The adhesion capability was calculated by measuring the absorbance at 595 nm and the results of one representative experiment is shown. c) Adhesion of NIM1 cells to ECM in the presence or absence of recombinant TIMP3 protein. The graph shows mean values from two different experiments. d) Adhesion of NIM1-T and NIM1-EV clones. The graph shows a representative experiment; the data represents mean values  $\pm$  SD. The asterisk indicates significant differences by the Student's t-test ( $p < 0.05$ ).

4.3.4. Effect of TIMP3 on cell migration and invasion

A wound healing assay was performed to investigate the migratory capability of NIM1-TIMP3 clones. As shown in Figure 4.9a the NIM1-TIMP3 clones showed reduced wound healing capability with respect to the NIM1-EV clones. At 24 hours the scratch of the control clones was completely healed, whereas the repair of the NIM1-TIMP3 clones was only 39 to 79%. Comparable results were obtained in the presence of recombinant TIMP3 protein which reduced the migration capability of NIM1 cells by approximately 50% at 8 and 24 hours after scratching (Figure 4.9b).

To further support these results, the effect of *TIMP3* silencing on the migration capability of K1 cells (derived from a PTC, carrying the *BRAFV600E* mutation and expressing high amount of *TIMP3* mRNA) was investigated. The results are shown in Figure 4.9c. K1 cells transiently transfected with *TIMP3* siRNA showed abrogation of *TIMP3* expression (Figure 4.9c, left). Concomitantly, a 2.3 fold increase of migration capability, with respect to control, was observed, as assessed by wound healing assay (Figure 4.9c, right).

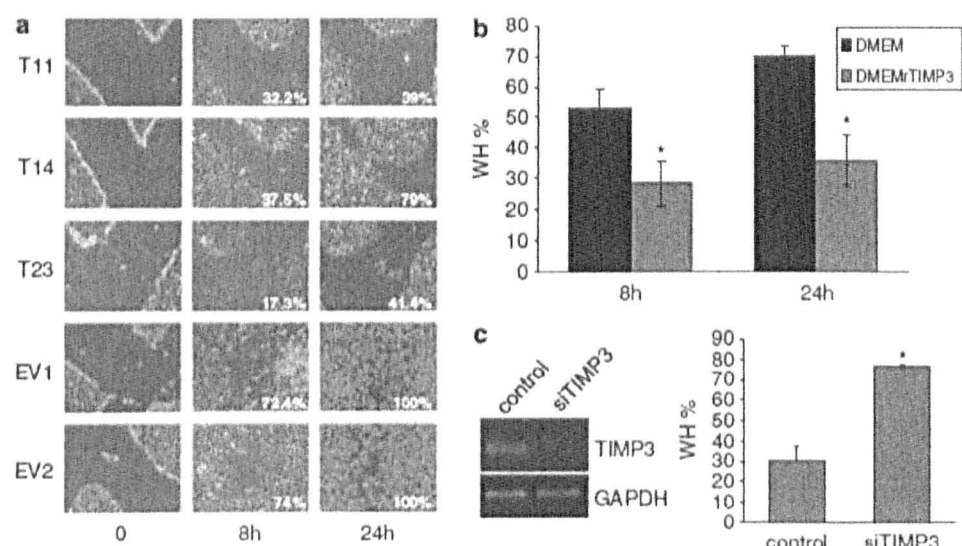


**Figure 4.9 Effect of TIMP3 expression on wound healing.** A scratch was applied to cell monolayer, and migration of the cells toward the “wound” was recorded by taking pictures at the indicated time points. a) NIM1-T and NIM1-EV clones; in each panel the percentage of wound healing, determined by dividing the migrated distance by the scratched distance, is indicated. b) NIM1 cells exposed (DMEM rTIMP3) or not (DMEM) to recombinant TIMP3 protein. Data are expressed as percentage of wound healing (WH %)

calculated by dividing the migrated distance by the scratched distance. c) K1 cells transfected with either control or *TIMP3* specific siRNAs. Left: *TIMP3* mRNA expression was checked by RT-PCR as described in Materials and Methods section. Right: Wound healing assay was performed in triplicates 48 hours after siRNA transfection. Data represent mean values  $\pm$  SD; the asterisk indicates differences significant by the Student's t-test ( $p < 0.05$ ).

Boyden chamber assays were then performed to investigate both the migratory and invasive capability of NIM1-*TIMP3* and NIM1-EV clones using their own CM as chemoattractant. In the migration assay all the NIM1-*TIMP3* clones showed a drastic reduction (78-87%) in migration with respect to the control NIM1-EV clones (Figure 4.10a, top). When the assay was performed in the presence of Matrigel, very similar results were obtained. The NIM1-*TIMP3* clones showing an invasion capability reduced by 86-95% with respect to NIM1-EV clones (Figure 4.10a, bottom).

To rule out the possibility that the above data could be ascribed to clone variability, we performed Boyden chamber assays in which NIM1 cells transiently transfected with *TIMP3-myc* construct or empty vector were exposed to their own or the other CM as chemoattractant. In this case the CM+ and CM- were derived from *TIMP3-myc* or empty vector transiently transfected cells, respectively. The results are reported in Figure 4.10b. NIM1-*TIMP3* transfected cells exposed to CM+ showed a reduction of migration (33%) in comparison with those exposed to CM-. Similarly, the migration of EV-transfected NIM1 cells was reduced by 49% in the presence of CM+ compared to CM-. The invasion assay showed similar results. The invasive capability of NIM1-*TIMP3* transfected cells in the presence of CM+ was reduced by 47% compared to that occurring in the presence of the CM-. Similarly, NIM1-EV cells showed a 51% reduction of invasion in the presence of CM+ with respect to that found in the presence of CM-. As reported above for the adhesion and wound healing assays, results consistent with those in the presence of CM+ were obtained by performing the invasion assay in the presence of recombinant *TIMP3* protein. A consistent reduction (41%) of invasiveness of NIM1-EV cells was detected.

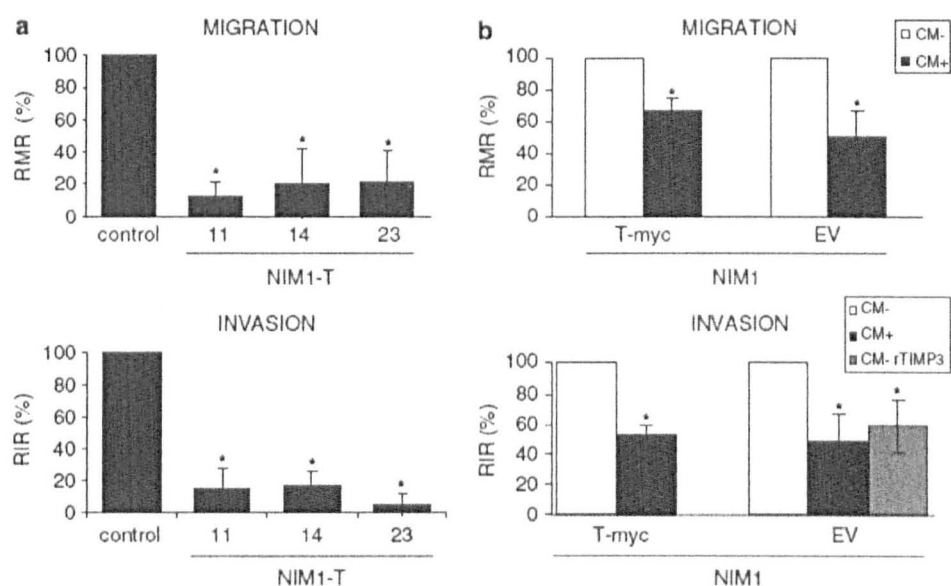


**Figure 4.10 Effect of TIMP3 expression on migration, invasion and anchorage-independent growth.** a) Migration and invasion of NIM1-T and NIM1-EV clones by Boyden chamber assays. Cells were seeded in the upper part of the Boyden chamber while their own conditioned media were used as chemoattractant in the bottom chamber. Migration and invasion rates are normalized over the control. RMR: relative migrating rate; RIR: relative invading rate. Data represent the mean values  $\pm$  SD of four independent experiments. The asterisk indicates significant differences using the Student's t-test ( $p < 0.05$ ). b) Migration and invasion of NIM1 cells transiently transfected with *TIMP3-myc* (T-myc) or empty vector (EV) and exposed to one of the following, their own or other conditioned medium (CM+ and CM-) as chemoattractant, or to recombinant TIMP3 protein (rTIMP3). The experiment was performed as in a.

#### 4.3.5. Effect of TIMP3 on anchorage-independent growth

Tumour cells display the capability to grow in the absence of adhesion. A soft agar assay was performed to investigate whether adhesion in the NIM1 cells is affected by TIMP3. The NIM1-TIMP3 clones and, as control, the NIM1-EV1 clone and untransfected NIM1 cells were used. After three weeks of incubation in soft agar the NIM1-TIMP3 clones formed colonies with efficiency reduced (68-91%) with respect to control cells (Figure 4.11, top). Moreover, the soft agar clones formed by NIM1-TIMP3 cells were smaller than those of the control cells (Figure 4.11 bottom).

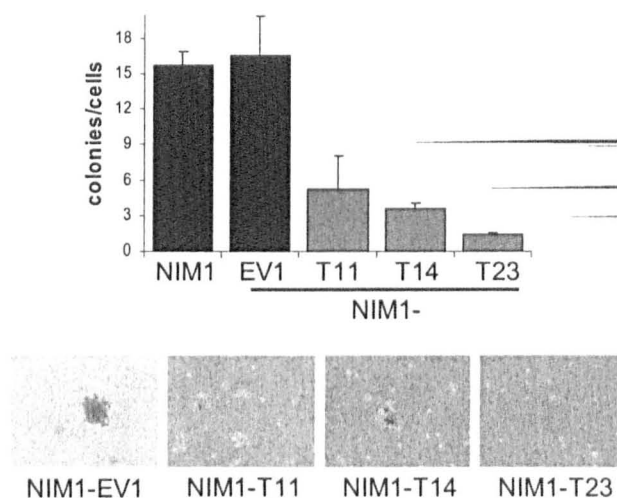


**Figure 4.11 Anchorage-independent growth in TIMP3 transfected and control cells.** Top: Colony-forming efficiency was determined by the ratio between number of colonies and number of plated cells. The asterisk indicates differences significant by the Student's t-test ( $p < 0.05$ ). Bottom: Representative pictures of colonies formed after 22 days of growth in soft agar.

#### 4.3.6. Analysis of proteins mediating TIMP3 effects

The status of several proteins, involved in the regulation of cell adhesion, migration and invasion by TIMP3 was investigated. Syndecan-4 and ALCAM are two proteins involved in cell adhesion and regulated by shedding mediated by ADAM17/TACE, a TIMP3-sensitive metalloprotease (Fata et al., 2001; Rosso et al., 2007). The soluble form of syndecan-4 was less abundant in the CM of the NIM1-TIMP3 clones with respect to the control cells, as demonstrated by immune dot blot (Figure 4.12a, top). Similarly, the level of the 96 kDa soluble form of ALCAM, detected by western blot, was reduced in the NIM1-TIMP3 clones with respect to the control cells (Figure 4.12a, bottom).

E-cadherin, an adhesion molecule whose deficiency in cancer cells promotes invasion (Margeanu et al., 2008), was undetectable in the naive NIM1 cells, a result in keeping with the metastatic origin of these cells, and its expression was not restored in

TIMP3-expressing clones. The expression of E-cadherin in human primary thyrocytes is shown as a control (Figure 4.12b).

Vimentin is involved in invasion and its expression is upregulated in several tumours, including PTC (Vasko et al., 2007). As shown in Figure 4.12c (top) the vimentin level in the NIM1-TIMP3 clones was reduced with respect to that present in the NIM1-EV cells.

The Cytokeratins 8/18 are regulators of integrin-dependent adhesion and migration (Bordeleau et al., 2010) and their levels were increased in the NIM1-TIMP3 clones with respect to control (Figure 4.12c, bottom).

On the whole these results indicate that TIMP3 regulates adhesion, invasion and migration of NIM1 cells by modulating the amount of syndecan-4, ALCAM, and vimentin and cytokeratins 8/18.

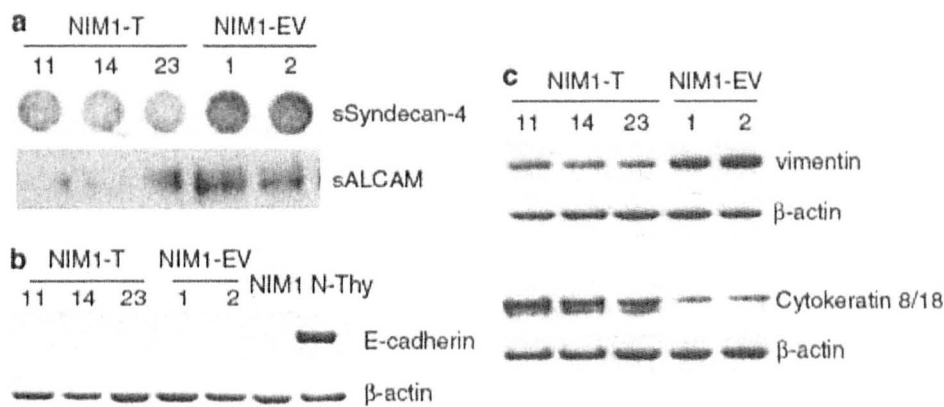


**Figure 4.12 Modulation of adhesion molecules by TIMP3 expression.** a) Analysis of shedding of Syndecan 4 by dot blot (upper panel) and ALCAM by Western blot (lower panel) in conditioned media of NIM1-EV and NIM1-T clones. Samples were normalized for cell number. b) Detection of E-cadherin and c) of vimentin and cytokeratins 8/18 expression in NIM-T and NIM-EV clones by Western blot analysis. β-actin was used as loading control for cell extracts. N-Thy indicates human primary thyrocytes.

#### 4.3.7. Effect of TIMP3 restoration in mouse tumour xenografts

To investigate the *in vivo* consequences of TIMP3 re-expression in NIM1 cells, the NIM1- TIMP3 clones (T11, T14 and T23) and NIM1 cells were injected into nude mice. Tumour growth was observed in 3/3 mice injected with the NIM1 cells. In mice xenografted with NIM1-T11 cells 3/3 takes were observed although regression occurred in 1/3 animal. In mice injected with the NIM1-T14 and NIM1-T23 clones tumour growth was observed in 2/3 mice. Collectively, the tumours produced by NIM1-TIMP3 clones grew more slowly than the NIM1 derived tumours (Table 4.1).

**Table 4.1** *In vivo* tumour growth of NIM1 cells and NIM1-TIMP3 clones<sup>a</sup>

<i>Cell line</i>	<i>Tumor-bearing mice</i>	<i>Regression</i>	<i>Days at 0.1 g</i>	<i>Days at 1 g</i>
NIM1	3/3	0/3	< 8	12 (12-18)
NIM1-T11	3/3	1/3	11 (< 8 to 14)	20, 38
NIM1-T14	2/3	0/2	10, 49	26, 62
NIM1-T23	2/3	0/2	11, 62	> 32, > 66

<sup>a</sup>Parental NIM1 cells and NIM1-TIMP3 clones ( $2 \times 10^6$ ) were inoculated subcutaneously into the left flank of athymic nude mice as described in Materials and Methods section. Tumour growth was assessed by evaluating tumour latency, ie days to reach 0.1 g, and by monitoring tumour weight (TW) twice a week. TW was estimated by the formula  $TW(g) = d^2 \times D / 2$  where d and D are the shortest and the longest diameters of the tumour, respectively, measured in cm.

As soon as the tumours were visible through the skin of the nude mice TIMP3-expressing tumours appeared to be paler than the NIM1-induced tumours. This difference was confirmed at excision of the tumours. In addition, TIMP3-expressing tumours were less hemorrhagic compared to the NIM1-induced tumours (data not shown). Cell cultures were established from the explanted tumours. Western blot analysis confirmed the expression of TIMP3 protein in tumour-derived cells (Figure 4.13a). In addition, functional

analysis of the xenograft-derived cells revealed that TIMP3-expressing cells maintain the reduction of wound healing, migration and invasion relative to NIM1 cells (Figure 4.13b, c, and d).

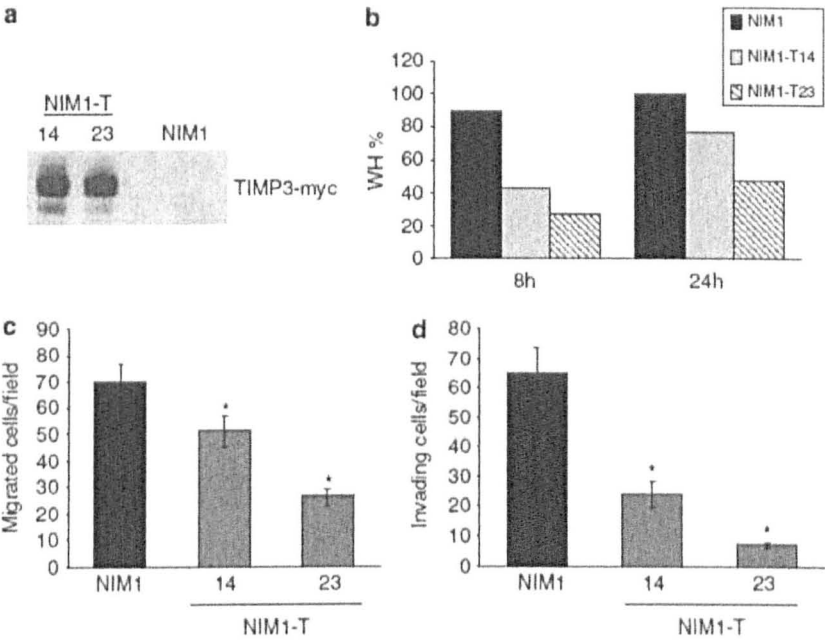


**Figure 4.13 Analysis of cell cultures established from tumours induced in nude mice by NIM1 and NIM1-T clones.** a) Detection of TIMP3-myc protein by Western blot analysis. b) Wound healing assay. A scratch was applied to cells grown in monolayer and the distances between the edges measured immediately, and then after 8 and 24 hours. Data are expressed as the percentage of wound healing (WH %) calculated by dividing the migrated distance by the scratched distance. Migration (c) and invasion (d) capabilities of xenograft-derived cell cultures measured by Boyden chamber assays. Cells were seeded in the upper part of the Boyden chamber while in the bottom part their own conditioned media were used as chemoattractant, as described in Material and methods. Data are expressed as number of migrated (c) or invading (d) cells per field. A representative experiment is shown; similar results were obtained in three independent experiments. Data represent mean values  $\pm$  SD. The asterisk indicates differences significant by the Student's t-test ( $p < 0.05$ ).

Histopathologically, both NIM1 and NIM1-TIMP3 subcutaneous tumour xenografts appeared as well-demarcated expansile multinodular growths. Tumour tissue was composed of large polygonal anaplastic epithelial cells arranged in small dense cellular lobules and papillary projections often delimiting central cystic spaces. These tumour units were supported by variable amounts of fibrovascular stroma and surrounded by a loose



capsular reaction with sparse infiltration of inflammatory cells. Locally extensive necro-hemorrhagic areas were consistently observed at the periphery of NIM1-induced tumours. Similar lesions were not observed in association with the NIM1-TIMP3-induced tumours (Figure 4.14 top panels, hematoxylin and eosin). Taken together, these findings may explain why grossly detectable hemorrhages were recorded in tumour xenografts deriving from the NIM1 cells but not from those induced by the NIM1-TIMP3 cells.

To assess the extent of vascularisation in tumour xenografts, the microvessel density was determined by IHC using an anti-mouse CD31 antibody (Figure 4.14, middle panels). The mean microvessel count in TIMP3-expressing tumours was reduced with respect to that present in the NIM1-induced tumours. The difference was statistically significant for the NIM1-T23 tumours.

In several human tumours, including thyroid cancer and related animal models, it has been observed that tumour angiogenesis correlates with the extent of macrophage infiltration (Dettoraki et al., 2009; Dhar et al., 1998; Russell et al., 2003). To investigate the presence of infiltrating macrophages in our *in vivo* tumour model their presence in the tumours was evaluated by IHC with an F4/80 antibody. As shown in Figure 4.14 (bottom panels, F4/80), the number of macrophages was significantly reduced in tumours expressing TIMP3 with respect to those induced by naive NIM1 cells.

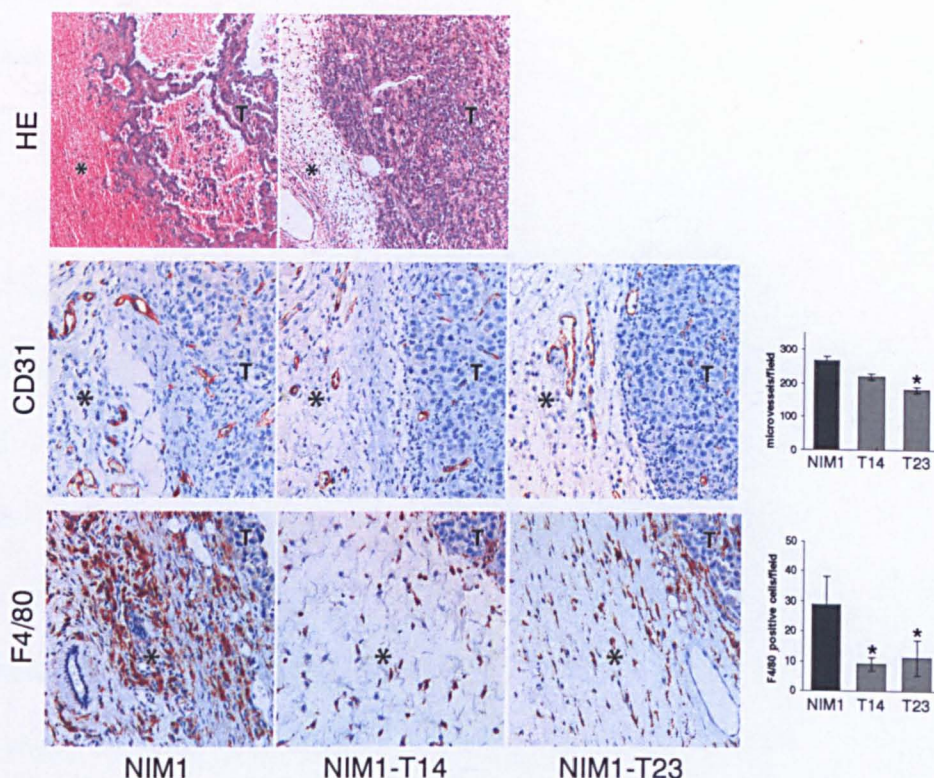


**Figure 4.14 Microscopic and immunohistochemical analysis of NIM1-TIMP3 and NIM1 induced tumours.** HE – left panel: NIM1-induced tumour xenograft where the periphery of the tumour is effaced by a locally extensive hemorrhagic area (\*) and few neoplastic papillary projections (T) are still present; right panel: in the NIM1-TIMP3-induced tumour xenograft, the periphery of the tumour is composed of solid lobules surrounded by a fibrovascular capsular reaction without any evidence of hemorrhagic lesions. CD31 – representative pictures of CD31 immunostaining in NIM1 (left panel), NIM1-T14 (central panel) and NIM1-T23 (right panel) tumour xenografts. T shows the position of the tumor lobules while (\*) denotes the tumour capsule-stroma (\*), F4/80 – representative pictures of F4/80 immunostaining in NIM1- (left panel), NIM1-T14 (central panel) and NIM1-T23 (right panel) induced tumour xenografts. Tumour capsule-stroma (\*), tumour lobules (T).

#### 4.4. Discussion

Using an integrated approach which included the analysis of gene expression data and functional studies, TIMP3 has been demonstrated to exert a negative regulatory role in thyroid carcinogenesis. Analysis of gene expression data produced in our laboratory demonstrated the consistent downregulation of *TIMP3* in PTC with respect to normal thyroid, and also highlighted an association with the tall cell variant. Downregulation of the *TIMP3* gene in PTCs with respect to normal thyroid was also observed by *in silico* analysis of three different public available gene expression data sets. Collectively the gene expression data support the notion that TIMP3 may exert an oncosuppressor role in PTC, a function also suggested by previous studies. For example, the *TIMP3* gene was found to be downregulated in primary thyrocytes infected with RET/PTC1 retroviral vector with respect to uninfected cells (Borrello et al., 2005). Moreover, *TIMP3* was identified as being within a group of tumour suppressor genes (also including *SLC5A8*, *DAPK*, *RARβ2*) which were hypermethylated in a consistent fraction (53%) of PTCs and was associated with tumour aggressiveness and *BRAF* mutation (Hu et al., 2006). In the present study promoter hypermethylation was also identified as the mechanism silencing *TIMP3* gene expression in the two PTC-derived tumour cell lines TPC1 and NIM1 with levels of *TIMP3* mRNA increasing upon treatment with the demethylating 5-Aza-C agent.

Different effects of TIMP3 restoration on tumour cell growth have been reported. Although no effects on the *in vitro* proliferation of murine neuroblastoma and melanoma cells have been observed (Spurbeck et al., 2002), TIMP3 expression in human melanoma, neuroblastoma and MPNST was reported to induce apoptosis (Ahonen et al., 2003; Mahller et al., 2008). The contribution of TIMP3 to thyroid carcinogenesis was therefore studied by restoring TIMP3 expression in the TIMP3-negative NIM1, a PTC-derived cell line. This was achieved by exposure of the NIM1 cells to TIMP3-containing conditioned

medium and by transient or stable transfection with *TIMP3-myc* cDNA. No effects on growth control, the induction of apoptosis or the activation levels of major signal transduction pathways known to function in NIM1 cells were observed. The lack of effect of TIMP3 on the growth rate of NIM1 cells might be related to their thyroid origin and/or to the advanced tumour stage they represent, being derived from a PTC metastasis. In this context it is worth noting that multiple elements contribute to the growth regulation of NIM1 cells. In addition to the *BRAFV600E* mutation, NIM1 cells carry a homozygous deletion of the tumour suppressor p16INK4 (Calabro et al., 1996), produce multiple cytokines including GM-CSF, IL-6, IL-11, and their growth is regulated by IL-1 through an autocrine mechanism (Tohyama et al., 1992; Zeki et al., 1993). Moreover, we have recently demonstrated that the growth of NIM1 cells is regulated by an autocrine TGF $\alpha$ /EGFR loop (Degl'Innocenti et al., 2010) and by the IGFBP7 pathway (Vizioli et al., 2010).

Although not involved in growth control in thyroid tumour models studied here, TIMP3 expression modified some features of the phenotype of treated NIM1 cells. Cells exposed to soluble TIMP3 protein or transfected with the TIMP3-myc construct showed increased adhesion and a reduced migratory and invasive capability. Analysis of some cell adhesion mediators in the TIMP3-expressing clones showed reduction of syndecan-4 and vimentin protein levels, decreased ALCAM shedding, but an increase of the epithelial marker cytokeratin. All these features, which are consistent with the inhibitory effect of TIMP3 on MMPs and on ADAM17/TACE, indicate a reduced degradation of the ECM, and suggest that the transformed phenotype of NIM1 cells can be modulated by TIMP3 restoration.

The most striking effect of TIMP3 restoration in NIM1 cells was observed in mouse tumour xenografts. When compared to TIMP3-negative NIM1-induced tumours, TIMP3-positive NIM1 expressing tumours showed consistently reduced growth and appeared paler and less hemorrhagic. In this context, histopathological examination confirmed the

presence of hemorrhagic areas in the NIM1 TIMP3-negative induced tumours, but not in the NIM-1 TIMP3-expressing tumours. In keeping with this, angiogenesis (assessed through the evaluation of microvessel density) was reduced in the NIM1 TIMP3-expressing tumours and this was associated with reduction of tumour infiltrating macrophages. The antiangiogenic effect of TIMP3 observed in the tumour xenografts suggests a link between the frequent increase of angiogenesis and TIMP3 downregulation detected in PTC (Akslen and LiVolsi, 2000; Hu et al., 2006). It has been described that the antiangiogenic effect of TIMP3 is related to its inhibition of VEGFA binding to VEGFR-2, thus attenuating downstream signalling (Qi et al., 2003), and that VEGFR inhibition is responsible for the anti-tumoural role of TIMP3 in several models (Ahonen et al., 2003; Mahller et al., 2008). Based on the evidence that NIM1 cells produce VEGFA (Melillo et al., 2010), the same mechanism could be responsible for the effects observed in our tumour xenograft model.

The reduction of infiltrating macrophages in the NIM1 TIMP3-expressing tumours is worth noting, since the extent of macrophage infiltration is associated with progression in thyroid epithelial tumours (Ryder et al., 2008). It has also been shown that the inhibition of VEGFA binding to VEGFR-2 reduces macrophage infiltration in orthotopic xenografts of pancreatic and breast tumours (Dineen et al., 2008; Roland et al., 2009). Thus, it is tempting to speculate that in the mouse xenograft tumour model the inhibitory effect of TIMP3 for VEGFA binding to VEGFR-2 may be responsible for reduction of both angiogenesis and macrophage infiltration, thus leading to restriction of *in vivo* tumour growth. Further studies are needed to dissect the mechanisms through which TIMP3 regulates angiogenesis and macrophage infiltration in PTC.

In summary, restoration of TIMP3 in the PTC-derived NIM1 cell line had no effect on growth rate; however, it reduced migration, invasion and anchorage independent growth and *in vivo* tumourigenicity, supporting a tumour suppressor role in thyroid carcinogenesis. (Figure 4.15)



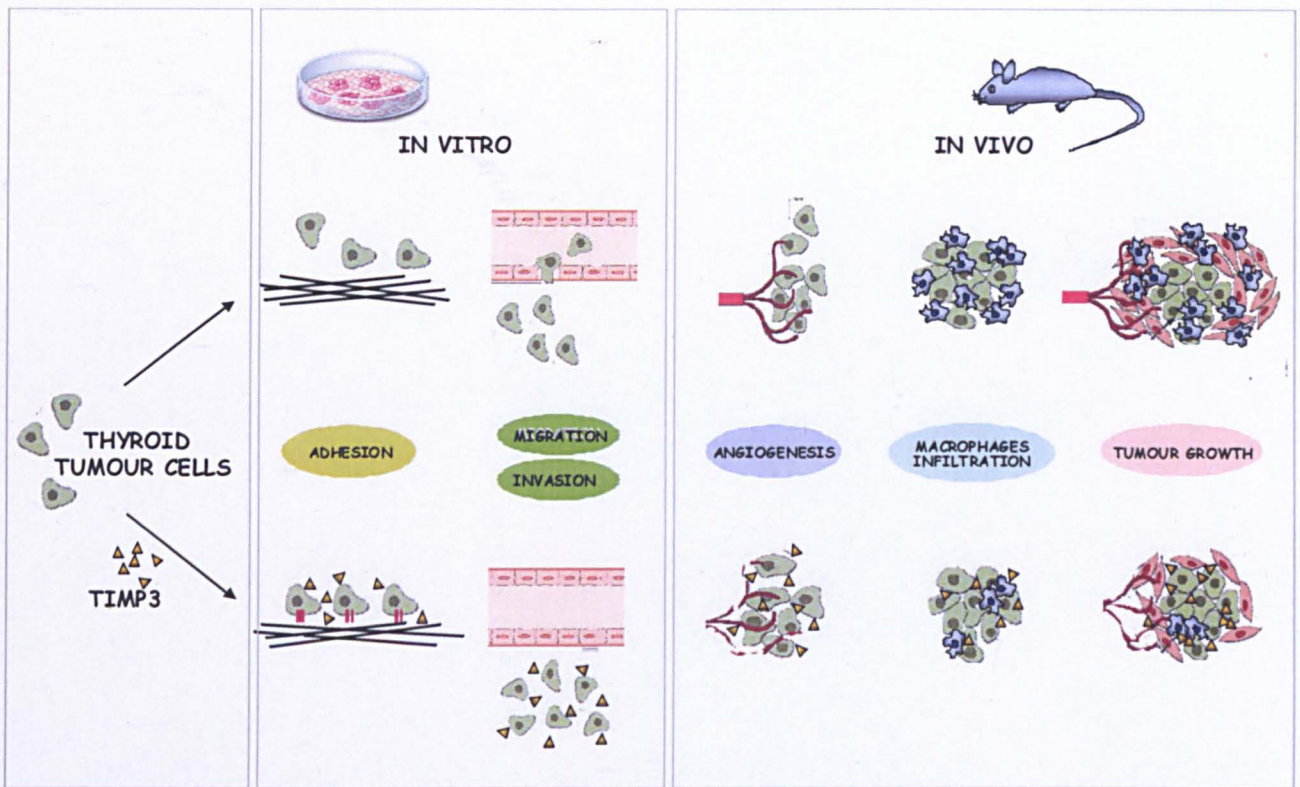


**Figure 4.15** *In vitro* and *in vivo* effects of TIMP3 restoration in thyroid tumour cells. Restoration of TIMP3 in the PTC-derived NIM1 cell line had no effect on growth rate; however, it reduced migration, invasion and anchorage independent growth and *in vivo* tumourigenicity, supporting a tumour suppressor role in thyroid carcinogenesis.



## 5.1 Introduction

### 5.1.1 S100A11

S100A11, also known as S100C and calgizzarin, is an EF hand-type  $\text{Ca}^{2+}$ -binding protein belonging to the S100 protein family. S100 proteins are named after their solubility in 100% saturated ammonium sulphate solution (Moore, 1965), and are small proteins with a molecular weight ranging from 9 to 14 kDa. Although the molecular structures of S100 proteins are similar, their expression profiles and cellular functions differ greatly depending on cell types and functional conditions. A large proportion of S100 proteins belong to the S100A family. In humans, 16 family members (S100A1 to S100A16) are currently known and they are clustered in a region of chromosome 1q21.

S100A11 has been proposed to have biological functions in the processes of endo- and exocytosis (Seemann et al., 1997), regulation of enzyme activity (Zhao et al., 2000), cell growth (Sakaguchi et al., 2000), apoptosis (Makino et al., 2004) and inflammation (Cecil et al., 2005). In addition, S100A11 has been identified as a ligand of the receptor for advanced glycation end products (RAGE), and could regulate the chondrocyte differentiation to hyperthrophy in osteoarthritis pathogenesis (Cecil et al., 2005).

One of the most widely accepted theories about the role of S100A11, has been proposed by Sakaguchi et al. (Sakaguchi and Huh, 2011), who presented S100A11 as a key mediator of calcium-induced growth inhibition in cultured normal human keratinocytes (NHK). An increase in extra-cellular calcium may cause phosphorylation of S100A11, with subsequent binding to nucleolin and translocation to the nucleus. S100A11 may then liberate Sp1/3 from nucleolin, leading to increased transcription of p21CIP1/WAF and p16INK4a which are negative regulators of cell growth (Figure 5.1). The same authors also showed that S100A11 mediated a TGF- $\beta$ -triggered signalling for growth suppression in a manner similar to that from high calcium (Sakaguchi et al., 2004). Notably, the S100-mediated pathway was deteriorated in human squamous carcinoma cell lines that are resistant to TGF- $\beta$  (Sonegawa



et al., 2007), indicating that it is at least partly involved in conferring human epithelial cancers resistance to TGF- $\beta$ .

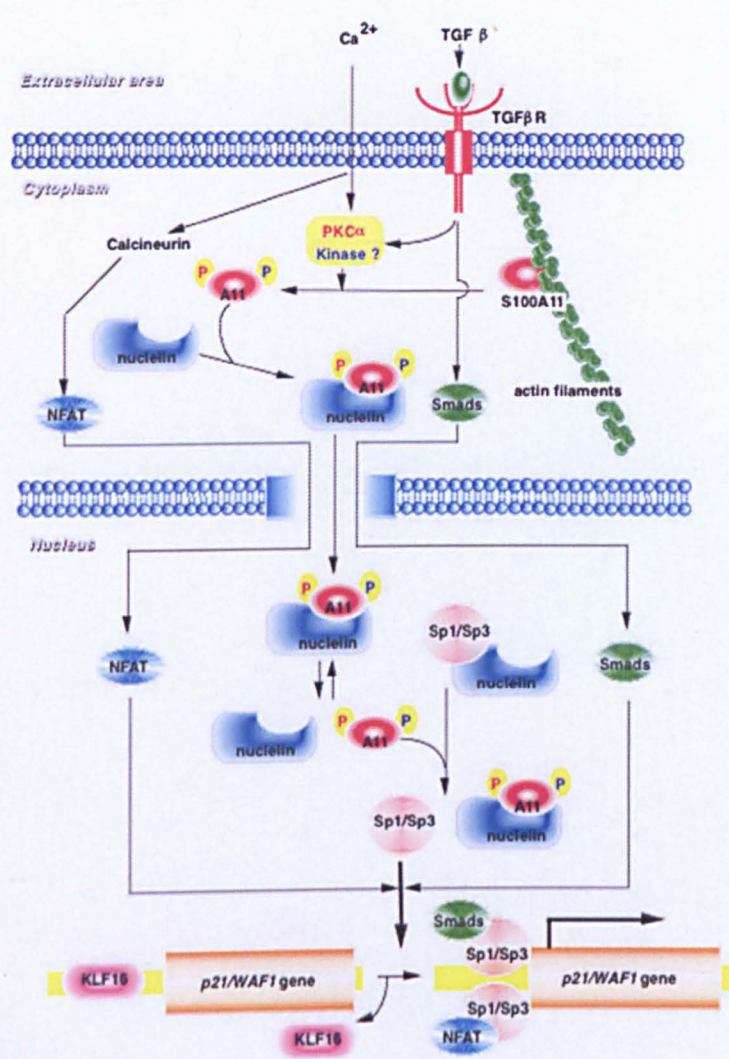


**Figure 5.1 Mechanism of S100A11-mediated growth inhibition in NHK cells.** High  $\text{Ca}^{2+}$  and TGF- $\beta$  stimulation promotes S100A11 phosphorylation, its binding to nucleolin and consequently translocation into the nucleus. S100A11 then liberates Sp1/3 from nucleolin, leading to increased transcription of p21CIP1/WAF and p16INK4a (from (Sakaguchi and Huh, 2011))

Another growth-suppressive function of S100A11 has been found in NHK, whose growth depends on arachidonic acids (Sakaguchi et al., 2007). Annexin 1 (ANXA1) complexed with S100A11 efficiently binds to and inhibits cPLA2, a rate limiting enzyme of the arachidonic cascade. Upon exposure of NHK to EGF, ANXA1 is cleaved at 12W, and the truncated ANXA1 loses binding capacity to S100A11, resulting in maintaining cPLA2 in an active state (Figure 5.2). In squamous cancer cells, this pathway was shown to be constitutively activated (Sakaguchi et al., 2007).

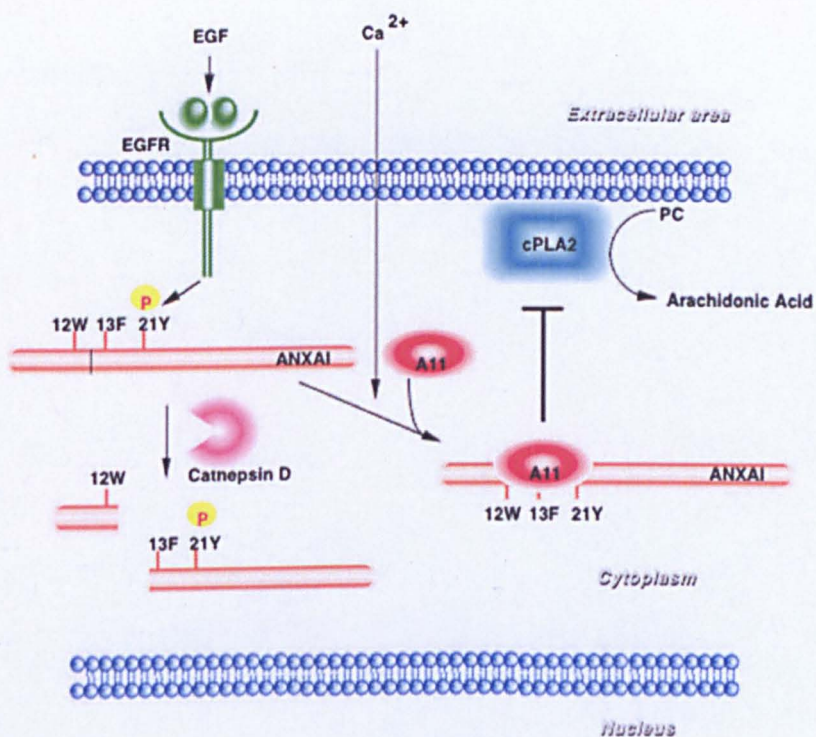


**Figure 5.2** Alternative mechanism of S100A11-mediated growth inhibition in NHK cells. EGF-activated EGFR leads to the cleavage of ANXA1. This hampers the formation of the complex with S100A11, resulting in loss of inhibition of cPLA2 activity, which is important for NHK growth (from (Sakaguchi and Huh, 2011))

More recently, the same authors have shown that in addition to being an essential mediator of growth suppression, S100A11 could also enhance growth of human keratinocytes through the induction of EGF, or other ligands of the EGF receptor, functioning as a dual mediator for growth regulation of epithelial cells (Sakaguchi et al., 2008). Extracellular



S100A11 binds to its receptor, RAGE, and this signal causes intracellular Akt phosphorylation. Activated Akt can phosphorylate CREB, which liberates CREB from the seventh AP-1 site of EGF promoter, and then, AP-1 binds to the spare site and triggers the transcription of EGF, and causes cell growth (Figure 5.3). Production and secretion of S100A11 are markedly enhanced in human squamous cancer cells. These findings indicate that S100A11 plays a dual role in growth regulation, being suppressive in cells and being promotive from outside of cells (Sakaguchi et al., 2008).

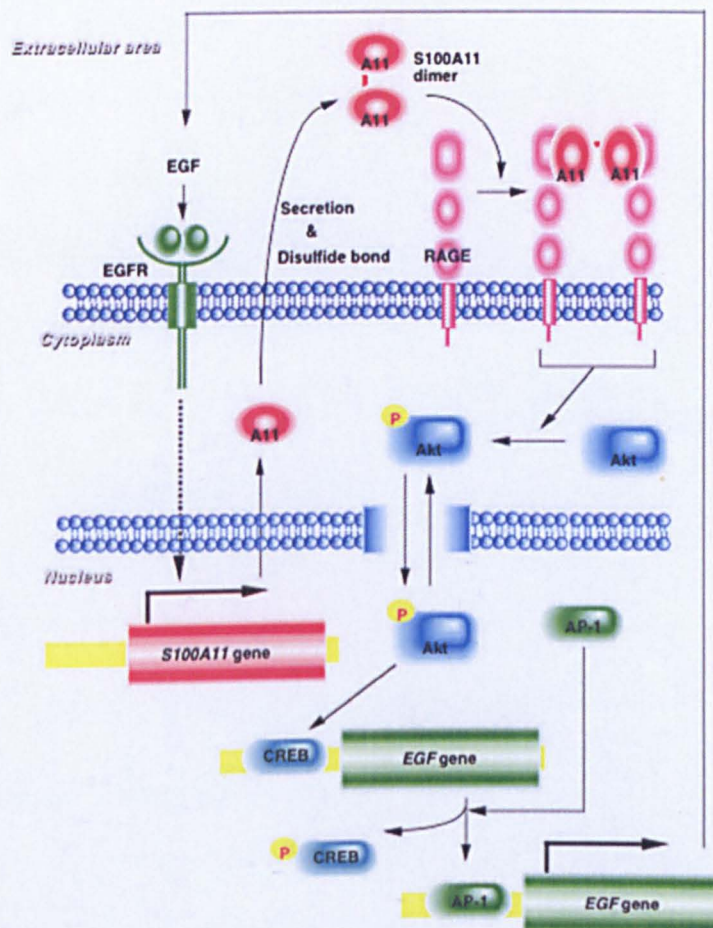


**Figure 5.3 Mechanism of S100A11-mediated growth promotion in NHK cells.** The EGF/EGFR pathway activation induces the expression and secretion of S100A11. The secreted S100A11 protein binds to RAGE and promotes the activation of Akt signalling pathway, resulting in the induction of EGF family proteins expression (from (Sakaguchi and Huh, 2011))

S100A11, as other members of its family, is supposed to regulate cytoskeleton dynamics and have a significant influence on cell morphology by interacting with the components of cytoskeleton. It has been shown that S100A11 can bind, in a  $\text{Ca}^{2+}$ -dependent manner, to the N-terminal domain of ANXA1. This interaction is indispensable for membrane localization of S100A11 (Sakaguchi et al., 2007). Besides ANXA1, S100A11 could interact with annexin II (Rintala-Dempsey et al., 2006) and annexin IV (Chang et al., 2007). It is proved that S100A11 can associate with actin (Sakaguchi et al., 2000; Zhao et al., 2000),  $\beta$ -tubulin (Broome and Eckert, 2004) and intermediate filaments (Bianchi et al., 2003). S100A11 also controls actin organization and causes the formation of the cells protrusions (Sakaguchi et al., 2000). S100A11 is shown to be essential for pseudopod protrusions and tumour cell migration and invasion. Knockdown of S100A11 in metastatic cells resulted in reduced actin cytoskeleton dynamics and induction of mesenchymal-epithelial transition (MET) (Shankar et al., 2010).

Among the biological roles of S100A11, a recent study demonstrates that it mediates hypoxia-induced mitogenic factor (HIMF)-induced smooth muscle cell migration, vesicular exocytosis and nuclear activation (Fan et al., 2011). In rat lung hypoxia resulted in transcriptional activation of the S100A11 promoter through hypoxia-inducible factor-1 (HIF-1) (Amano et al., 2003).

More recently, the involvement of S100A11 in DNA repair mechanisms has been demonstrated. Murzik et al. (Murzik et al., 2008) found a specific interaction of S100A11 and Rad54B, a DNA-dependent ATPase, involved in recombinational repair of DNA damage. S100A11/Rad54B foci are spatially associated with sites of DNA double-strand breaks (DSBs). Furthermore, downregulation of S100A11 by siRNA abolished Rad54B targeting to DSBs and drastically reduced p21WAF1/CIP1 protein levels, that are normally increased in cells undergoing DNA repair. Gorsler et al. (Gorsler et al., 2010) found that DNA damage induces a nucleolin-mediated translocation of S100A11 from the cytoplasm to the nucleus, resulting in the increase of p21WAF1/CIP1 protein level. This translocation is impeded by

inhibition of the phosphorylation activity of PKC $\alpha$ . These observations suggest that regulation of the subcellular distribution of S100A11 plays an important role in DNA damage response and p21-mediated cell cycle control.

There have been various speculations about the specific function of S100A11 in cancer and tumour promoting, as well as tumour suppressor roles proposed. A tumour promoting role has been suggested by a large number of studies of different tumour types.

In neoplasms such as colon cancer (Tanaka et al., 1995; Wang et al., 2008), uveal malignant melanoma (Van Ginkel et al., 1998), and anaplastic large cell lymphoma (Rust et al., 2005). S100A11 was highly expressed. S100A11 expression was also found significantly increased in leiomyoma compared with myometrium and suppression of S100A11 by siRNA led to apoptosis in human uterine smooth muscle tumour cells (Kanamori et al., 2004). S100A11 could also sustain the cell growth of squamous carcinoma cell lines (Sakaguchi et al., 2008) and may be involved in prostate cancer development and progression (Rehman et al., 2004). By gene expression analysis Mori *et al.* (Mori et al., 2004) found *S100A11* gene overexpressed in gastric adenocarcinoma specimens with respect to non-cancerous mucosa, and this was associated with the presence of lymph node metastasis. This suggested that *S100A11* gene expression status could be useful to predict gastric cancers with lymph node metastases. By immunohistochemical analysis, a significant high level of S100A11 in primary non small cell lung carcinoma (NSCLC) tissues was associated with higher tumour-node metastasis stage and positive lymph node status, suggesting S100A11 involvement in promoting invasion and metastasis (Tian et al., 2007). Hao *et al.* found that both mRNA and protein levels of S100A11 were overexpressed in adenocarcinomas (ADC) and squamous cell carcinomas (SCC) compared with paired non-cancerous lung tissues, while S100A11 was detected downregulated in small cell lung cancers (SCLC). They found S100A11 protein level increased in the sera of NSCLC patients. When *S100A11* was knocked down in lung

adenocarcinoma cells the cell proliferation was significantly inhibited *in vitro* and *in vivo* (Hao et al., 2012).

However, on the other hand, S100A11 could act as a tumour suppressor in some cancers.

Kondo et al. (Kondo et al., 2002) found a decrease in the S100A11 immunostaining levels in some tumours, such as lung, breast, kidney, prostate, uterus and testis. S100A11 is also downregulated in esophageal squamous cell carcinoma (Ji et al., 2004). In pancreatic tumours, it has been proposed that overexpression of S100A11 may be an early tumourigenic event and then expression of S100A11 may be decreased during subsequent progression to a more malignant phenotype (Ohuchida et al., 2006). Low expression of S100A11 was associated with poor survival of bladder cancer patients, and its expression was suppressed during early development of bladder cancer (Memon et al., 2005). In breast cancer, there is controversy regarding the expression pattern, subcellular localization and functions of S100A11. Kondo et al. (Kondo et al., 2002) found that the expression of S100A11 was decreased in breast tumour cells and found a prevalent cytoplasmic staining in normal tissues. Cross et al. (Cross et al., 2005) found that S100A11 displayed increased expression in breast carcinoma and the subcellular localization changed from a strictly nuclear-localization in normal tissue to a more cytoplasmic-localization in tumour tissues suggesting that, in breast carcinomas, the loss of nuclear translocation may lead to the inability to control or suppress cell growth.

### 5.1.2. *S100A11* and thyroid cancer

Different studies of gene expression profiling reported *S100A11* as a gene differentially expressed in thyroid carcinogenesis. Jarzab *et al.* (Jarzab *et al.*, 2005) found *S100A11* in a list of genes whose expression is increased in PTC in comparison with normal samples. In the analysis performed by Stolf *et al.* (Stolf *et al.*, 2005), *S100A11* was found overexpressed in papillary carcinomas as compared to normal thyroid, adenomas and goiter. More recently, *S100A11* was found overexpressed in PTC with respect to benign thyroid tissue, however not included among genes able to discriminate between the follicular and classical variant of PTC (Finn *et al.*, 2007).

Concomitantly with gene expression studies, *S100A11* was also analysed by immunohistochemistry. By comparative 2-dimensional gel electrophoresis of microdissected cells from tumours and normal tissue, Torres-Cabala *et al.* (Torres-Cabala *et al.*, 2004) identified *S100A11*, among several proteins belonging to different categories, highly expressed in papillary thyroid carcinoma. By immunohistochemical analysis, *S100A11* protein was found expressed in the nuclei of normal tissue, hyperplastic nodules and follicular adenomas and carcinomas, whereas PTC showed a strong, but cytoplasmatic, pattern of staining. These findings suggested that immunohistochemical staining of *S100A11* could be helpful in the pathological assessment of thyroid lesions, especially in cases in which follicular variants of PTC and FTC are considered in the differential diagnosis. In a subsequent study, the same authors proposed *S100A11*, in association with galectin-1 and galectin-3, helpful in discriminating between benign and malignant thyroid lesions (Torres-Cabala *et al.*, 2006).

## 5.2 Aims of the chapter

The aim of this chapter is to study the involvement of S100A11 in thyroid carcinogenesis. We tried to gain insight into the relevance of S100A11 in PTC biology, performing analysis of gene expression data sets and functional studies in different cellular models. In particular, in the PTC-derived K1 cell line we investigated:

- the sub-cellular localization of S100A11;
- a possible interaction of S100A11 with the EGF/EGFR pathway;
- the effect of RNA interference-mediated knockdown of S100A11 expression, by performing *in vitro* and *in vivo* studies.

In parallel, we assessed the effect of *S100A11* gene modulation on the transforming potential of the PTC-associated *TRK-T3* oncogene in NIH3T3 cells, which represent a useful model for studying *in vitro* oncogene activity.



### 5.3 Results

#### 5.3.1. Expression analysis of *S100A11* in PTC samples and PTC-derived cell lines

*S100A11* expression has been proposed as a discriminating factor between benign and malignant thyroid disease (Torres-Cabala et al., 2006). Expression level of *S100A11* gene was first investigated by analyzing cDNA microarray data previously produced in our laboratory. Data were obtained using RNA from a collection of 9 normal thyroid tissues (N) and 31 PTCs. Analysis of the expression levels of *S100A11* in all the samples showed that *S100A11* was significantly overexpressed in a large percentage of PTC cases (19 out of 32, 59.4 %) ( $p < 0.01$ ) (Figure 5.4).



**Figure 5.4 cDNA array expression of *S100A11* gene.** Graphic representation of the expression level in normal thyroid samples (N, green) and papillary thyroid carcinomas (PTC, blue). The expression level (relative expression, RE) of the *S100A11* gene in all the tissue samples hybridized on the array was measured as log ratio between the expression level of the specimens and that of the reference. Gene showing a positive log ratio value (ie more expressed in the thyroid sample than in the reference) is called upregulated; that with a negative log ratio value is called downregulated.

*S100A11* expression in PTC was also analysed by performing metanalysis of several publicly available data sets. As shown in Figure 5.5, in Jarzab (Jarzab et al., 2005)(a), Huang (Huang et al., 2001a) (b) and Reyes (Reyes, 2006) (c) data sets, a significant increased expression of *S100A11* ( $p<0.05$ ) was observed in PTC samples in comparison with controlateral normal tissues. In the Vasko data set (Vasko et al., 2007)(d), such increase of expression was statistically significant only comparing the invasive regions of PTCs with the corresponding normal region. Collectively, data obtained in our laboratory and meta-analysis strongly indicate that *S100A11* is frequently overexpressed in PTC.

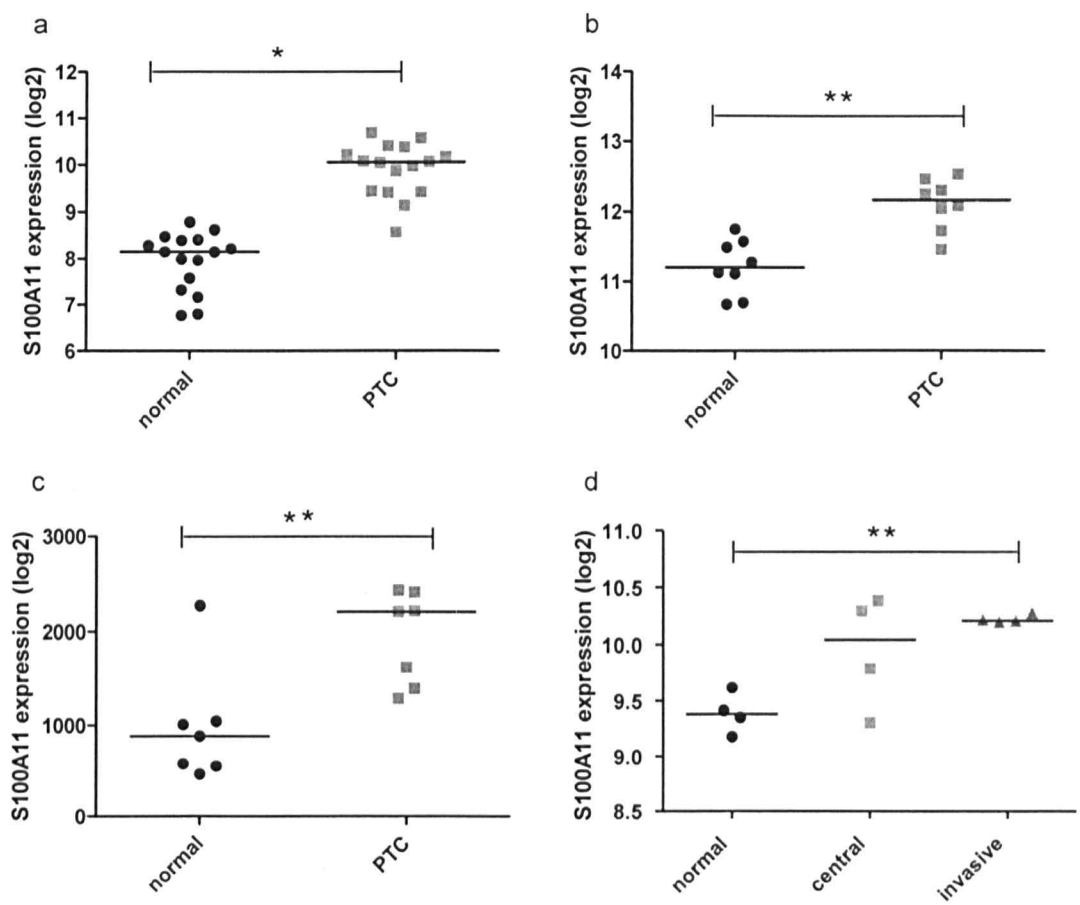


**Figure 5.5 Meta-analysis of *S100A11* gene expression levels in PTC in four different data sets.** Data are reported as scatter plots of log2 values and median is recorded. In Jarzab (a) Huang (b) and Reyes (c) data sets *S100A11* expression was increased in PTC when compared with the normal thyroid in paired tissues samples ( \*\*  $p<0.01$  or \*  $p<0.05$  by Wilcoxon paired test). In the Vasko data set (d) a statistically significant increase of *S100A11* expression was found in the invasive regions of PTC in comparison with the corresponding normal region (\*\*  $p<0.01$  by Wilcoxon paired test).



We analysed the expression of *S100A11* mRNA in a panel of PTC-derived cell lines by reverse transcriptase-PCR (RT-PCR). The following cell lines were used: TPC1, NIM1, BCPAP and K1. Except for TPC1 which carries *RET/PTC1* oncogene, the other cell lines harbour the *BRAFV600E* mutation (details of the mutational status of these cell lines are reported in table 3.2 of material and methods section). As control, we used the Nthy-ori 3-1 cells (N-Thy), normal human thyrocytes immortalized by the SV40 large T antigen, and normal thyrocytes (N), derived from normal thyroid tissue.

The experiment reported in Figure 5.6a showed that *S100A11* mRNA was abundantly expressed in all PTC-derived cell lines, whereas it was barely detectable in the controls.

The data were also confirmed by quantitative real time analysis (5.6b).

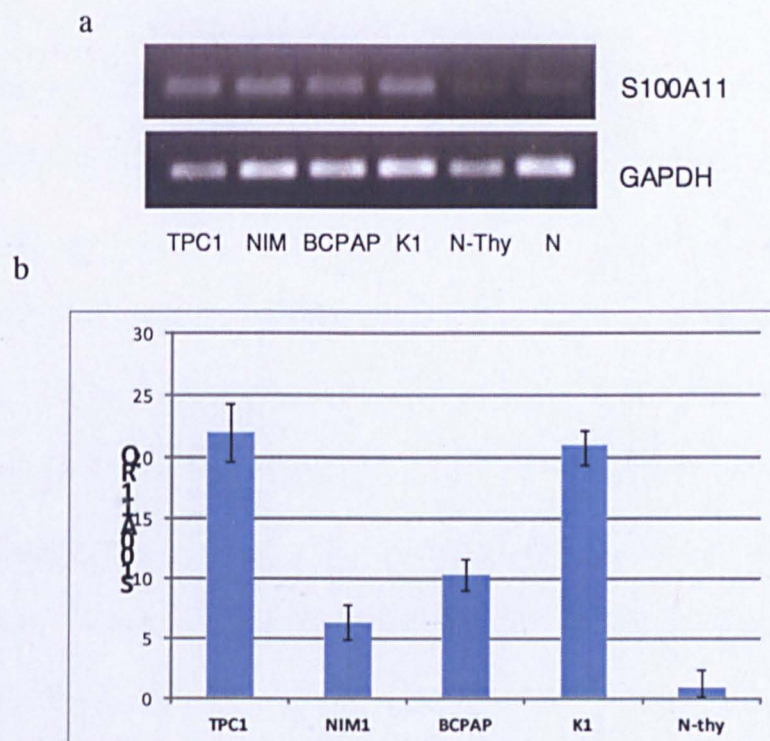


**Figure 5.6** Detection of *S100A11* expression in a panel of PTC-derived cell lines a) *S100A11* mRNA expression by RT-PCR analysis; *GAPDH* gene was used as loading control; b) *S100A11* mRNA expression by real time RT-PCR (N-Thy: NThy-Ori 3-1 cell line, N: normal thyrocytes); RQ, relative quantity of *S100A11* mRNA normalised for HPRT housekeeping gene expression)

### 5.3.2 Analysis of cellular localization of S100A11

Based on the results of *S100A11* mRNA expression reported above, as a model for our studies we selected K1 cell line, derived from a PTC, carrying the *BRAFV600E* mutation, and tumourigenic in nude mice as demonstrated in previous studies (Ferrario et al., 2008).

S100A11 has been demonstrated to play different roles depending on its cellular localization. With respect to the thyroid, S100A11 was found mostly nuclear in normal tissue, whereas cytoplasmic in PTC (Torres-Cabala et al., 2004). To assess S100A11 localization in PTC-derived cell lines, we performed cellular fractioning of K1 cells and investigated the presence of S100A11 in nuclear and cytoplasmic fraction by western blot analysis with the anti-S100A11 antibody. The quality of cytoplasmic and nuclear fractions was assessed using  $\beta$ -tubulin and NBS1 antibodies, respectively. As shown in Figure 5.7 a, we found that S100A11 localized in the cytoplasm and was absent in nuclear fraction of K1 cells. The cytoplasmic localization was also observed in other thyroid derived cell lines (data not shown). According to the model proposed by Sagakuci *et al* in human primary keratinocytes, an increase of extracellular  $\text{Ca}^{2+}$  or TGF- $\beta$  stimulation promotes nuclear translocation of S100A11 and consequently cell growth arrest through the induction of p21 expression. We then investigated whether in our cellular model S100A11 was able to translocate into the nucleus upon  $\text{Ca}^{2+}$  or TGF- $\beta$  stimulation. We treated K1 cells with different concentrations of  $\text{Ca}^{2+}$  (10 mM and 1.5 mM) for 6 hours and then performed cell fractionation. In untreated cells the S100A11 protein was mainly present in the cytoplasmic fraction, whereas after  $\text{Ca}^{2+}$  stimulus we observed a dose dependent increase of S100A11 level in the nuclear fractions (Figure 5.7 b). The analysis of K1 cells treated with  $\text{Ca}^{2+}$  1.5 mM for different times showed an increase of S100A11 protein in the nuclear fraction after 1hour of treatment, followed by a slight decrease after 16 and 24 hours. In parallel, the analysis of cytoplasmic fractions showed an opposite effect: after 1h we observed a striking decrease of the amount of S100A11 protein up to a slight increase

at 16 and 24 hours (Figure 5.7 c). Concomitantly, we investigated the effect of  $\text{Ca}^{2+}$  stimulation on the expression of p21 and S100A11 proteins. As shown in western blot analysis of whole cell extracts, the amount of both proteins remained unchanged after  $\text{Ca}^{2+}$  treatment (Figure 5.7 d).

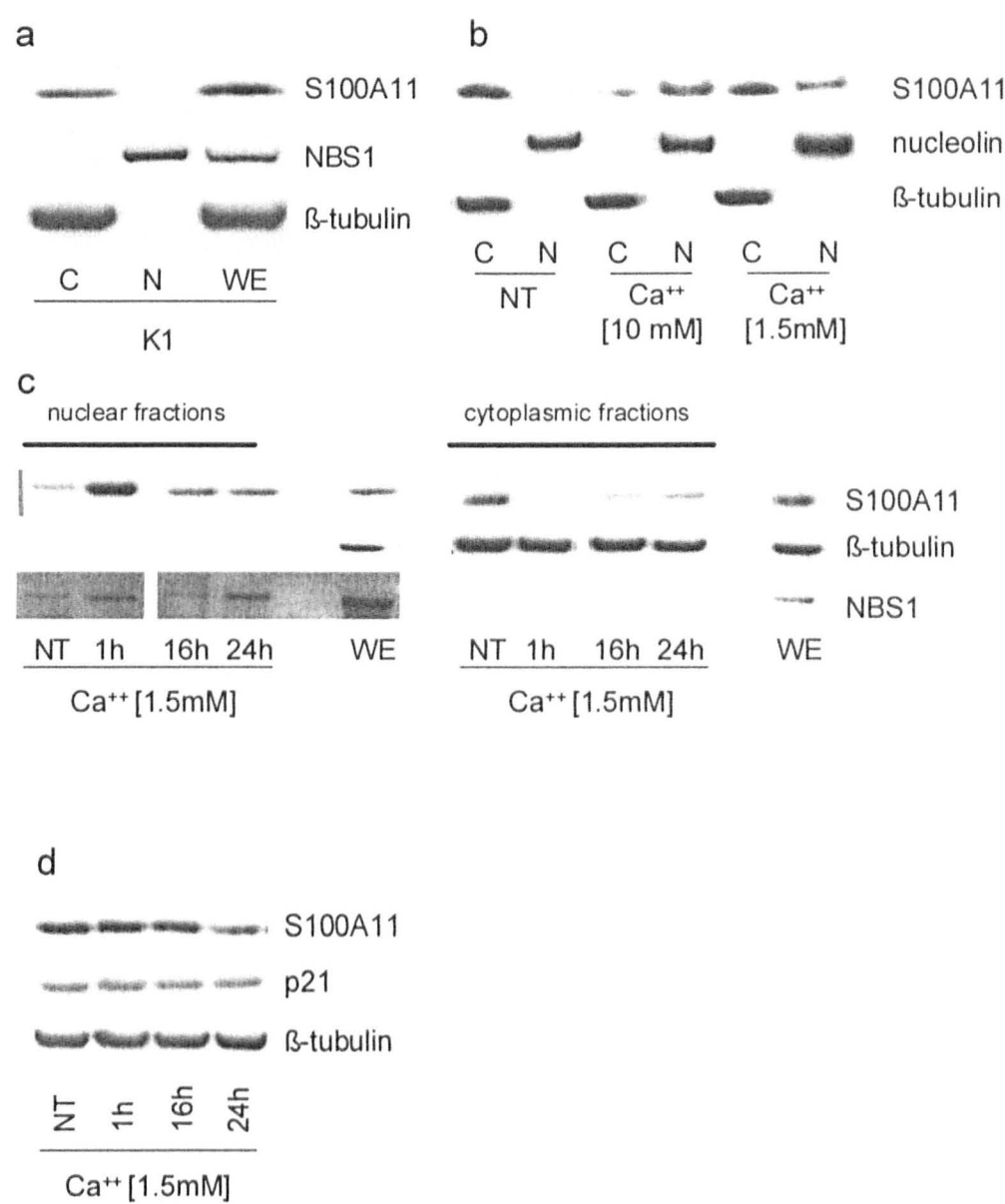


**Figure 5.7 Analysis of S100A11 localization after  $\text{Ca}^{2+}$  stimulation.** a) western blot analysis of S100A11 expression after K1 cells fractionation (C: cytoplasmic fraction; N: nuclear fraction; WE: whole protein extract); b) K1 cells were treated for 6 hours at different  $\text{Ca}^{2+}$  concentration (10 and 1.5 mM) and fractionated for the analysis of S100A11 expression.; c) S100A11 expression in K1 nuclear fractions (left panel) and cytoplasmic fractions (right panel) after treatment with  $\text{Ca}^{2+}$  at the indicated time points. The quality of cytoplasmic and nuclear fractions was assessed using  $\beta$ -tubulin and NBS1 (nucleolin for Figure b) antibodies, respectively; d) analysis of S10A11 and p21 expression in whole protein extracts of K1 cells treated with  $\text{Ca}^{2+}$  at the indicated time points.  $\beta$ -tubulin was used as loading control for cell extracts.

In order to investigate the effect of TGF- $\beta$  on S100A11 localization, we treated K1 cells with TGF- $\beta$  for 1 and 8 hours. Cell fractionation showed that in untreated cells and in cells treated for 1 hour, the S100A11 protein was mainly cytoplasmic; after 8 hours of treatment, S100A11 was equally found in nuclear and cytoplasmic fractions, indicating a nuclear translocation (Figure 5.8 a). NBS1 and  $\beta$ -tubulin distributions are shown as control for nuclear and cytoplasmic fraction quality, respectively. Moreover, the treatment of K1 cells with TGF- $\beta$  at different time points did not alter the total protein levels of S100A11 (5.8 b). As control, the increase of SMAD2 phosphorylation, indicating the efficacy of the TGF- $\beta$  treatment, is shown (Figure 5.8 b).

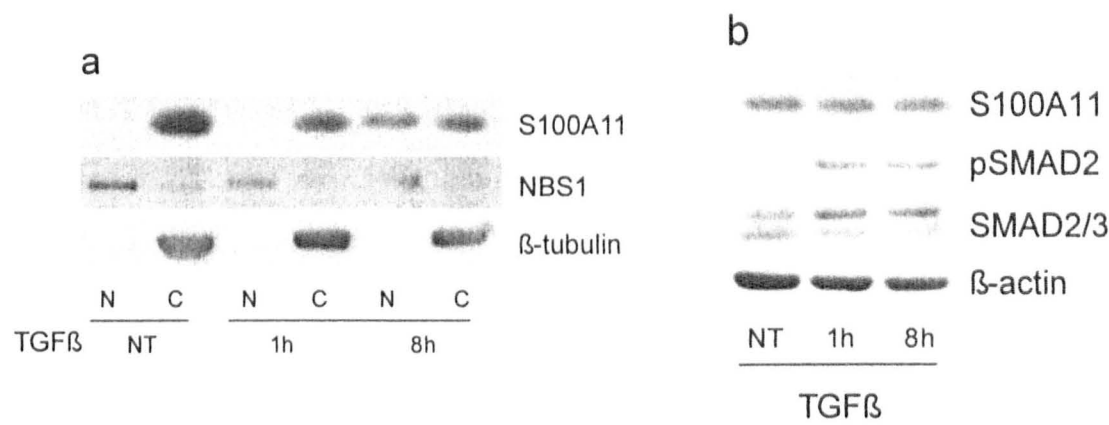


**Figure 5.8 Analysis of S100A11 localization after TGF- $\beta$  stimulation.** a) K1 cells were treated with TGF- $\beta$  (10ng/ml) for 1 and 8 hours and fractionated for the analysis of S100A11 expression (C: cytoplasmic fraction; N: nuclear fraction); the quality of cytoplasmic and nuclear fractions was assessed using  $\beta$ -tubulin and NBS1 antibodies, respectively; b) analysis of S100A11, pSMAD2 and SMAD2/3 protein expression after treatment of K1 cells with TGF- $\beta$  (10ng/ml) at the indicated time points.  $\beta$ -actin was used as loading control for cell extracts.

### 5.3.3 Analysis of interaction between S100A11 and EGF/EGFR pathway

According to the model proposed by Sagakuci *et al* in human primary keratinocytes, S100A11 could have a growth promoting role related to its involvement in the EGF/EGFR pathway. To investigate whether the cross-talk between S100A11 and EGF/EGFR takes place also in thyroid tumour cells, we first analysed the effect of EGF on S100A11 levels in K1 cells. As shown in Figure 5.9 a, treatment of K1 cells with EGF for different time points did not alter S100A11 protein levels. To investigate whether S100A11 affected the EGF-triggered signalling, we analysed the EGFR, AKT and ERK 1/2 phosphorylation in K1 cells transiently transfected with S100A11-myc construct, treated or not with EGF. As control, untransfected and empty vector (EV) transfected cells were used (the details of S100A11-myc expression plasmid are reported in material and methods section). As shown in Figure 5.9 b (left panel), in untreated cells basal phosphorylation of EGFR, AKT and ERK 1/2 was not altered by S100A11 overexpression. Similarly, cells overexpressing S100A11-myc protein showed comparable levels of EGF-induced EGFR, AKT and ERK 1/2 phosphorylation as control cells. These data indicate the lack of the effect of S100A11 on EGF-triggered pathways. In keeping with this result, the activation of these pathways was not altered in S100A11-silenced cells in comparison with the control (Figure 5.9 b, right panel). (Details for S100A11 silencing are reported in the next paragraph). The control of S100A11 overexpression and downregulation in K1 cells is shown in Figure 5.8 c.

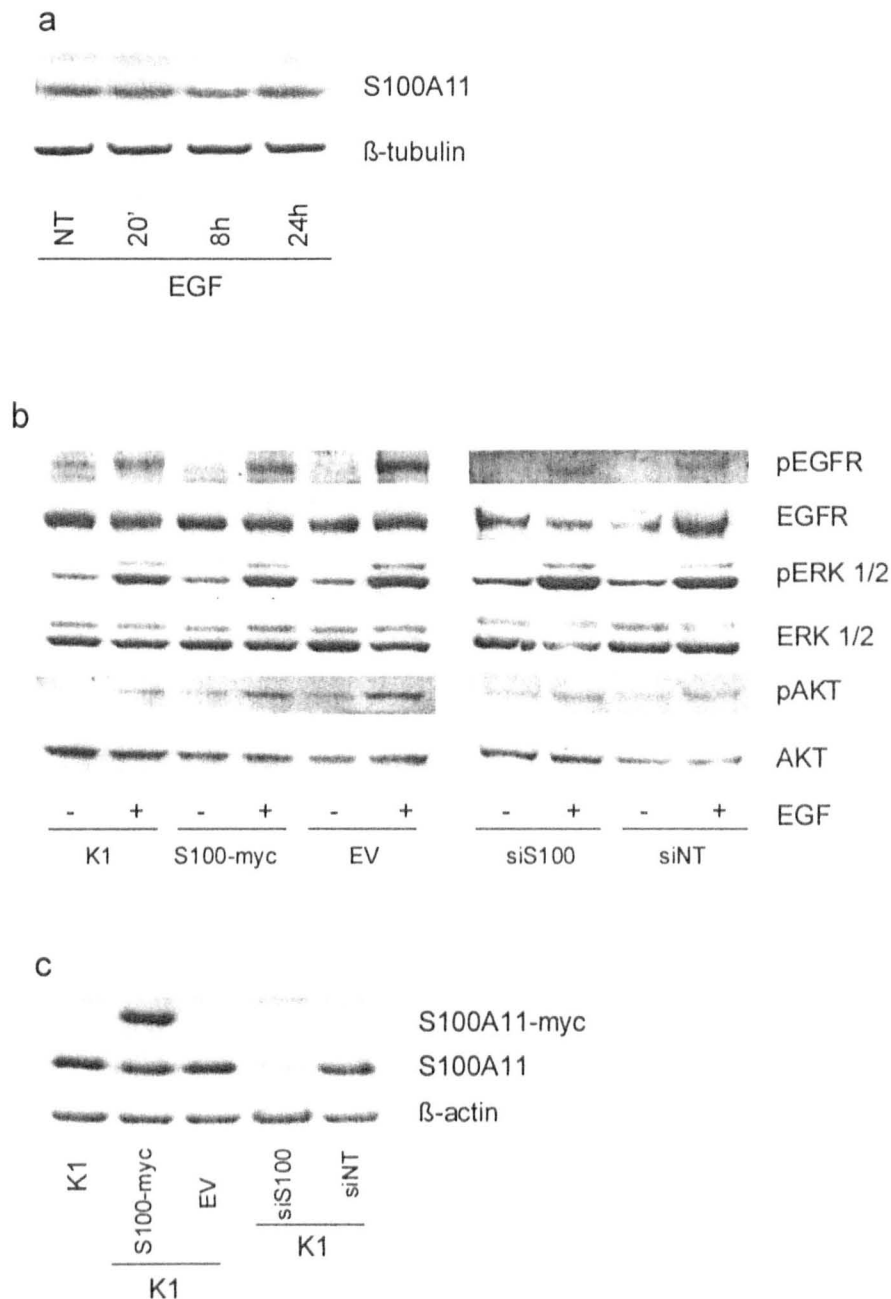


**Figure 5.9 Analysis of interaction between S100A11 and EGF/EGFR pathway.** a) western blot analysis S100A11 expression after treatment of K1 cells with EGF (20 ng/ml) at the indicated time points. β-tubulin was used as loading control for cell extracts; b) western blot analysis of the EGFR, AKT and ERK 1/2 phosphorylation of parental K1 cells and K1 cells transiently transfected with S100A11-myc construct (left panel) or S100-silenced K1 cells (siS100) (right panel), treated or not with EGF (20ng/ml) for 20 minutes. (EV: empty vector, siNT (si Non Targeting)). Total EGFR, ERK 1/2 and AKT were used as loading control of cell extracts; c) S100A11 expression in K1 cells transiently transfected with S100A11-myc construct and in S100A11-silenced K1 cells. β-actin was used as loading control of cell extracts (the same panel was used in Figure5.10)



### 5.3.4. Effect of *S100A11* silencing

#### 5.3.4.1 Transient silencing of *S100A11*

In order to investigate the biological effect of *S100A11* silencing, K1 cells were transiently transfected with specific *S100A11* small interfering RNAs (siS100). As control, non targeting small interfering RNAs (siNT) were used. Western blot analysis showed that *S100A11* protein was efficiently knocked-down after 72 hours from siRNAs transfection (Figure 5.10 a). The analysis at different time points showed that the abrogation of *S100A11* expression was maintained at least until day seven after transfection.

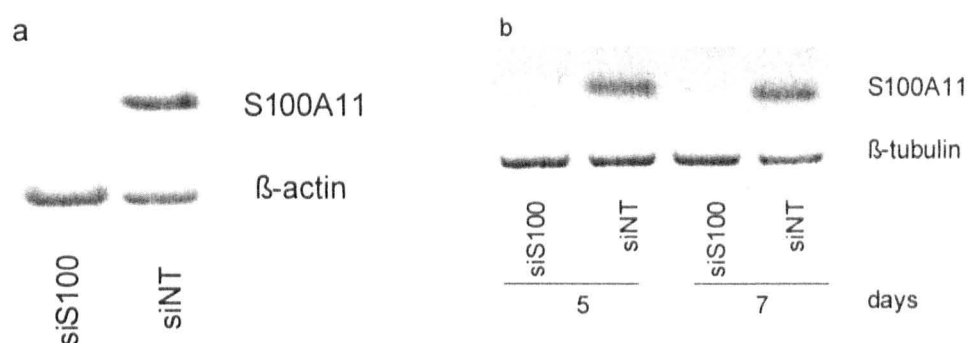


**Figure 5.10 Transient silencing of *S100A11* in K1 cells.** Western blot analysis of *S100A11* expression in K1 cells transiently transfected with small interfering RNAs (siS100 and siNT (Non Targeting)) as control. The analysis was carried out 72 hours (a) and 5 and 7 days after transfection (b).  $\beta$ -actin and  $\beta$ -tubulin were used as loading control for cell extracts (the same panel a was used in Figure 5.9)

To investigate whether the loss of *S100A11* expression affected cellular proliferation, K1 cells were transfected with siRNAs and cell growth analysis was performed after 72 hours and followed for a further 3 days. As shown in Figure 5.11 a *S100A11*-silenced K1 cells (K1 siS100) displayed the same growth rate as control cells (K1 siNT). Flow cytometric analysis performed 72 hours after transfection showed that K1 siS100 cells had a similar cell cycle distribution in comparison with control cells (Figure 5.11 b).

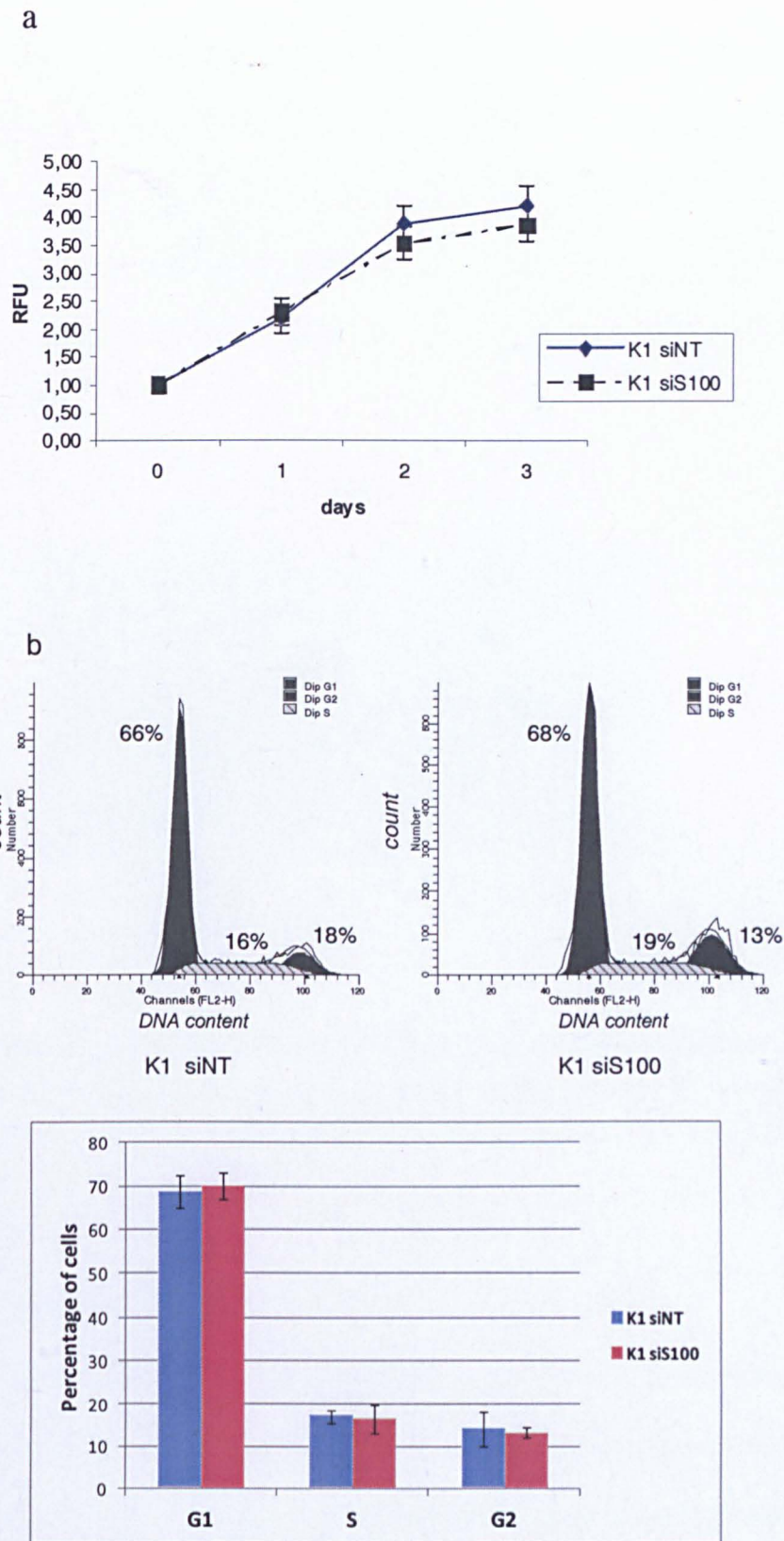


**Figure 5.11 Effect of transient *S100A11* silencing on growth rate.** a) proliferation of K1 cells transiently transfected with specific siRNAs (siS100 and control siNT). The analysis was carried out after 72 hours of transfection and conducted for 3 days. The growth rate was determined by the alamarBlue Assay. At the indicated time points, the relative fluorescence unit (RFU) was determined and data were normalized for values at day 1; b) top: flow cytometric analysis of K1 cells after 72 hours from transfection with siS100 and siNT RNAs; percentage of cell cycle distribution is shown; bottom: the data represent the percentage average of cells in different stages of the cell cycle of three independent experiments.

The effect of S100A11 silencing on cell proliferation was also assayed by colony forming assay. K1 siS100 cells and K1 siNT cells were plated at low density 96 hours after transfection and cultured for 7 days. No difference between the two samples was observed, as both produced colonies with similar efficiency and dimension.

Collectively, these data indicate that the knockdown of S100A11 protein does not affect K1 cell growth

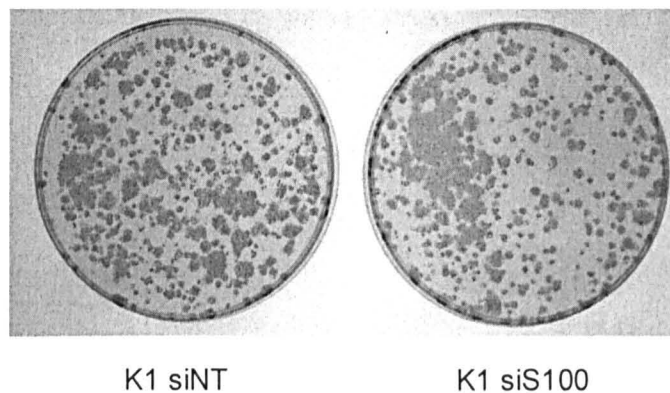


**Figure 5.12** Analysis of the effect of S100A11 on growth rate by colony forming assay. K1 cells were transfected with specific siRNAs (siS100 and siNT). After 96 hours from transfection, a total of 2000 cells were plated into 60mm Petri dishes; colonies were fixed and stained after 7 days. Representative pictures are reported.

#### 5.3.4.2 Stable silencing of *S100A11*

We investigated the long term effect of a stable S100A11 knockdown using short-hairpin RNA technology. K1 cells were transfected with four independent expression vectors carrying the shRNA cassette specific for *S100A11* gene downregulation (sh1, sh2, sh3 and sh4) and a vector containing a non effective (scrambled) shRNA cassette (sh scr), as control, and analysed 3 days later. The most efficient silencing of S100A11 was observed in K1-sh1 and K1-sh2 cells, showing S100A11 protein level reduced by 50% and 82%, respectively, with respect to K1-sh scr cells (Figure 5.13 b). Cells were grown under

antibiotic selection and used for further studies. The S100A11 knockdown was periodically monitored and found maintained at least for 80 days (data not shown).

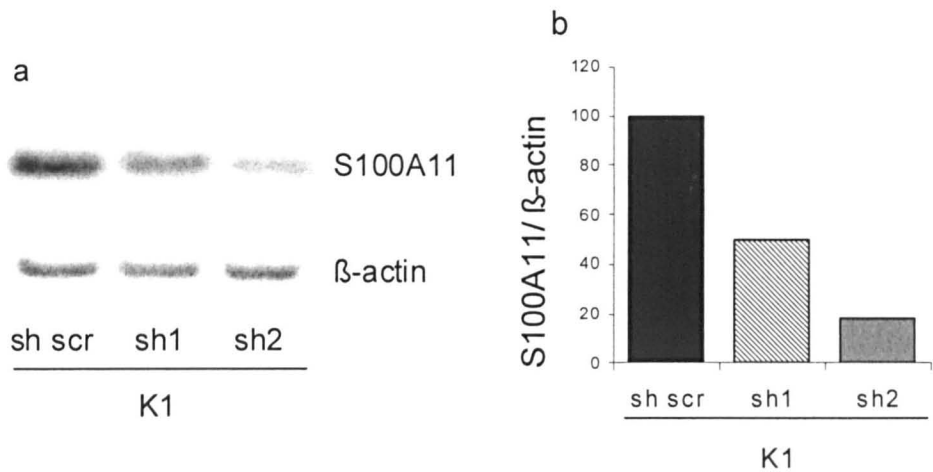


**Figure 5.13 Knockdown of S100A11 expression in K1 cells.** a) western blot analysis of S100A11 expression in K1 cells after 72 hours from transfection with sh1 and sh2. A scrambled shRNA (sh scr) was used as control.  $\beta$ -actin was used as loading control for cell extracts; b) the graph represents the densitometric analysis of the bands. Data are reported as ratio of S100A11/ $\beta$ -actin and normalized for the sh scr value.

Similarly to the analysis carried out for the transient S100A11 silencing, we next investigated the effect of the stable silencing of S100A11 on cellular proliferation. As shown in Figure 5.14a, K1-sh1 and K1-sh2 transfected cells showed the same growth rate in comparison with the control (K1-sh scr) and the parental K1 cells. In parallel, cells were analysed for the activation of the major signal transduction pathways by western blot. The same level of ERK and AKT phosphorylation was observed in K1-sh1 and -sh2 in comparison with the controls (Figure 5.14 b).

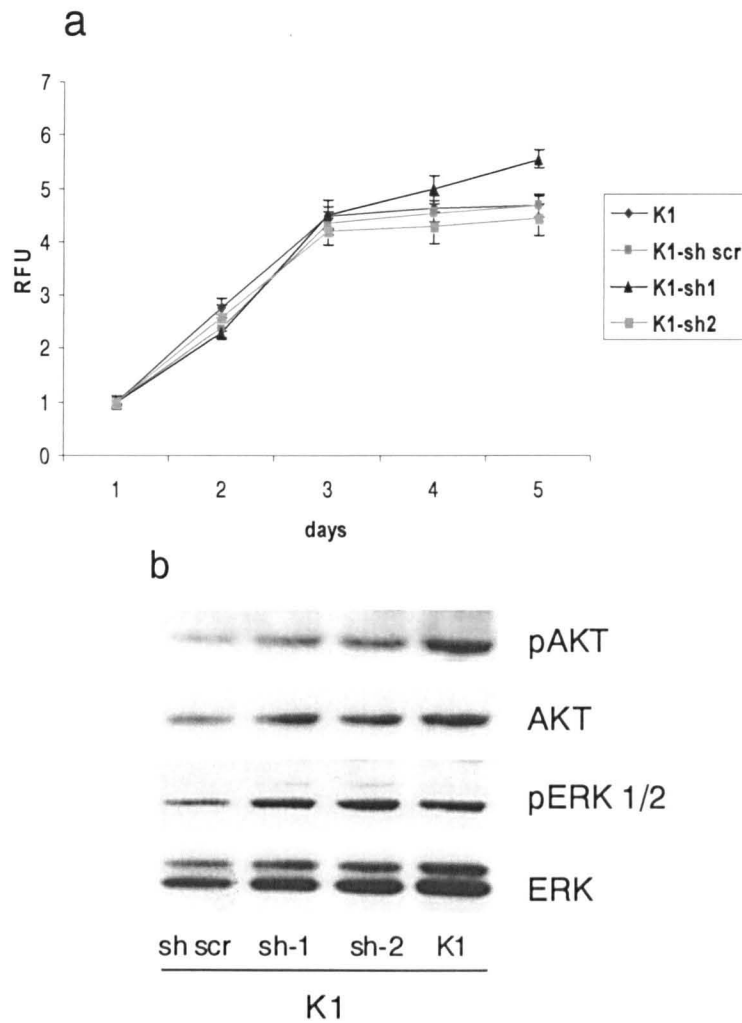


**Figure 5.14 Analysis of stable S100A11 silencing on growth rate.** a) proliferation analysis of K1-sh1 and K1-sh2 cells. K1-sh scr and parental K1 cells were used as control. The growth rate was determined by the alamarBlue Assay. At the indicated time points, the relative fluorescence unit (RFU) was determined and data were normalized for values at day 1; b) western blot analysis of AKT and ERK1/2 phosphorylation in S100A11-silenced cells. Total AKT and ERK1/2 were used as loading control for cell extracts.

We investigated whether S100A11 was necessary for anchorage-independent growth of K1 cells by performing a soft agar assay with K1-sh1 and -sh2 cells and K1-sh scr cells as control. After 3 weeks of incubation, soft agar colonies were counted. As shown in Figure 5.15a, K1-sh1 and -sh2 cells formed colonies with efficiency reduced (56%) with respect to control cells. Moreover, clones formed by S100 silenced cells were smaller than those of the control cells. Representative pictures at different magnification are reported in Figure 5.15 b.

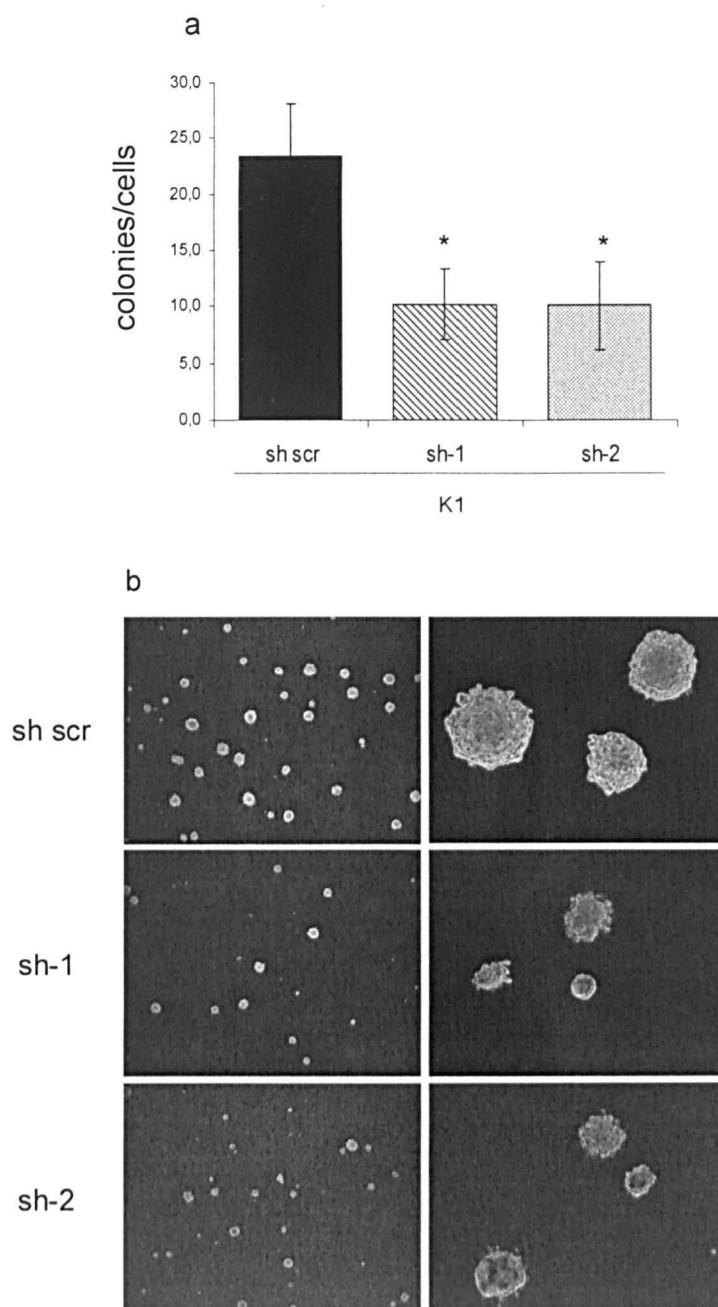


**Figure 5.15 Anchorage-independent growth of stable S100A11-silenced K1 cells.** A total number of 2500 cells were seeded in 60mm Petri dishes. After 3 weeks, the number of soft agar colonies was counted. a) Colony-forming efficiency was determined by the ratio between number of colonies and the number of plated cells. Asterisk indicates differences significant by the Student's *t*-test ( $p < 0.01$ ); b) representative pictures of colonies at different magnification are reported

### 5.3.4.3 Effect of stable *S100A11* silencing in mouse tumour xenografts

To investigate possible *in vivo* effects of *S100A11* silencing, we tested the tumourigenicity of K1-sh1 and -sh2 cells. As control, we used K1-sh scr cells, displaying tumourigenicity similar to the parental K1 cell line (data not shown). Cells were subcutaneously injected into nude mice and results are summarized in table 5.1. Tumour bearing mice were 9/10 for K1-sh scr sample, 10/10 and 8/10 for K1-sh1 and -sh2 samples, respectively. All the samples showed a similar tumour latency. In Figure 5.16 a, tumour growth rate of each cell line is reported. Collectively, we did not observe any differences in tumourigenicity of *S100A11*-silenced cells in comparison with control cells. Twenty eight days after the injection, tumours were excised and analysed for *S100A11* expression. Western blot analysis showed that the *S100A11* silencing was maintained in K1-sh1 and -sh2 derived xenografts over this period (Figure 5.16 b).

**Table 5.1** *In vivo* tumour growth of K1-sh1, -sh2 and -sh scr cells

<i>cell line</i>	<i>tumour-bearing mice</i>	<i>Days at 0.1g</i>	<i>Days at 1 g</i>
<i>K1- sh scr</i>	9/10	17(14-20)	26(21->28)
<i>K1- sh1</i>	10/10	13(11-24)	24(20->28)
<i>K1 sh-2</i>	8/10	13(11-15)	25(22-28)

K1-sh1, -sh2 and -sh scr cells ( $2.5 \times 10^6$ ) were inoculated subcutaneous into the left flank of athymic nude mice as described in Materials and Methods section. Tumour growth was assessed by evaluating tumour latency, ie days to reach 0.1 g, and by monitoring tumor weight (TW) twice a week. TW was estimated by the formula  $TW(g)=d^2 \times D/2$  where d and D are the shortest and the longest diameters of the tumour, respectively, measured in cm.

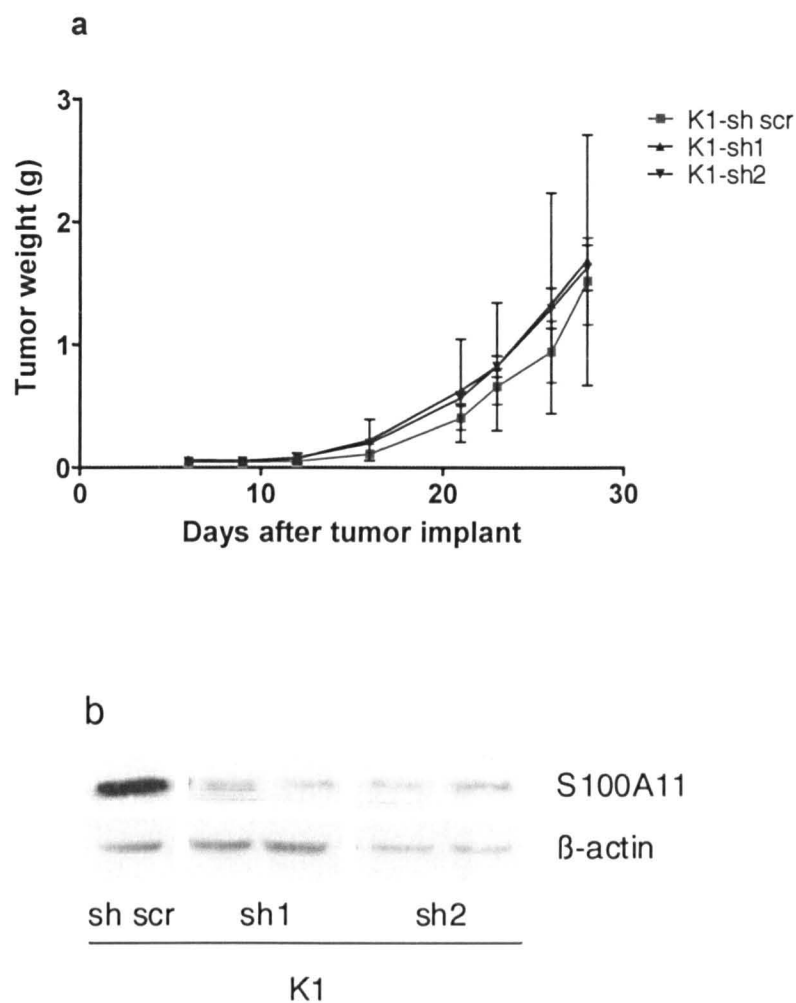


**Figure 5.16 *In vivo* tumourigenicity assay.** a) tumour growth after subcutaneously injection of K1-sh1, -sh2, -sh scr cells into the left flank of athymic nude mice. Tumour growth was monitored twice a week from day 10 to day 28; Each data point represent the mean  $\pm$  SD of 10, 8 and 9 primary tumours respectively; b) the expression of S100A11 protein in tumour explants was determined by western blot.  $\beta$ -actin was used as loading control of protein extracts.



### 5.3.5 Effect of *S100A11* on the transforming potential of *TRK-T3* oncogene

#### 5.3.5.1 *S100A11* enhances “*in vitro*” *TRK-T3* transforming activity

In the previous paragraphs we described the effect of *S100A11* silencing on tumourigenic properties of K1, a PTC-derived cell line and carrying *BRAFV600E* mutation. Here we described an alternative approach aimed to determine the effect of *S100A11* gene modulation on the transforming potential of a PTC-related oncogene, namely *TRK-T3*. We first investigated the biological consequences of concomitant stable expression of *TRK-T3* and *S100A11* in the NIH3T3 cellular system, which represents a useful model for studying *in vitro* oncogene activity. By performing focus forming assay, NIH3T3 cells were transfected with *S100A11* cDNA construct, producing a *myc*-tagged protein, and *TRK-T3* cDNA construct, alone or in combination (details of these constructs are reported in material and methods section). For all the constructs similar transfection efficiency was observed (data not shown).

As shown in Figure 5.17, *TRK-T3* transfection was able to transform, as expected, NIH3T3 cells, as previously demonstrated in our laboratory (Roccato et al., 2003); on the contrary, no transforming activity was detected for *S100A11*. When *S100A11* was transfected in addition to *TRK-T3*, we observed the enhancement of the transforming capability of the latter.

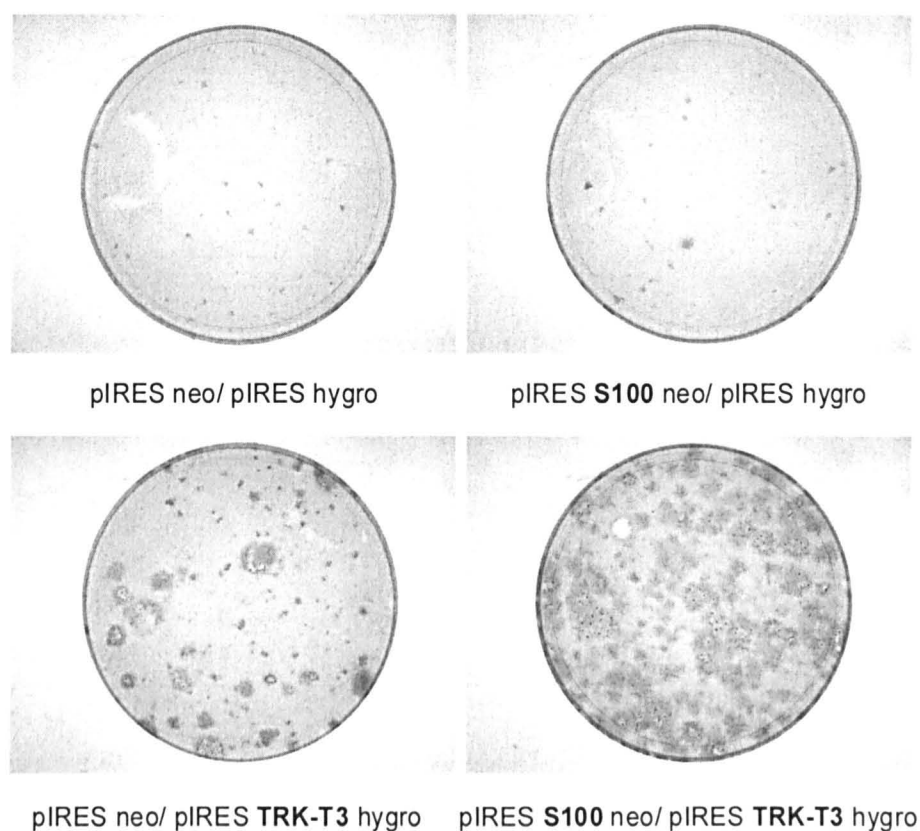


**Figure 5.17 Transforming activity of S100A11 and TRK-T3 proteins.** NIH3T3 cells were transfected with S100A11 and TRK-T3 plasmids. Empty vectors were used as control. All the constructs showed similar transfection efficiency. Focus formation assay was performed and representative plates derived from this experiment are shown.

#### 5.3.5.2 Biochemical and biological analysis of T3/S100 foci

From the above focus forming assay, we isolated transformed foci expressing the exogenous TRK-T3 protein (T3 foci: 2A and 2F) and TRK-T3 protein in addition to S100A11 protein (T3/S100 foci. 6D and 6F) (Figure 5.18 a ). No morphological differences among them were observed, since both of them displayed the typical NIH3T3 transformed phenotype, marked by loss of contact inhibition and spindle-shaped morphology (data not shown). Immunodot blot assay of conditioned media with antibody against the myc-epitope showed that 6D and 6F cells secreted the S100A11 protein (5.18

b). We next characterized these transformed foci for the major signal transduction pathways. Western blot analysis showed that all the foci showed the same level of ERKs and AKT activation (5.18 c, d).

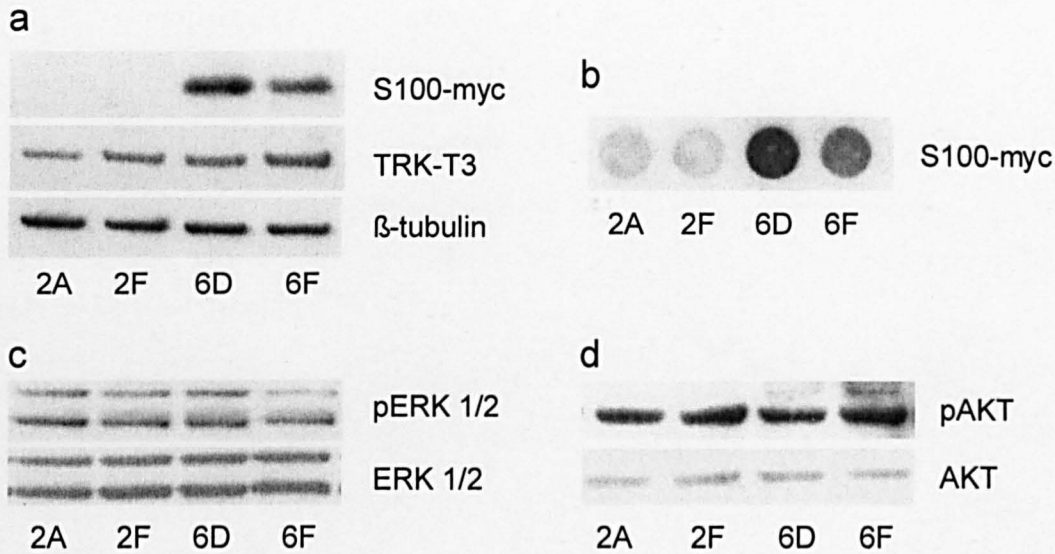


**Figure 5.18 Biochemical analysis of T3/S100 foci.** a) Western blot analysis of S100A11 and TRK-T3 expression in 2 (A,F) and 6(D,F) foci.  $\beta$ -tubulin was used as loading control for cell extracts; b) dot blot analysis of S100A11 secretion in conditioned media produced by transformed foci. Samples were normalized for cell number; c) and d) detection of ERK1/2 and AKT phosphorylation in transformed foci. Total ERK and AKT were used as loading control for cell extracts.

To investigate whether S100A11 affected cell proliferation, we determined the growth rate of the transformed foci. 2A and F foci, expressing TRK-T3 protein, and 6D and 6F foci, expressing both TRK-T3 and S100A11 proteins, displayed the same growth rate (Figure 5.19). This result was also confirmed by flow cytometric analysis of transformed foci isolated from a previous and similar focus forming assay (data not shown). These data are in keeping with the lack of effect of S100A11 on cell proliferation previously observed in K1 cellular model.

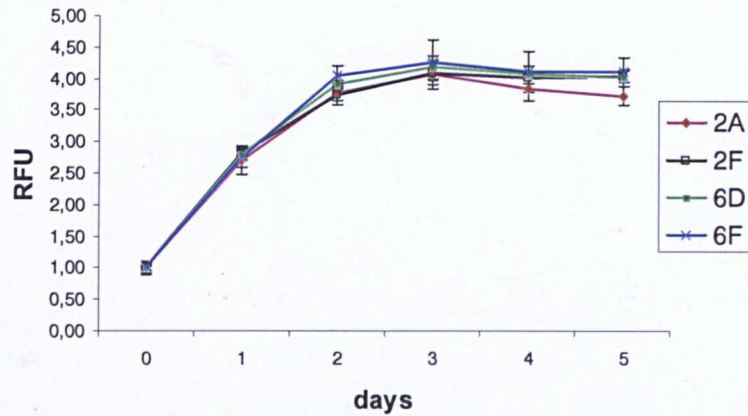


**Figure 5.19 Analysis of cell proliferation of T3/S100 foci.** Proliferation of 2 (A,F) and 6 (D,F) cells determined by the alamarBlue Assay. At the indicated time points, the relative fluorescence unit (RFU) was determined and data were normalized for values at day 1.

Several studies reported the importance of S100A11 on cell invasion. In order to investigate this issue, we performed invasion assay of 2F and 6F foci. Cells were allowed to invade through a matrigel coated transwell toward 10% FBS for 48 hours and subsequently measured through a fluorescence-based detection. As shown in Figure 5.20, 6F cells displayed a 3.5 fold increase of invasion capability with respect to 2F cells, suggesting that S100A11 enhances this property.

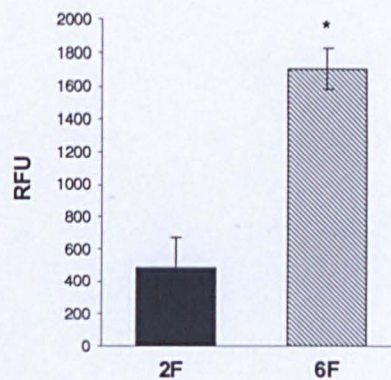


**Figure 5.20 Invasion analysis of 2F and 6F cells.**  $2 \times 10^5$  cells were allowed to invade toward 10% FBS for 48 hours. The invading cells were detected by using a fluorescent dye. Relative fluorescence unit (RFU) was determined by the ratio between the fluorescence of invading cells and total cell number. The asterisk indicates differences significant by the Student's t-test (\* $p < 0.01$ ).



Then we investigated whether S100A11 was also involved in the anchorage independent-growth, as previously demonstrated in K1 cell study. A soft agar colony forming assay of 2F and 6F foci was performed. After three weeks of incubation in soft agar, 6F cells formed colonies with efficiency 3.5 fold increased with respect to 2F cells (Figure 5.21 a). Moreover, 6F colonies showed an increase in size in comparison with the control. Representative pictures at different magnification are reported in Figure 5.21 b.

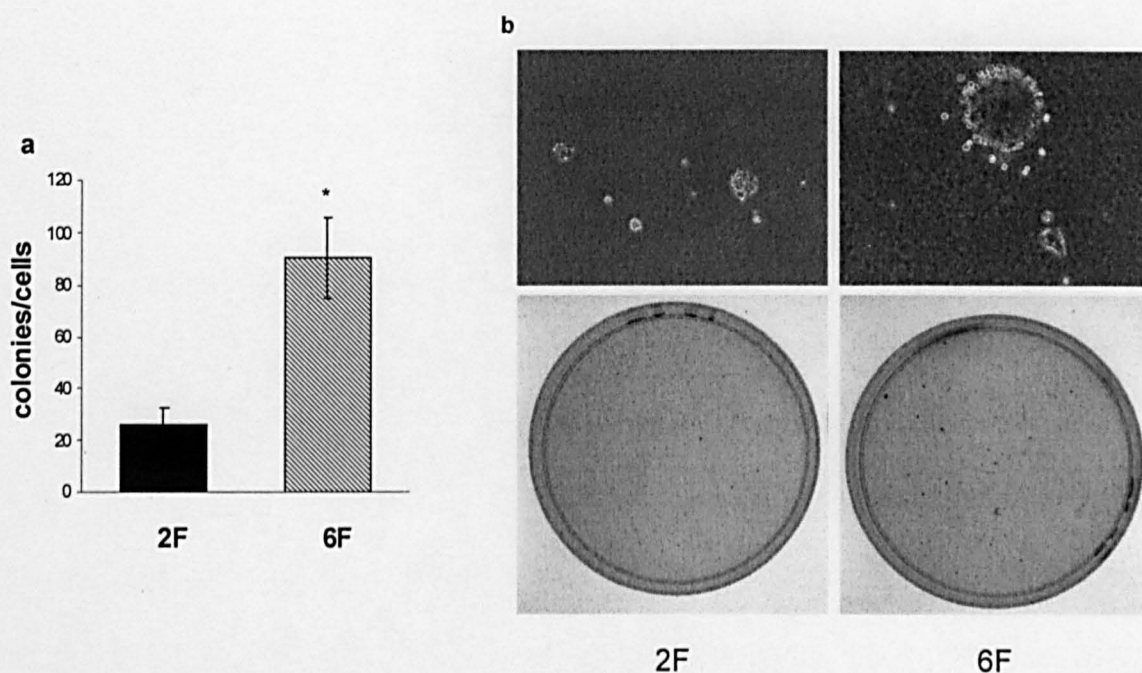


**Figure 5.21 Anchorage-independent growth of 2F and 6F foci.** A total number of  $2 \times 10^4$  cells were seeded in 60mm Petri dishes. After 3 weeks, the number of soft agar colonies were counted. a) Colony forming efficiency was determined by the ratio between number of colonies and the number of plated cells. Asterisk indicates differences significant by the Student's *t*-test ( $p < 0.01$ ); b) representative pictures of colonies at different magnification are reported.

### 5.3.5.3 Analysis of the tumourigenic capability of T3/S100 foci

To gain more insight into the contribution of S100A11 to the enhanced transforming potential of TRK-T3, an *in vivo* tumourigenicity assay was performed. Transformed NIH3T3 cells, expressing TRK-T3 (focus 2F) or TRK-T3 in association with S100A11 (focus 6F), were injected into nude mice. The expression of TRK-T3 and S100A11-myc proteins before injection was confirmed by western blot ( Figure 5.22).

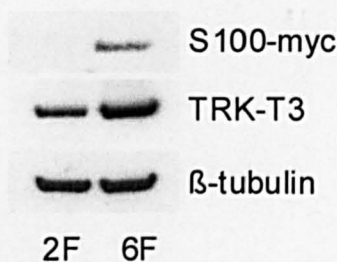


**Figure 5.22** Analysis of 2F and 6F cells before injection in nude mice. Detection of S100A11 and TRK-T3 expression by western blot analysis.  $\beta$ -tubulin was used as loading control for cell extracts.

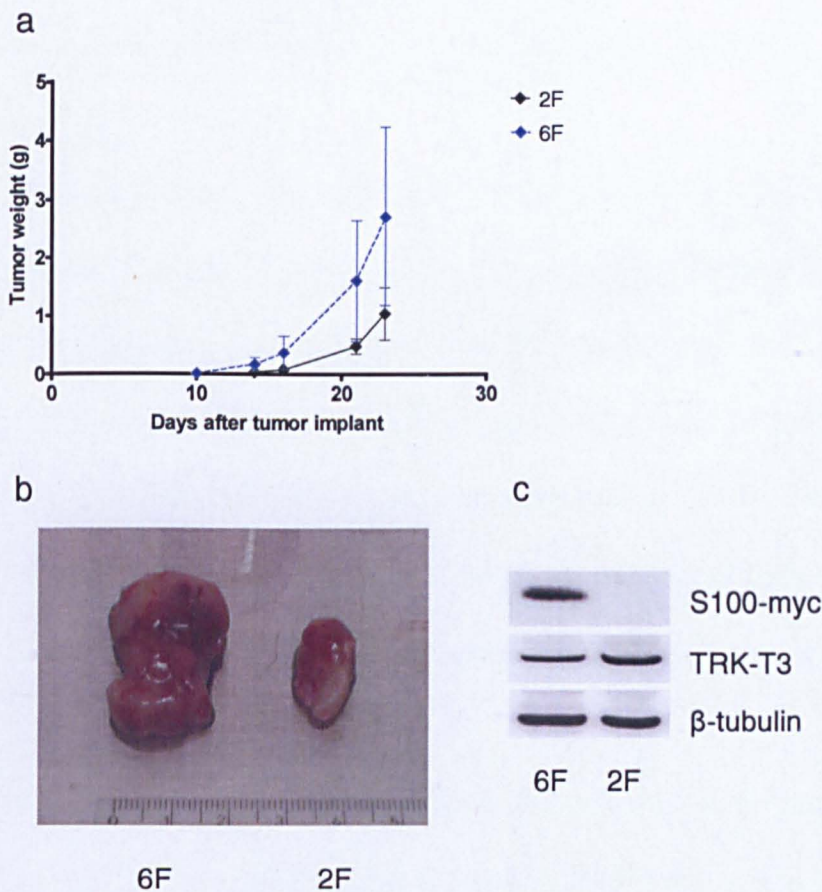
For each cell line, different doses (  $2 \times 10^5$ ,  $4 \times 10^4$ ,  $1 \times 10^4$  cells ) were used. As reported in table 5.2, the difference in tumourigenicity was more evident with the intermediate dose. As shown in figure 5.23 a, tumours produced by 6F cells grew faster than those by 2F cells. Representative pictures of tumour explants are reported in Figure 5.23 b. Cell cultures were established from the explanted tumours. Western blot analysis confirmed the expression of S100A11 and TRK-T3 proteins in tumour-derived cells (Figure 5.23 c).



Table 5.2 *In vivo* tumour growth of T3/S100 foci

n. cells	2F			6F		
	Takes	days at		Takes	days at	
		0.1g	1g		0.1g	1g
2 x 10 <sup>5</sup>	6/6	13(11-14)	21(18-21)	6/6	11(10-13)	18(17-19)
4 x 10 <sup>4</sup>	6/6	16.5(15-19)	23(22-25)	6/6	13.5(12-15)	20(17-23)
1 x 10 <sup>4</sup>	6/6	20(17-23)	27.5(25-30)	5/5	18.5(17-20)	25(20-24)

2F (TRK-T3 expressing NIH3T3 cells) and 6F (S100A11/TRK-T3 expressing NIH3T3 cells) were inoculated at different doses subcutaneously into the left flank of athymic nude mice as described in Materials and Methods section. Tumour growth was assessed by evaluating tumour latency, ie days to reach 0.1 g, and by monitoring tumour weight (TW) twice a week. TW was estimated by the formula  $TW(g)=d \times D/2$  where d and D are the shortest and the longest diameters of the tumour, respectively, measured in cm.



**Figure 5.23 Tumour xenografts analysis.** a) volumes of tumours derived from 2F and 6F cells injection (intermediate dose) in nude mice. Each data point represent the mean  $\pm$  SD of six primary tumours. \*  $p<0.01$ ; b) representative pictures of tumour xenografts from mice 23 days from injection; c) western blot analysis of S100A11 and TRK-T3 expression of cell cultures established from tumours induced by 6F and 2F foci in nude mice.  $\beta$ -tubulin was used as loading control for cell extracts.

## 5.4 Discussion

Despite the many studies focusing on S100A11, its role in cancer is still controversial. In fact, although a large amount of data supports the role of S100A11 in the oncogenesis of several types of tumours; many authors propose S100A11 as a tumour suppressor.

In different studies of gene expression, *S100A11* was found overexpressed in papillary thyroid cancer with respect to normal thyroid tissue. Moreover, Torres-Cabala *et al.* reported, by immunohistochemical analysis, a high S100A11 expression in PTC. Even though these studies confirm a strong association between the S100A11 expression and the papillary histotype, the functional role of this protein in thyroid carcinogenesis is unknown. For this purpose, we studied the relevance of S100A11 in PTC biology by different approaches.

Analysis of gene expression data produced in our laboratory demonstrated a consistent upregulation of *S100A11* in PTC with respect to normal thyroid. Our results were corroborated by analysing four publicly available microarray data sets. The mechanism leading to the upregulation of S100A11 in tumours, and in particular, in thyroid cancers, is still unknown. The *S100* genes are clustered on human chromosome 1q21. Gain of this region is a recurrent chromosome aberration in many cancers, including thyroid (Kjellman *et al.*, 2001), and could be responsible for the overexpression of S100 proteins.

We analysed a panel of PTC-derived cell lines, and found that all of them express high levels of *S100A11* mRNA. Among them, we focused on the K1 cell line as an *in vitro* model to investigate the contribution of S100A11 upregulation to the thyroid tumour phenotype. Since an opposite role of S100A11 it has been demonstrated, being pro-tumoural when in the cytoplasm and tumour suppressor in the nucleus, we first checked its cellular localization. Interestingly, we found that in K1 cells, as well as in other PTC-



derived cell lines, S100A11 was mainly localized into the cytoplasm. This is in keeping with the observations of Torres-Cabala *et al.* who found a cytoplasmatic pattern of S100A11 staining in PTC, and a nuclear staining in normal thyroid. We then asked whether in our model S100A11 was retained into the cytoplasm and nuclear translocation was hampered. In agreement with the model proposed by Sakaguchi *et al.* for human normal keratinocytes, after treatment of K1 cells with  $\text{Ca}^{2+}$ , we observed a nuclear translocation of S100A11. However, conversely to the keratinocyte model, S100A11 translocation did not lead to an increase of the level of p21, a negative regulator of cell growth. We demonstrated that also TGF- $\beta$  stimulation was able to promote the nuclear translocation of S100A11. These observations indicate that in K1 cells this capability is preserved although not involved in the regulation of cell proliferation.

The cytoplasmic function of S100A11 in our cellular model remains to be investigated. The importance of S100A11 is known in cytoskeleton remodelling, pseudopodial formation and in epithelial to mesenchymal transition (Shankar et al., 2010). The involvement of S100A11 in these processes in thyroid tumour cells deserves further investigation.

It has been demonstrated in human keratinocytes that a crosstalk between S100A11 and the EGF/EGFR pathway exists, resulting in the promotion of cell growth. We did not observe an increase of S100A11 mRNA and protein levels in K1 cells treated with EGF. Moreover, overexpression or silencing of S100A11 had no effect on the activation of the EGFR pathway following EGF stimulation. The absence of S100A11 involvement in the enhancement of this pathway could have some explanations. First, it has been demonstrated that in K1, as well as in other thyroid cancer cell lines, a functional TGFA/EGFR autocrine signalling loop exists, and it sustains cell proliferation (Degl'Innocenti et al., 2010). Second, the K1 cell line, in addition to the *BRAFV600E* mutation, also carries the *E542K* mutation of the *PI3KCA* gene (Pilli et al., 2009), leading

to a basal constitutive high level of Akt phosphorylation. Overall, the constitutive activation of EGFR and Akt could overcome the moderate effect of S100A11.

To further study the function of S100A11 in thyroid cancer, we transiently and stably knocked-down S100A11 protein in K1 cells. With both approaches we did not observe any effect of S100A11 on K1 growth rate, in keeping with the lack of effect of S100A11 on the expression of the negative growth regulator p21. Cells stably silenced for S100A11 showed no difference in the adhesion and migratory capability, but showed a significant anchorage-independent growth reduction. Finally, using mouse tumour xenografts, we observed that *in vivo* the K1 cells with silenced S100A11 grow at the same rate as the parental cell line. Even though we did not observe any differences in the growth of primary tumours, we could not exclude that S100A11 silencing might affect the formation of distant metastasis as observed in other tumour types. Moreover, analysis of gene expression data sets of thyroid tumour samples could be taken into account in order to find a possible association of S100A11 expression with clinical-pathological features, in particular the presence of metastases. To investigate the involvement of S100A11 in the metastatic process with our experimental model, preliminary studies evaluating the metastatic potential of K1 cells, and the employment of an appropriate *in vivo* metastasis assay will be required.

Except for the reduction of anchorage-independent growth, on the whole we did not observe any effect of S100A11 silencing in K1 cells by our *in vitro* and *in vivo* studies, and this could be due to different reasons. One could be related to the efficiency of S100A11 knockdown, which although great might not be enough to observe a detectable effect. Furthermore, the lack of S100A11 in our cellular context could be counterbalanced by the activation of compensatory mechanisms. Such mechanisms could involve other members of the S100 family such as S100A2 and S100A4, associated with invasion and metastasis and overexpressed in thyroid cancer (Ito et al., 2005; Zou et al., 2005); or S100B, known to form heterodimers with S100A11 and to associate with vimentin intermediate filaments

(Bianchi et al., 2003). In this respect, it would be worth investigating whether the expression of S100 genes is concomitantly modulated in thyroid tumours and cell line.

The second part of our studies focused on the investigation of a possible cooperation between the *S100A11* gene and PTC-associated oncogenes. By performing co-transfection experiments in NIH3T3 cells, we showed that the *S100A11* gene was able to enhance the transforming capability of the *TRK-T3* oncogene. The characterization of transformed NIH3T3 foci expressing TRK-T3 alone or in combination with S100A11 showed that the latter was not involved in the regulation of cell proliferation. Instead, S100A11 was able to enhance the invasion and anchorage-independent growth triggered by *TRK-T3* oncogene. It remains to investigate the mechanism through which S100A11 modulates these capabilities. *In vivo* tumourigenicity assays revealed that the TRK-T3/S100A11 expressing tumours showed significant increased growth in comparison with those expressing only TRK-T3. This striking effect could be attributed to S100A11 secretion-related function. It has been demonstrated that in normal human keratinocytes and squamous cell carcinoma S100A11 is secreted and promotes cell growth through the onset of a positive feedback loop with the EGF/EGFR pathway. Moreover, the enhancement of this pathway is also related to the S100A11 promotion of different cytokines and other different EGFR ligands (Sakaguchi et al., 2008). It has also been demonstrated that a crosstalk between S100A11 and inflammation takes place in chondrocytes. Cytokines such as TNF- $\alpha$  and CXCL8 upregulate S100A11 secretion, which in turn promotes osteoarthritis progression through an increased collagen production. (Cecil et al., 2005). Collectively, this information allow us to hypothesize that the effect of secreted S100A11 on tumour growth, inflammation and formation of the extracellular matrix, may be responsible for the enhanced tumourigenicity of *TRK-T3* oncogene. Further studies, including histopathological analysis of tumour xenografts, are needed in order to validate these hypotheses.

In summary, we found different effects of the S100A11 modulation in two different cellular models. In the K1 cell line we observed that S100A11 was localized both in

cytoplasm and in the nucleus. The latter localization did not influence the levels of p21, a negative regulator of cell growth. Moreover, the S100A11 involvement in the EGF/EGFR pathway was not detectable. The effect of S100A11 silencing was evident on the anchorage-independent growth, while not affecting the *in vitro* and *in vivo* cell growth, suggesting that S100A11 modulation differently affects the various tumour cell properties.

Using the other model, the NIH3T3 cells, we observed that S100A11 was able to enhance the transforming capability of TRK-T3. Although performed in an experimental model, these data highlight the capability of S100A11 to cooperate with PTC-associated oncogenes.

In summary, by comparing the results obtained in the two models, several analogies emerge, as well as some differences. In both cases, *in vitro* cell growth was unaffected whereas anchorage-independent growth was affected. However, *in vivo* tumour growth was increased only in the NIH3T3 model. These differences can be ascribed to the different cellular context. As reported above, in K1 cells the effect of S100A11 could be masked by the activation of compensatory mechanisms, at variance with the NIH3T3 model. Furthermore, it has been clearly shown by others that S100A11 can display different functions on cellular types and tumours.

In conclusion, our work indicates a role of S100A11 in thyroid cancer, whose full elucidation requires more efforts in order to assess whether its modulation could result in a therapeutic strategy.

**6. CITED1 studies**

## 6.1 Introduction

### 6.1.1 *CITED1 (CBP/p300-Interacting Transactivators with glutamic acid (E) and aspartic acid (D)-rich C-terminal domain 1).*

CITED1 (also named melanocyte-specific gene 1 (*MSG1*) since initially believed to be melanocyte-specific), is a part of family of transcriptional cofactors that regulates diverse CBP/p300 transcriptional responses. CITED1 enhances transcriptional responses involving TGF- $\beta$ /Smad4 and it also functions as a selective coactivator for estrogen-dependent transcription (Yahata et al., 2000; Yahata et al., 2001). These effects are dependent on interactions between CITED1 and CBP/p300. Moreover, the transcriptional activity of CITED1 is regulated by phosphorylation in a cell cycle-dependent manner (Shi et al., 2006).

Expression analysis suggests that CITED1 may play a role in the pathogenesis of tumours such as malignant melanoma (Sedghizadeh et al., 2005), Wilms tumour (Lovvorn et al., 2007) and PTC (Prasad et al., 2004). In particular, in different microarray studies *CITED1* was found overexpressed in PTC (Jarzab et al., 2005; Prasad et al., 2004). Moreover, Aldred *et al.* reported that *CITED1* belongs to a list of five genes (*CITED1*, *CAV1*, *CAV2*, *IGFBP6* and *CLDN10*) capable of distinguishing between PTC and FTC (Aldred et al., 2004). It was also proposed as a highly sensitive and specific diagnostic marker, useful in differentiating PTC from benign and malignant thyroid tumours (Ducena et al., 2011). CITED1, in association with Galectin-3, fibronectin-1, HBME1 and cytokeratin-19 has been proposed for the differential diagnosis of thyroid tumours (Prasad et al., 2005). The mechanism leading to upregulation of *CITED1* gene expression in PTC compared to normal thyroid is still unclear. Sassa *et al.* reported a positive association of *BRAF* mutation with CITED1 overexpression, concomitantly to hypomethylation of the CpGs in the promoter region of *CITED1* gene (Sassa et al., 2011).

### 6.1.2 *Aims of CITED1 studies*

A large number of studies reported the importance of *CITED1* in thyroid carcinogenesis and, in particular, in the papillary histotype. To gain more insight into the role of *CITED1* in this neoplasia, we planned to follow different approaches including the analysis of gene expression data sets and functional studies. Our aims are to:

- 1) validate our gene expression data;
- 2) analyse the effect of *CITED1* gene silencing in a selected tumour cell line;
- 3) investigate the effect of *CITED1* on transforming activity of PTC-associated oncogenes.

## 6.2 Preliminary results

1) We explored the expression level of the *CITED1* gene by analyzing cDNA microarray data produced in our laboratory. The sample collection was the same used for TIMP3 and S100A11 analysis. As reported in Figure 6.1, the expression levels of *CITED1* are upregulated in a great proportion of PTC in comparison with normal thyroid tissue (N) (paired t-test  $p < 0.01$ ). These findings are in keeping with the data on *CITED1* overexpression in PTC reported by a large number of gene expression and immunohistochemical studies.

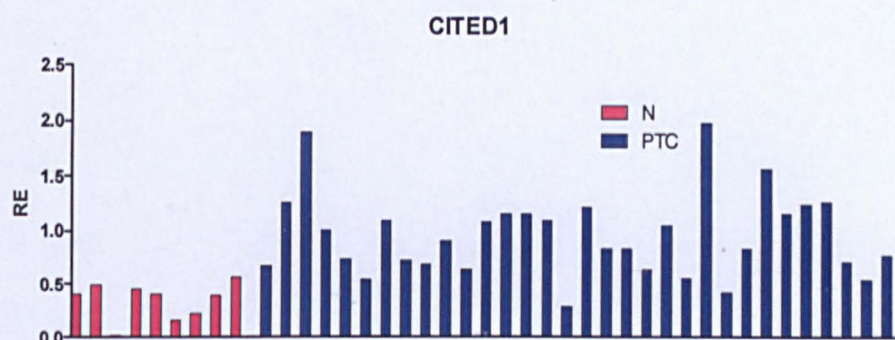


**Figure 6.1 cDNA array expression of *CITED1* gene.** Graphic representation of the expression level in normal thyroid samples (N, red) and papillary thyroid carcinomas (PTC, blue). The expression level (relative expression, RE) of the *CITED1* gene in all the tissue samples hybridized on the array was measured as log ratio between the expression level of the specimens and that of the reference.



2) An expression analysis of the *CITED1* gene in a panel of thyroid cell lines has been performed (Figure 6.2). We investigated the expression of *S100A11* by reverse transcriptase-PCR (RT-PCR) in the following cell lines: TPC1, NIM1, BCPAP and K1. Except for TPC1, which carries *RET/PTC1* oncogene, the other thyroid tumour cell lines are characterized by the *BRAFV600E* mutation. As a control, we used the Nthy-ori 3-1 cells (N-Thy), normal human thyrocytes immortalized by the SV40 large T antigen, and normal thyrocytes (N) derived from normal thyroid tissue. The aim was to select a cell line that overexpresses this gene and then to validate a siRNA sequence against *CITED1*. BCPAP and K1 cell lines, could be considered good candidates for our studies. Reagents for silencing of this gene have been selected and will be tested shortly.

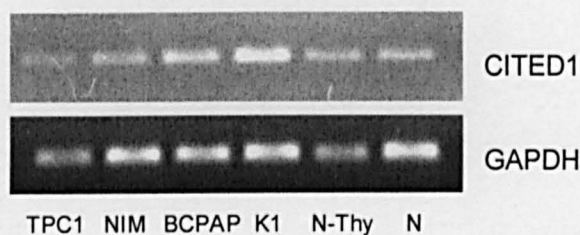


**Figure 6.2 *CITED1* mRNA expression by RT-PCR.** Analysis of a panel of PTC-derived cell lines; *GAPDH* gene was used as loading control; (N-Thy: N-Thy-Ori 3-1 cell line, N: normal thyrocyte)

3) We produced *CITED1-myc* expression vectors as tools for the proposed functional studies. *CITED1* cDNA has been amplified from HeLa cells and cloned into *pcDNA3* or *pIres* vectors, both carrying the myc epitope (details of these plasmids are reported in material and methods section). cDNA constructs have been transiently transfected into HEK293T cells and shown to express the expected protein by western blot analysis with anti-myc antibody (Figure 6.3).



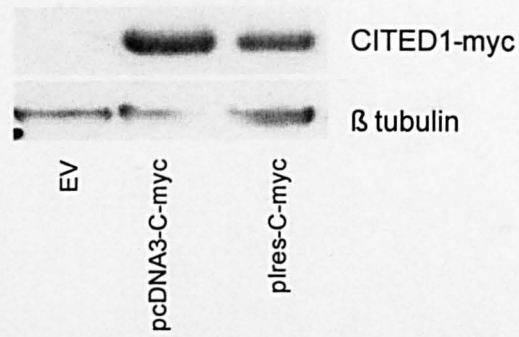


**Figure 6.3 Expression of CITED1-myc protein in HEK293T cells.** Cells transiently transfected with *pcDNA3-CITED1myc* and *pIRES-CITED1myc* constructs were analysed by western blot for the expression of CITED1myc protein using anti-myc antibody. As a control, empty vector (EV)-transfected HEK293T cells were used.  $\beta$ -tubulin was used as loading control for cell extracts.



## 7. *Insulin-like growth factor-binding protein 7 (IGFBP7)*

As anticipated in the aim of the thesis section, our studies were also addressed to the investigation of the role of *Insulin-like growth factor-binding protein 7 (IGFBP7)*, one of the genes whose expression was differentially regulated in PTC with respect to normal thyroid. Even though not strictly related to the PhD project, this analysis is part of a larger study conducted by our laboratory, aimed at the dissection of the role of genes differentially expressed in thyroid carcinogenesis, in which the candidate collaborated.

The results are hereafter summarized.

IGFBP7, also called IGFBP-rP1 or MAC25, is a member of the IGFBP superfamily, including 16 secreted proteins binding IGFs with variable affinity (Burger et al., 2005). IGFBP7 binds IGFs with low affinity, but in contrast, recognizes insulin with high affinity, and thereby modifies its metabolism, distribution, and ability to bind to the insulin receptor (Yamanaka et al., 1997). IGFBP7 has also IGF/insulin-independent actions.

A large body of evidence suggests that *IGFBP7* functions as an oncosuppressor gene in human prostate, breast, lung and colorectal cancer, as it regulates cell proliferation, cell adhesion, cellular senescence, and angiogenesis (Akaogi et al., 1996; Burger et al., 2005; Chen et al., 2007; Ruan et al., 2006; Sato et al., 2007; Sprenger et al., 1999; Wilson et al., 2002). *IGFBP7* is silenced by promoter hypermethylation in several neoplastic tissues, including colorectal and gastric cancers (Ahmed et al., 2003; Kanemitsu et al., 2000; Lin et al., 2007). More recently, IGFBP7 has been shown to mediate senescence in melanocytes, and to suppress melanoma growth *in vivo* by inducing apoptosis (Wajapeyee et al., 2008).

In our laboratory, we investigate the role of IGFBP7 in PTC. Analysis of expression levels in microarray datasets highlighted that *IGFBP7* was downregulated in a consistent fraction of PTC, with respect to normal thyroid. To address the functional consequences of IGFBP7 downregulation we used the PTC-derived NIM1 cell line, in which the expression of IGFBP7 is lacking. Exposure to soluble IGFBP7 protein or restoration of IGFBP7

expression by cDNA transfection reduced growth rate, migration, anchorage independent growth and tumorigenicity of NIM1 cells. We provide evidence that the effects of IGFBP7 are related to apoptosis. We also performed immunohistochemical analysis for IGFBP7 expression in thyroid tumour samples including microcarcinomas, PTCs and ATCs. We found that microcarcinoma expressed high levels of IGFBP7 whereas PTC expressed variable (from low to moderate) levels. Significantly, expression of IGFBP7 was not detectable in ATC. These data indicate that IGFBP7 protein expression is progressively lost during thyroid tumour progression.

Overall, our data suggest that *IGFBP7* gene exerts an oncosuppressor role in thyroid epithelial carcinogenesis.

Details of the study can be found in the attached reprint of the papers:

- 1) MG Vizioli *et al.* (2010): "*IGFBP7: an oncosuppressor gene in thyroid carcinogenesis*" *Oncogene* 29(26), 3835-44;);
- 2) MG Vizioli *et al.* (2011) "*Evidence of oncogene-induced senescence in thyroid carcinogenesis*" *Endocr Relat Cancer*, Dec 1; 18(6):743-757; )

## **8. General discussion and future plans**

## **8. General discussion and future plans**

Papillary thyroid carcinoma (PTC) is characterized by specific and well known alterations, all converging on the activation of the RTK/RAS/BRAF/MAPK pathway. Even though the identification of these alterations has provided a great contribution to the understanding of PTC pathogenesis, the molecular mechanisms underlying the development of these neoplasias are still far from being completely elucidated. In particular, the role of tumour suppressor genes in thyroid malignancies is not completely understood.

In the past few years microarray technology has become a powerful tool to analyse global gene expression profiles and has provided answers to fundamental questions regarding tumour biology, early detection, prognosis and follow-up. Several groups have determined the gene expression profile of thyroid tumours. These studies allowed discrimination between benign and malignant lesions, and between PTC and FTC. In addition to the identification of diagnostic and prognostic markers, gene expression has the potential to unveiling genes involved in the pathogenesis of thyroid tumours and possible new therapeutic targets. Recent reports highlight the power of gene expression analysis as a tool for the identification, among others, of putative oncosuppressor genes. Some genes identified as down-regulated in the context of gene expression studies, were classified as tumour suppressors by functional studies, as their re-expression modulated transformed properties of thyroid carcinoma cell lines. Restoration of MT1G (Ferrario et al., 2008), CBX7 (Pallante et al., 2008), and ABI3BP (Latini et al., 2008) in thyroid tumour cell lines lacking their expression affected cell growth and transformed properties. On the other hand, gene expression analyses of thyroid cancer identified the upregulation of several genes, involved in different cellular functions such as adhesion, signal transduction, EMT and inflammation, subsequently found to act as tumour promoters. TWIST1 and Polo-like Kinase 1 were found upregulated in anaplastic thyroid carcinoma (ATC) and shown to exert a tumour promoter role. In particular, functional studies revealed that TWIST1 plays

important roles in determining the anaplastic thyroid cancer phenotype, in terms of promotion of cell migration, invasion and resistance to apoptosis (Salerno et al., 2011), whereas functional studies showed that Polo-like Kinase 1 is involved in cell transformation and is proposed as a promising target for the molecular therapy of ATC (Nappi et al., 2009).

Based on the evident importance of functional studies for the discovery of new players in thyroid carcinogenesis, we decided to start from a gene expression analysis of thyroid tumour samples in order to identify putative tumour suppressor or tumour promoter candidates. In this work, we decided to dissect the functional role of *Tissue Inhibitor of Metalloproteases-3 (TIMP-3)*, *S100/calgizzarin* and *CITED1(CBP/p300-Interacting Transactivators with glutamic acid (E) and aspartic acid (D) rich C-terminal domain 1)* genes for which a role in the pathogenesis of PTC was also suggested by recently published gene and protein expression data. In our microarray analysis, these genes were found differentially expressed in PTC compared to normal thyroid tissue. The study of these selected genes allowed us to obtain important information about their role in PTC.

Using an integrated approach, including analysis of gene expression data and functional studies, we demonstrated that TIMP3 exerts a negative regulatory role in thyroid carcinogenesis. In addition to the inhibitor role on migratory and invasive capabilities of the PTC-derived NIM1 cells, our data showed that the most striking effect of TIMP3 was observed *in vivo*, as it reduced the NIM1 tumourigenicity by repressing angiogenesis and macrophage infiltration. Our future plans are to better dissect the mechanisms through which TIMP3 is able to modulate the inflammatory microenvironment. Even though the reduction of inflammation could be generally attributed to the negative role of TIMP3 on angiogenesis and on the reduction of the pro-inflammatory TNF-alpha cytokine shedding, we think that, in addition to these general mechanisms, TIMP3 might act through the involvement of other thyroid specific mediators. To clarify this issue, the characterization of soluble molecules produced by NIM1, in the presence or the absence of TIMP3, will be

undertaken. In conclusion, some authors reported that TIMP3 overexpression in tumour cells suppress primary tumour growth and angiogenesis, indicating its involvement in the earliest aspect of tumour development. On the other hand, it has been demonstrated a decreased TIMP3 expression at the invasive front of tumour, suggesting that its regional loss may facilitate tumour invasion and metastasis. All these data suggest as TIMP3 may contribute to all stages of malignant progression. In the context of thyroid tumours the downregulation of TIMP3, concomitant with the *BRAF* mutation, is associated with several aggressive features of PTC, including extrathyroidal invasion, lymph node metastasis, multifocality and advanced tumour stages. On the basis these evidences, TIMP3 could be considered a good prognostic marker of PTC.

The second part of the thesis dealt with the dissection of the role of S100A11 in PTC. Functional studies revealed that S100A11 could have different functions depending on cellular context. In K1 cells, we found the finely tuning of S100A11 expression might modulate some cellular capabilities such as anchorage-independent growth, whereas no effect was observed on cellular proliferation and *in vivo* tumourigenicity. Our future plans are to investigate whether S100A11 might be involved in other important cellular processes such as the remodelling of cytoskeleton and the epithelial to mesenchymal transition, features which could be related to cellular invasive and metastatic capabilities. Moreover, we plan to perform meta-analysis of publicly available gene expression data sets of thyroid tumours in order to investigate a possible association of S100A11 expression with clinical-pathological features, such as presence of metastases. We hypothesize that effect of S100A11 modulation on K1 cells could be masked by the presence of other members of the S100A family, such as S100A4 and S100A2 which are found overexpressed in PTC. In this respect, we plan to investigate whether members of S100 family are concomitantly modulated in thyroid tumour and cell lines. On the other hand, co-transfection studies in NIH3T3 cells allowed us to observe a cooperation between S100A11 and TRK-T3 oncogene. We plan to carry out more detailed studies in order to



investigate how this cooperation occurs. Moreover, we are also interested in understanding whether this cooperation is specific for *TRK-T3* oncogene or is common to the other PTC-associated oncogenes. Since the striking effect of S100A11 was found in the tumourigenic capability of transformed NIH3T3, our aim is to verify whether it could be attributed to the secretion-related function of S100A11, known to be involved in the regulation of growth promotion, inflammation and formation of extracellular matrix. Our plan is to perform histopathological analysis of mouse tumour xenografts of transformed NIH3T3 in order to validate these hypotheses. Even though from our studies the role of S100A11 role has only been partially elucidated, some evidences indicate as S100A11 could be involved in conferring to the cell a transformed phenotype, such as the capability to grow in an anchorage-independent manner, thus suggesting a putative role of S100A11 in the metastatic process. In keeping with this, some authors reported as S100A11 is overexpressed in primary tumours with metastatic potential.

On the whole, our studies contributed to the dissection of the role of these genes in thyroid carcinogenesis. In particular, the modulation of TIMP3 and S100A11 expression was involved in the alteration of important processes such as adhesion, invasion and EMT, in keeping with the concept that PTC are characterized by the modulation of genes belonging to these onthology classes. So, through different mechanisms, the loss of TIMP3 in addition to the overexpression of S100A11, could act together to modulate the PTC phenotype. We hypothesize that the major contribution of these molecules could reside in the stage of progression from primary tumour to distant metastases, even though we can not exclude their importance in the promotion of primary tumour onset. From a clinical point of view, it would be interesting to investigate whether in PTC samples the TIMP3 downregulation is associated with the concomitant S100A11 overexpression and whether they could be considered possible prognostic markers of PTC.

Many studies reported the involvement of CITED1 in PTC biology. All of them analysed the expression level of CITED1, suggesting a putative tumour promoter role in

the context of thyroid cancer. Moreover, some authors proposed it as a powerful diagnostic marker of PTC. Our aims are to better dissect mechanisms leading to CITED1 overexpression, to investigate its effect on transforming activity of PTC-associated oncogenes and the effect of its silencing on the phenotype of a PTC-derived cellular model.

In conclusion, our studies allowed the identification of specific cellular properties in which TIMP3 and S100A11 are involved. The function of CITED1 remains to be investigated. Even though more efforts to better elucidate their functional role are needed, our studies revealed that they might be considered important players in the complex network of alterations of thyroid carcinogenesis.

The value of this study, from a translational stand point, lies in identifying putative biomarkers of PTC. Further studies are needed to evaluate whether these genes could be considered a “molecular signature” that could be associated with clinical outcome (prognosis), recurrence and survival or putative new targets for thyroid cancer treatment.

## Reference List

- Abubaker,J., Jehan,Z., Bavi,P., Sultana,M., Al-Harbi,S., Ibrahim,M., Al-Nuaim,A., Ahmed,M., Amin,T., Al-Fehaily,M., Al-Sanea,O., Al-Dayel,F., Uddin,S., and Al-Kuraya,K.S. (2008). Clinicopathological analysis of papillary thyroid cancer with PIK3CA alterations in a Middle Eastern population. *J Clin Endocrinol. Metab* 93, 611-618.
- Adeniran,A.J., Zhu,Z., Gandhi,M., Steward,D.L., Fidler,J.P., Giordano,T.J., Biddinger,P.W., and Nikiforov,Y.E. (2006). Correlation between genetic alterations and microscopic features, clinical manifestations, and prognostic characteristics of thyroid papillary carcinomas. *Am. J Surg. Pathol.* 30, 216-222.
- Ahmed,S., Yamamoto,K., Sato,Y., Ogawa,T., Herrmann,A., Higashi,S., and Miyazaki,K. (2003). Proteolytic processing of IGFBP-related protein-1 (TAF/angiomodulin/mac25) modulates its biological activity. *Biochem. Biophys. Res Commun.* 310, 612-618.
- Ahonen,M., Poukkula,M., Baker,A.H., Kashiwagi,M., Nagase,H., Eriksson,J.E., and Kahari,V.M. (2003). Tissue inhibitor of metalloproteinases-3 induces apoptosis in melanoma cells by stabilization of death receptors. *Oncogene.* 22, 2121-2134.
- Airaksinen,M.S. and Saarma,M. (2002). The GDNF family: signalling, biological functions and therapeutic value. *Nat Rev Neurosci* 3, 383-394.
- Akaogi,K., Okabe,Y., Sato,J., Nagashima,Y., Yasumitsu,H., Sugahara,K., and Miyazaki,K. (1996). Specific accumulation of tumor-derived adhesion factor in tumor blood vessels and in capillary tube-like structures of cultured vascular endothelial cells. *Proc. Natl Acad. Sci U. S. A.* 93, 8384-8389.
- Akslen,L.A. and LiVolsi,V.A. (2000). Increased angiogenesis in papillary thyroid carcinoma but lack of prognostic importance. *Hum. Pathol* 31, 439-442.
- Akslen,L.A. and Varhaug,J.E. (1995). Oncoproteins and tumor progression in papillary thyroid carcinoma: presence of epidermal growth factor receptor, c-erbB-2 protein, estrogen receptor related protein, p21-ras protein, and proliferation indicators in relation to tumor recurrences and patient survival. *Cancer* 76, 1643-1654.
- Aldred,M.A., Huang,Y., Liyanarachchi,S., Pellegata,N.S., Gimm,O., Jhiang,S., Davuluri,R.V., de la,C.A., and Eng,C. (2004). Papillary and follicular thyroid carcinomas show distinctly different microarray expression profiles and can be distinguished by a minimum of five genes. *J Clin Oncol* 22, 3531-3539.
- Amano,H., Maruyama,K., Naka,M., and Tanaka,T. (2003). Target validation in hypoxia-induced vascular remodeling using transcriptome/metabolome analysis. *Pharmacogenomics. J* 3, 183-188.
- Anand-Apte,B., Bao,L., Smith,R., Iwata,K., Olsen,B.R., Zetter,B., and Apte,S.S. (1996). A review of tissue inhibitor of metalloproteinases-3 (TIMP-3) and experimental analysis of its effect on primary tumor growth. *Biochem. Cell Biol.* 74, 853-862.
- Angell,J.E., Lindner,D.J., Shapiro,P.S., Hofmann,E.R., and Kalvakolanu,D.V. (2000). Identification of GRIM-19, a novel cell death-regulatory gene induced by the interferon-

beta and retinoic acid combination, using a genetic approach. *J Biol Chem* 275, 33416-33426.

Arighi,E., Borrello,M.G., and Sariola,H. (2005). RET tyrosine kinase signaling in development and cancer. *Cytokine and Growth Factor Reviews* 16, 441-467.

Bachman,K.E., Herman,J.G., Corn,P.G., Merlo,A., Costello,J.F., Cavenee,W.K., Baylin,S.B., and Graff,J.R. (1999). Methylation-associated silencing of the tissue inhibitor of metalloproteinase-3 gene suggest a suppressor role in kidney, brain, and other human cancers. *Cancer Res.* 59, 798-802.

Barden,C.B., Shister,K.W., Zhu,B., Guter,G., Greenblatt,D.Y., Zeiger,M.A., and Fahey,T.J., III (2003). Classification of follicular thyroid tumors by molecular signature: results of gene profiling. *Clin Cancer Res* 9, 1792-1800.

Barski,D., Wolter,M., Reifengerger,G., and Riemenschneider,M.J. (2010). Hypermethylation and transcriptional downregulation of the TIMP3 gene is associated with allelic loss on 22q12.3 and malignancy in meningiomas. *Brain Pathol* 20, 623-631.

Basolo,F., Caligo,M.A., Pinchera,A., Fedeli,F., Baldanzi,A., Miccoli,P., Iaconi,P., Fontanini,G., and Pacini,F. (2000). Cyclin D1 overexpression in thyroid carcinomas: relation with clinico-pathological parameters, retinoblastoma gene product, and Ki67 labeling index. *Thyroid* 10, 741-746.

Baverstock,K., Egloff,B., Pinchera,A., Ruchti,C., and Williams,D. (1992). Thyroid cancer after Chernobyl. *Nature* 359, 21-22.

Bianchi,R., Giambanco,I., Arcuri,C., and Donato,R. (2003). Subcellular localization of S100A11 (S100C) in LLC-PK1 renal cells: Calcium- and protein kinase c-dependent association of S100A11 with S100B and vimentin intermediate filaments. *Microsc. Res Tech.* 60, 639-651.

Bongarzone,I., Monzini,N., Borrello,M.G., Carcano,C., Ferraresi,G., Arighi,E., Mondellini,P., Della Porta,G., and Pierotti,M.A. (1993). Molecular characterization of a thyroid tumor-specific transforming sequence formed by the fusion of ret tyrosine kinase and the regulatory subunit RI $\alpha$  of cyclic AMP-dependent protein kinase A. *Mol. Cell. Biol.* 13, 358-366.

Bordeleau,F., Galarneau,L., Gilbert,S., Loranger,A., and Marceau,N. (2010). Keratin 8/18 modulation of protein kinase C-mediated integrin-dependent adhesion and migration of liver epithelial cells. *Mol Biol Cell.* 21(10), 1698-1713.

Borrello,M.G., Alberti,L., Fischer,A., Degl'Innocenti D., Ferrario,C., Gariboldi,M., Marchesi,F., Allavena,P., Greco,A., Collini,P., Pilotti,S., Cassinelli,G., Bressan,P., Fugazzola,L., Mantovani,A., and Pierotti,M.A. (2005). Induction of a proinflammatory programme in normal human thyrocytes by the RET/PTC1 oncogene. *Proc. Natl Acad. Sci U. S. A* 102, 14825-14830.

Borup,R., Rossing,M., Henao,R., Yamamoto,Y., Krogdahl,A., Godballe,C., Winther,O., Kiss,K., Christensen,L., Hogdall,E., Bennedbaek,F., and Nielsen,F.C. (2010). Molecular signatures of thyroid follicular neoplasia. *Endocr. Relat Cancer* 17, 691-708.

Bounacer,A., Schlumberger,M., Wicker,R., Du-Villard,J.A., Caillou,B., Sarasin,A., and Suarez,H.G. (2000). Search for NTRK1 proto-oncogene rearrangements in human thyroid tumours originated after therapeutic radiation. *Br. J Cancer* 82, 308-314.

- Bounacer,A., Wicker,R., Caillou,B., Cailleux,A.F., Sarasin,A., Schlumberger,M., and Suarez,H.G. (1997). High prevalence of activating *ret* proto-oncogene rearrangements in thyroid tumors from patients who had received external radiation. *Oncogene 15*, 1263-1273.
- Brabant,G., Hoang-Vu,C., Cetin,Y., Dralle,H., Scheumann,G., Molne,J., Hansson,G., Jansson,S., Ericson,L.E., and Nilsson,M. (1993). E-cadherin: a differentiation marker in thyroid malignancies. *Cancer Res 53*, 4987-4993.
- Brecelj,E., Frkovic,G.S., Auersperg,M., and Bracko,M. (2005). Prognostic value of E-cadherin expression in thyroid follicular carcinoma. *Eur J Surg. Oncol 31*, 544-548.
- Brilli,L. and Pacini,F. (2011). Targeted therapy in refractory thyroid cancer: current achievements and limitations. *Future. Oncol 7*, 657-668.
- Broome,A.M. and Eckert,R.L. (2004). Microtubule-dependent redistribution of a cytoplasmic cornified envelope precursor. *J Invest Dermatol 122*, 29-38.
- Brzezinski,J., Migodzinski,A., Gosek,A., Tazbir,J., and Dedecjus,M. (2004). Cyclin E expression in papillary thyroid carcinoma: relation to staging. *Int J Cancer 109*, 102-105.
- Brzezinski,J., Migodzinski,A., Toczek,A., Tazbir,J., and Dedecjus,M. (2005). Patterns of cyclin E, retinoblastoma protein, and p21Cip1/WAF1 immunostaining in the oncogenesis of papillary thyroid carcinoma. *Clin Cancer Res 11*, 1037-1043.
- Burger,A.M., Leyland-Jones,B., Banerjee,K., Spyropoulos,D.D., and Seth,A.K. (2005). Essential roles of IGBP-3 and IGFBP-rP1 in breast cancer. *Eur J Cancer 41*, 1515-1527.
- Buttel,I., Fechter,A., and Schwab,M. (2004). Common fragile sites and cancer: targeted cloning by insertional mutagenesis. *Ann. N. Y. Acad. Sci 1028*, 14-27.
- Butti,M.G., Bongarzone,I., Ferraresi,G., Mondellini,P., Borrello,M.G., and Pierotti,M.A. (1995). A sequence analysis of the genomic regions involved in the rearrangements between TPM3 and NTRK1 genes producing TRK oncogenes in papillary thyroid carcinomas. *Genomics 28*, 15-24.
- Calabro,V., Strazzullo,M., La,M.G., Fedele,M., Paulin,C., Fusco,A., and Lania,L. (1996). Status and expression of the p16INK4 gene in human thyroid tumors and thyroid-tumor cell lines. *Int J Cancer 67*, 29-34.
- Castro,P., Eknaes,M., Teixeira,M.R., Danielsen,H.E., Soares,P., Lothe,R.A., and Sobrinho-Simoes,M. (2005). Adenomas and follicular carcinomas of the thyroid display two major patterns of chromosomal changes. *J Pathol 206*, 305-311.
- Caudill,C.M., Zhu,Z., Ciampi,R., Stringer,J.R., and Nikiforov,Y.E. (2005). Dose-dependent generation of RET/PTC in human thyroid cells after in vitro exposure to gamma-radiation: a model of carcinogenic chromosomal rearrangement induced by ionizing radiation. *J Clin. Endocrinol. Metab. 90*, 2364-2369.
- Cecil,D.L., Johnson,K., Rediske,J., Lotz,M., Schmidt,A.M., and Terkeltaub,R. (2005). Inflammation-induced chondrocyte hypertrophy is driven by receptor for advanced glycation end products. *J Immunol 175*, 8296-8302.
- Cerutti,J.M., Delcelo,R., Amadei,M.J., Nakabashi,C., Maciel,R.M., Peterson,B., Shoemaker,J., and Riggins,G.J. (2004). A preoperative diagnostic test that distinguishes

benign from malignant thyroid carcinoma based on gene expression. *J Clin Invest* 113, 1234-1242.

Chang,N., Sutherland,C., Hesse,E., Winkfein,R., Wiehler,W.B., Pho,M., Veillette,C., Li,S., Wilson,D.P., Kiss,E., and Walsh,M.P. (2007). Identification of a novel interaction between the Ca(2+)-binding protein S100A11 and the Ca(2+)- and phospholipid-binding protein annexin A6. *Am J Physiol Cell Physiol* 292, C1417-C1430.

Chen,Y., Pacyna-Gengelbach,M., Ye,F., Knosel,T., Lund,P., Deutschmann,N., Schluns,K., Kotb,W.F., Sers,C., Yasumoto,H., Usui,T., and Petersen,I. (2007). Insulin-like growth factor binding protein-related protein 1 (IGFBP-rP1) has potential tumour-suppressive activity in human lung cancer. *J Pathol.* 211, 431-438.

Chen,Y.T., Kitabayashi,N., Zhou,X.K., Fahey,T.J., III, and Scognamiglio,T. (2008). MicroRNA analysis as a potential diagnostic tool for papillary thyroid carcinoma. *Mod. Pathol.* 21, 1139-1146.

Ciampi,R., Giordano,T.J., Wikenheiser-Brokamp,K., Koenig,R.J., and Nikiforov,Y.E. (2007). HOOK3-RET: a novel type of RET/PTC rearrangement in papillary thyroid carcinoma. *Endocr. Relat Cancer* 14, 445-452.

Ciampi,R., Knauf,J.A., Kerler,R., Gandhi,M., Zhu,Z., Nikiforova,M.N., Rabes,H.M., Fagin,J.A., and Nikiforov,Y.E. (2005). Oncogenic AKAP9-BRAF fusion is a novel mechanism of MAPK pathway activation in thyroid cancer. *J Clin Invest* 115, 94-101.

Collins,B.J., Chiappetta,G., Schneider,A.B., Santoro,M., Pentimalli,F., Fogelfeld,L., Gierlowski,T., Shore-Freedman,E., Jaffe,G., and Fusco,A. (2002). RET expression in papillary thyroid cancer from patients irradiated in childhood for benign conditions. *J Clin. Endocrinol. Metab.* 87, 3941-3946.

Colonna,M., Guizard,A.V., Schvartz,C., Velten,M., Raverdy,N., Molinie,F., Delafosse,P., Franc,B., and Grosclaude,P. (2007). A time trend analysis of papillary and follicular cancers as a function of tumour size: a study of data from six cancer registries in France (1983-2000). *Eur J Cancer* 43, 891-900.

Cross,S.S., Hamdy,F.C., Deloulme,J.C., and Rehman,I. (2005). Expression of S100 proteins in normal human tissues and common cancers using tissue microarrays: S100A6, S100A8, S100A9 and S100A11 are all overexpressed in common cancers. *Histopathology.* 46, 256-269.

Curcio,F., Ambesi-Impiombato,F.S., Perrella,G., and Coon,H.G. (1994). Long-term culture and functional characterization of follicular cells from adult normal human thyroids. *Proc. Natl Acad. Sci U. S. A* 91, 9004-9008.

Dal,M.L., Lise,M., Zambon,P., Falcini,F., Crocetti,E., Serraino,D., Cirilli,C., Zanetti,R., Vercelli,M., Ferretti,S., Stracci,F., De,L., V, Busco,S., Tagliabue,G., Budroni,M., Tumino,R., Giacomini,A., and Franceschi,S. (2011). Incidence of thyroid cancer in Italy, 1991-2005: time trends and age-period-cohort effects. *Ann. Oncol* 22, 957-963.

Davies,L. and Welch,H.G. (2006). Increasing incidence of thyroid cancer in the United States, 1973-2002. *JAMA.* 295, 2164-2167.

De Cecco,L., Marchionni,L., Gariboldi,M., Reid,J.F., Lagonigro,M.S., Caramuta,S., Ferrario,C., Bussani,E., Mezzanzanica,D., Turatti,F., Delia,D., Daidone,M.G., Oggionni,M., Bertuletti,N., Ditto,F., Raspagliesi,S., Pilotti,S., Pierotti,M.A., Canevari,S.,

and Schneider,C. (2004). Gene expression profiling of advanced ovarian cancer: characterization of a molecular signature involving fibroblast growth factor 2. *Oncogene* 23, 8171-8183.

Degl'Innocenti,D., Alberti,C., Castellano,G., Greco,A., Miranda,C., Pierotti,M.A., Seregni,E., Borrello,M.G., Canevari,S., and Tomassetti,A. (2010). Integrated ligand-receptor bioinformatic and in vitro functional analysis identifies active TGFA/EGFR signaling loop in papillary thyroid carcinomas. *PLoS. One.* 5(9), e12701.

Detoraki,A., Staiano,R.I., Granata,F., Giannattasio,G., Prevete,N., de,P.A., Ribatti,D., Genovese,A., Triggiani,M., and Marone,G. (2009). Vascular endothelial growth factors synthesized by human lung mast cells exert angiogenic effects. *J Allergy Clin Immunol* 123, 1142-9, 1149.

Detours,V., Delys,L., Libert,F., Weiss,S.D., Bogdanova,T., Dumont,J.E., Franc,B., Thomas,G., and Maenhaut,C. (2007). Genome-wide gene expression profiling suggests distinct radiation susceptibilities in sporadic and post-Chernobyl papillary thyroid cancers. *Br. J Cancer.* 97, 818-825.

Detours,V., Versteyhe,S., Dumont,J.E., and Maenhaut,C. (2008). Gene expression profiles of post-Chernobyl thyroid cancers. *Curr. Opin. Endocrinol. Diabetes Obes.* 15, 440-445.

Detours,V., Wattel,S., Venet,D., Hutsebaut,N., Bogdanova,T., Tronko,M.D., Dumont,J.E., Franc,B., Thomas,G., and Maenhaut,C. (2005). Absence of a specific radiation signature in post-Chernobyl thyroid cancers. *Br. J Cancer.* 92, 1545-1552.

Dhar,D.K., Kubota,H., Kotoh,T., Tabara,H., Watanabe,R., Tachibana,M., Kohno,H., and Nagasue,N. (1998). Tumor vascularity predicts recurrence in differentiated thyroid carcinoma. *Am J Surg.* 176(5), 442-447.

Di Renzo,M., Olivero,M., Ferro,S., Prat,M., Bongarzone,I., Pilotti,S., Belfiore,A., Costantino,A., Vigneri,R., Pierotti,M.A., and Comoglio,P.M. (1992). Overexpression of the c-met/HGF receptor gene in human thyroid carcinomas. *Oncogene* 7, 2549-2553.

Dineen,S.P., Lynn,K.D., Holloway,S.E., Miller,A.F., Sullivan,J.P., Shames,D.S., Beck,A.W., Barnett,C.C., Fleming,J.B., and Brekken,R.A. (2008). Vascular endothelial growth factor receptor 2 mediates macrophage infiltration into orthotopic pancreatic tumors in mice. *Cancer Res* 68, 4340-4346.

Dohan,O., De,I., V, Paroder,V., Riedel,C., Artani,M., Reed,M., Ginter,C.S., and Carrasco,N. (2003). The sodium/iodide Symporter (NIS): characterization, regulation, and medical significance. *Endocr. Rev.* 24, 48-77.

Ducena,K., Abols,A., Vilmanis,J., Narbutis,Z., Tars,J., Andrejeva,D., Line,A., and Pirags,V. (2011). Validity of multiplex biomarker model of 6 genes for the differential diagnosis of thyroid nodules. *Thyroid Res* 4, 11.

Durante,C., Haddy,N., Baudin,E., Leboulleux,S., Hartl,D., Travagli,J.P., Caillou,B., Ricard,M., Lumbroso,J.D., De,V.F., and Schlumberger,M. (2006). Long-term outcome of 444 patients with distant metastases from papillary and follicular thyroid carcinoma: benefits and limits of radioiodine therapy. *J Clin Endocrinol. Metab* 91, 2892-2899.

Elisei,R., Shiohara,M., Koeffler,H.P., and Fagin,J.A. (1998). Genetic and epigenetic alterations of the cyclin-dependent kinase inhibitors p15INK4b and p16INK4a in human thyroid carcinoma cell lines and primary thyroid carcinomas. *Cancer* 83, 2185-2193.

Ensinger,C., Kremser,R., Prommegger,R., Spizzo,G., and Schmid,K.W. (2006). EpCAM overexpression in thyroid carcinomas: a histopathological study of 121 cases. *J Immunother.* 29, 569-573.

Erickson,L.A., Yousef,O.M., Jin,L., Lohse,C.M., Pankratz,V.S., and Lloyd,R.V. (2000). p27kip1 expression distinguishes papillary hyperplasia in Graves' disease from papillary thyroid carcinoma. *Mod. Pathol* 13, 1014-1019.

Esapa,C.T., Johnson,S.J., Kendall-Taylor,P., Lennard,T.W., and Harris,P.E. (1999). Prevalence of Ras mutations in thyroid neoplasia. *Clin Endocrinol. (Oxf)* 50, 529-535.

Eustatia-Rutten,C.F., Corssmit,E.P., Biermasz,N.R., Pereira,A.M., Romijn,J.A., and Smit,J.W. (2006). Survival and death causes in differentiated thyroid carcinoma. *J Clin Endocrinol. Metab* 91, 313-319.

Ezzat,S., Zheng,L., Kolenda,J., Safarian,A., Freeman,J.L., and Asa,S.L. (1996). Prevalence of activating ras mutations in morphologically characterized thyroid nodules. *Thyroid* 6, 409-416.

Fagin,J.A., Matsuo,K., Karmakar,A., Chen,D.L., Tang,S.H., and Koeffler,H.P. (1993). High prevalence of mutations of the p53 gene in poorly differentiated human thyroid carcinomas. *J. Clin. Invest.* 91, 179-184.

Fagin,J.A. and Mitsiades,N. (2008). Molecular pathology of thyroid cancer: diagnostic and clinical implications. *Best. Pract. Res Clin Endocrinol. Metab* 22, 955-969.

Fagin,J.A., Tang,S.H., Zeki,K., Di,L.R., Fusco,A., and Gonsky,R. (1996). Reexpression of thyroid peroxidase in a derivative of an undifferentiated thyroid carcinoma cell line by introduction of wild-type p53. *Cancer Res* 56, 765-771.

Fan,C., Fu,Z., Su,Q., Angelini,D.J., Van,E.J., and Johns,R.A. (2011). S100A11 mediates hypoxia-induced mitogenic factor (HIMF)-induced smooth muscle cell migration, vesicular exocytosis, and nuclear activation. *Mol Cell Proteomics* 10, M110.

Fata,J.E., Leco,K.J., Voura,E.B., Yu,H.Y., Waterhouse,P., Murphy,G., Moorehead,R.A., and Khokha,R. (2001). Accelerated apoptosis in the Timp-3-deficient mammary gland. *J Clin Invest.* 108, 831-841.

Fedele,M., Palmieri,D., Chiappetta,G., Pasquinelli,R., De,M., I, Arra,C., Palma,G., Valentino,T., Pierantoni,G.M., Viglietto,G., Rothstein,J.L., Santoro,M., and Fusco,A. (2009). Impairment of the p27kip1 function enhances thyroid carcinogenesis in TRK-T1 transgenic mice. *Endocr. Relat Cancer.* 16, 483-490.

Fenton,C.L., Lukes,Y., Nicholson,D., Dinanuer,C.A., Francis,G.L., and Tuttle,R.M. (2000). The ret/PTC mutations are common in sporadic papillary thyroid carcinoma of children and young adults. *J Clin Endocrinol. Metab* 85, 1170-1175.

Ferby,I., Reschke,M., Kudlacek,O., Knyazev,P., Pante,G., Amann,K., Sommergruber,W., Kraut,N., Ullrich,A., Fassler,R., and Klein,R. (2006). Mig6 is a negative regulator of EGF receptor-mediated skin morphogenesis and tumor formation. *Nat. Med.* 12, 568-573.

Ferrario,C., Lavagni,P., Gariboldi,M., Miranda,C., Losa,M., Cleris,L., Formelli,F., Pilotti,S., Pierotti,M.A., and Greco,A. (2008). Metallothionein 1G acts as an oncosuppressor in papillary thyroid carcinoma. *Lab Invest.* 88, 474-481.



- Figge,J., del Rosario,A.D., Gerasimov,G., Dedov,I., Bronstein,M., Troshina,K., Alexandrova,G., Kallakury,B.V., Bui,H.X., Bratslavsky,G., and . (1994). Preferential expression of the cell adhesion molecule CD44 in papillary thyroid carcinoma. *Exp Mol Pathol* 61, 203-211.
- Finley,D.J., Arora,N., Zhu,B., Gallagher,L., and Fahey,T.J., III (2004a). Molecular profiling distinguishes papillary carcinoma from benign thyroid nodules. *J Clin Endocrinol Metab* 89, 3214-3223.
- Finley,D.J., Zhu,B., Barden,C.B., and Fahey,T.J., III (2004b). Discrimination of benign and malignant thyroid nodules by molecular profiling. *Ann Surg* 240, 425-436.
- Finn,S.P., Smyth,P., Chill,S., Streck,C., O'Regan,E.M., Flavin,R., Sherlock,J., Howells,D., Henfrey,R., Cullen,M., Toner,M., Timon,C., O'Leary,J.J., and Sheils,O.M. (2007). Expression microarray analysis of papillary thyroid carcinoma and benign thyroid tissue: emphasis on the follicular variant and potential markers of malignancy. *Virchows Arch* 450, 249-260.
- Fischer,A.H., Bond,J.A., Taysavang,P., Battles,O.E., and Wynford-Thomas,D. (1998). Papillary thyroid carcinoma oncogene (RET/PTC) alters the nuclear envelope and chromatin structure. *Am. J Pathol.* 153, 1443-1450.
- Fitzgerald,M.L., Wang,Z., Park,P.W., Murphy,G., and Bernfield,M. (2000). Shedding of syndecan-1 and -4 ectodomains is regulated by multiple signaling pathways and mediated by a TIMP-3-sensitive metalloproteinase. *J Cell Biol* 148, 811-824.
- Fluge,O., Bruland,O., Akslen,L.A., Lillehaug,J.R., and Varhaug,J.E. (2006). Gene expression in poorly differentiated papillary thyroid carcinomas. *Thyroid* 16, 161-175.
- Fornari,F., Gramantieri,L., Ferracin,M., Veronese,A., Sabbioni,S., Calin,G.A., Grazi,G.L., Giovannini,C., Croce,C.M., Bolondi,L., and Negrini,M. (2008). MiR-221 controls CDKN1C/p57 and CDKN1B/p27 expression in human hepatocellular carcinoma. *Oncogene* 27, 5651-5661.
- Foukakis,T., Gusnanto,A., Au,A.Y., Hoog,A., Lui,W.O., Larsson,C., Wallin,G., and Zedenius,J. (2007). A PCR-based expression signature of malignancy in follicular thyroid tumors. *Endocr. Relat Cancer* 14, 381-391.
- Frattoni,M., Ferrario,C., Bressan,P., Balestra,D., De Cecco,L., Mondellini,P., Bongarzone,I., Collini,P., Gariboldi,M., Pilotti,S., Pierotti,M.A., and Greco,A. (2004). Alternative mutations of *BRAF*, *RET* and *NTRK1* are associated with similar but distinct gene expression patterns in papillary thyroid cancer. *Oncogene* 23, 7436-7440.
- Frisk,T., Foukakis,T., Dwight,T., Lundberg,J., Hoog,A., Wallin,G., Eng,C., Zedenius,J., and Larsson,C. (2002). Silencing of the PTEN tumor-suppressor gene in anaplastic thyroid cancer. *Genes Chromosomes. Cancer* 35, 74-80.
- Gabriely,G., Wurdinger,T., Kesari,S., Esau,C.C., Burchard,J., Linsley,P.S., and Krichevsky,A.M. (2008). MicroRNA 21 promotes glioma invasion by targeting matrix metalloproteinase regulators. *Mol Cell Biol.* 28, 5369-5380.
- Garcia-Rostan,G., Camp,R.L., Herrero,A., Carcangiu,M.L., Rimm,D.L., and Tallini,G. (2001). Beta-catenin dysregulation in thyroid neoplasms: down-regulation, aberrant nuclear expression, and CTNNB1 exon 3 mutations are markers for aggressive tumor phenotypes and poor prognosis. *Am. J Pathol.* 158, 987-996.

Garcia-Rostan,G., Costa,A.M., Pereira-Castro,I., Salvatore,G., Hernandez,R., Hermsem,M.J., Herrero,A., Fusco,A., Cameselle-Teijeiro,J., and Santoro,M. (2005). Mutation of the PIK3CA gene in anaplastic thyroid cancer. *Cancer Res.* *65*, 10199-10207.

Garcia-Rostan,G., Zhao,H., Camp,R.L., Pollan,M., Herrero,A., Pardo,J., Wu,R., Carcangiu,M.L., Costa,J., and Tallini,G. (2003). ras mutations are associated with aggressive tumor phenotypes and poor prognosis in thyroid cancer. *J Clin Oncol.* *21*, 3226-3235.

Garofalo,M., Di,L.G., Romano,G., Nuovo,G., Suh,S.S., Ngankea,A., Taccioli,C., Pichiorri,F., Alder,H., Secchiero,P., Gasparini,P., Gonelli,A., Costinean,S., Acunzo,M., Condorelli,G., and Croce,C.M. (2009). miR-221&222 regulate TRAIL resistance and enhance tumorigenicity through PTEN and TIMP3 downregulation. *Cancer Cell.* *16*, 498-509.

Ghossein,R. and LiVolsi,V.A. (2008). Papillary thyroid carcinoma tall cell variant. *Thyroid* *18*, 1179-1181.

Gild,M.L., Bullock,M., Robinson,B.G., and Clifton-Bligh,R. (2011). Multikinase inhibitors: a new option for the treatment of thyroid cancer. *Nat. Rev. Endocrinol.* *7*, 617-624.

Giordano,T.J., Au,A.Y., Kuick,R., Thomas,D.G., Rhodes,D.R., Wilhelm,K.G., Jr., Vinco,M., Misek,D.E., Sanders,D., Zhu,Z., Ciampi,R., Hanash,S., Chinnaiyan,A., Clifton-Bligh,R.J., Robinson,B.G., Nikiforov,Y.E., and Koenig,R.J. (2006). Delineation, functional validation, and bioinformatic evaluation of gene expression in thyroid follicular carcinomas with the PAX8-PPARG translocation. *Clin Cancer Res.* *12*, 1983-1993.

Giordano,T.J., Kuick,R., Thomas,D.G., Misek,D.E., Vinco,M., Sanders,D., Zhu,Z., Ciampi,R., Roh,M., Shedden,K., Gauger,P., Doherty,G., Thompson,N.W., Hanash,S., Koenig,R.J., and Nikiforov,Y.E. (2005). Molecular classification of papillary thyroid carcinoma: distinct BRAF, RAS, and RET/PTC mutation-specific gene expression profiles discovered by DNA microarray analysis. *Oncogene.* *24(44)*, 6646-6656.

Gorsler,T., Murzik,U., Ulbricht,T., Hentschel,J., Hemmerich,P., and Melle,C. (2010). DNA damage-induced translocation of S100A11 into the nucleus regulates cell proliferation. *BMC Cell Biol* *11*, 100.

Greco,A., Borrello,M.G., Miranda,C., Degl'Innocenti,D., and Pierotti,M.A. (2009). Molecular pathology of differentiated thyroid cancer. *Q. J Nucl. Med. Mol Imaging.* *53*, 440-453.

Greco,A., Mariani,C., Miranda,C., Lupas,A., Pagliardini,S., Pomati,M., and Pierotti,M.A. (1995). The DNA rearrangement that generates the *TRK-T3* oncogene involves a novel gene on chromosome 3 whose product has a potential coiled-coil domain. *Mol. Cell. Biol.* *15*, 6118-6127.

Greco,A., Roccato,E., and Pierotti,M.A. (2004). TRK oncogenes in papillary thyroid carcinoma. In *Molecular basis of thyroid cancer*, N.R.Farid, ed. (Boston: Kluwer Academic Publishers), pp. 207-219.

Grieco,M., Santoro,M., Berlingieri,M.T., Melillo,R.M., Donghi,R., Bongarzone,I., Pierotti,M.A., Della Porta,G., Fusco,A., and Vecchio,G. (1990). PTC is a novel rearranged form of the ret proto-oncogene and is frequently detected in vivo in human thyroid papillary carcinomas. *Cell* *60*, 557-563.

Griffith,O.L., Melck,A., Jones,S.J., and Wiseman,S.M. (2006). Meta-analysis and meta-review of thyroid cancer gene expression profiling studies identifies important diagnostic biomarkers. *J Clin Oncol.* 24, 5043-5051.

Grodski,S., Brown,T., Sidhu,S., Gill,A., Robinson,B., Learoyd,D., Sywak,M., Reeve,T., and Delbridge,L. (2008). Increasing incidence of thyroid cancer is due to increased pathologic detection. *Surgery* 144, 1038-1043.

Gschwind,A., Hart,S., Fischer,O.M., and Ullrich,A. (2003). TACE cleavage of proamphiregulin regulates GPCR-induced proliferation and motility of cancer cells. *EMBO J* 22, 2411-2421.

Gu,P., Xing,X., Tanzer,M., Rocken,C., Weichert,W., Ivanauskas,A., Pross,M., Peitz,U., Malfertheiner,P., Schmid,R.M., and Ebert,M.P. (2008). Frequent loss of TIMP-3 expression in progression of esophageal and gastric adenocarcinomas. *Neoplasia.* 10, 563-572.

Guan,H., Ji,M., Hou,P., Liu,Z., Wang,C., Shan,Z., Teng,W., and Xing,M. (2008). Hypermethylation of the DNA mismatch repair gene hMLH1 and its association with lymph node metastasis and T1799A BRAF mutation in patients with papillary thyroid cancer. *Cancer.* 113, 247-255.

Guarino,V., Faviana,P., Salvatore,G., Castellone,M.D., Cirafici,A.M., De,F., V, Celetti,A., Giannini,R., Basolo,F., Melillo,R.M., and Santoro,M. (2005). Osteopontin is overexpressed in human papillary thyroid carcinomas and enhances thyroid carcinoma cell invasiveness. *J Clin Endocrinol. Metab* 90, 5270-5278.

Hao,J., Wang,K., Yue,Y., Tian,T., Xu,A., Hao,J., Xiao,X., and He,D. (2012). Selective expression of S100A11 in lung cancer and its role in regulating proliferation of adenocarcinomas cells. *Mol Cell Biochem.* 359, 323-332.

Haq,M. and Harmer,C. (2005). Differentiated thyroid carcinoma with distant metastases at presentation: prognostic factors and outcome. *Clin Endocrinol. (Oxf)* 63, 87-93.

He,H., Jazdzewski,K., Li,W., Liyanarachchi,S., Nagy,R., Volinia,S., Calin,G.A., Liu,C.G., Franssila,K., Suster,S., Kloos,R.T., Croce,C.M., and de la,C.A. (2005). The role of microRNA genes in papillary thyroid carcinoma. *Proc. Natl Acad Sci U. S. A.* 102, 19075-19080.

He,Y., Cui,Y., Wang,W., Gu,J., Guo,S., Ma,K., and Luo,X. (2011). Hypomethylation of the hsa-miR-191 locus causes high expression of hsa-mir-191 and promotes the epithelial-to-mesenchymal transition in hepatocellular carcinoma. *Neoplasia* 13, 841-853.

Hoque,M.O., Rosenbaum,E., Westra,W.H., Xing,M., Ladenson,P., Zeiger,M.A., Sidransky,D., and Umbricht,C.B. (2005). Quantitative assessment of promoter methylation profiles in thyroid neoplasms. *J Clin Endocrinol. Metab.* 90, 4011-4018.

Hou,P., Ji,M., and Xing,M. (2008). Association of PTEN gene methylation with genetic alterations in the phosphatidylinositol 3-kinase/AKT signaling pathway in thyroid tumors. *Cancer.* 113, 2440-2447.

Hou,P., Liu,D., Shan,Y., Hu,S., Studeman,K., Condouris,S., Wang,Y., Trink,A., El-Naggar,A.K., Tallini,G., Vasko,V., and Xing,M. (2007a). Genetic alterations and their relationship in the phosphatidylinositol 3-kinase/Akt pathway. *Clinical Cancer Research* 13, 1161-1170.

Hou,P., Liu,D., and Xing,M. (2007b). Functional characterization of the T1799-1801del and A1799-1816ins BRAF mutations in papillary thyroid cancer. *Cell Cycle*. 6, 377-379.

Hu,S., Liu,D., Tufano,R.P., Carson,K.A., Rosenbaum,E., Cohen,Y., Holt,E.H., Kiseljak-Vassiliades,K., Rhoden,K.J., Tolaney,S., Condouris,S., Tallini,G., Westra,W.H., Umbricht,C.B., Zeiger,M.A., Califano,J.A., Vasko,V., and Xing,M. (2006). Association of aberrant methylation of tumor suppressor genes with tumor aggressiveness and BRAF mutation in papillary thyroid cancer. *Int J Cancer*. 119, 2322-2329.

Huang,Y., Prasad,M., Lemon,W.J., Hampel,H., Wright,F.A., Kornacker,K., LiVolsi,V., Frankel,W., Kloos,R.T., Eng,C., Pellegata,N.S., and de la,C.A. (2001a). Gene expression in papillary thyroid carcinoma reveals highly consistent profiles. *Proc. Natl Acad. Sci U. S. A* 98, 15044-15049.

Huang,Y., Prasad,M., Lemon,W.J., Hampel,H., Wright,F.A., Kornacker,K., LiVolsi,V., Frankel,W., Kloos,R.T., Eng,C., Pellegata,N.S., and de la,C.A. (2001b). Gene expression in papillary thyroid carcinoma reveals highly consistent profiles. *Proc. Natl Acad. Sci U. S. A*. 98(26), 15044-15049.

Hundahl,S.A., Fleming,I.D., Fremgen,A.M., and Menck,H.R. (1998). A National Cancer Data Base report on 53,856 cases of thyroid carcinoma treated in the U.S., 1985-1995 [see comments]. *Cancer*. 83, 2638-2648.

Hunt,J.L., LiVolsi,V.A., Baloch,Z.W., Swalsky,P.A., Bakker,A., Sasatomi,E., Finkelstein,S., and Barnes,E.L. (2003). A novel microdissection and genotyping of follicular-derived thyroid tumors to predict aggressiveness. *Hum. Pathol* 34, 375-380.

Hunt,J.L., Yim,J.H., and Carty,S.E. (2006). Fractional allelic loss of tumor suppressor genes identifies malignancy and predicts clinical outcome in follicular thyroid tumors. *Thyroid* 16, 643-649.

Ito,T., Seyama,T., Iwamoto,K.S., Hayashi,T., Mizuno,T., Tsuyama,N., Dohi,K., Nakamura,N., and Akiyama,M. (1993). In vitro irradiation is able to cause RET oncogene rearrangement. *Cancer Res*. 53, 2940-2943.

Ito,Y., Arai,K., Nozawa,R., Yoshida,H., Hirokawa,M., Fukushima,M., Inoue,H., Tomoda,C., Kihara,M., Higashiyama,T., Takamura,Y., Miya,A., Kobayashi,K., Matsuzuka,F., and Miyauchi,A. (2009). S100A8 and S100A9 expression is a crucial factor for dedifferentiation in thyroid carcinoma. *Anticancer Res* 29, 4157-4161.

Ito,Y., Yoshida,H., Tomoda,C., Uruno,T., Miya,A., Kobayashi,K., Matsuzuka,F., Kakudo,K., Kuma,K., and Miyauchi,A. (2005). Expression of S100A2 and S100A6 in thyroid carcinomas. *Histopathology* 46, 569-575.

Jarzab,B., Wiench,M., Fujarewicz,K., Simek,K., Jarzab,M., Oczko-Wojciechowska,M., Wloch,J., Czarniecka,A., Chmielik,E., Lange,D., Pawlaczek,A., Szpak,S., Gubala,E., and Swierniak,A. (2005). Gene expression profile of papillary thyroid cancer: sources of variability and diagnostic implications. *Cancer Res* 65, 1587-1597.

Jazdzewski,K., Murray,E.L., Franssila,K., Jarzab,B., Schoenberg,D.R., and de la,C.A. (2008). Common SNP in pre-miR-146a decreases mature miR expression and predisposes to papillary thyroid carcinoma. *Proc. Natl Acad. Sci U. S. A*. 105, 7269-7274.

- Jhiang,S.M., Sagartz,J.E., Tong,Q., Parker-Thornburg,J., Capen,C.C., Cho,J.Y., Xing,S., and Ledent,C. (1996b). Targeted expression of the ret/PTC1 oncogene induces papillary thyroid carcinomas. *Endocrinology* 137, 375-378.
- Jhiang,S.M., Sagartz,J.E., Tong,Q., Parker-Thornburg,J., Capen,C.C., Cho,J.Y., Xing,S., and Ledent,C. (1996a). Targeted expression of the ret/PTC1 oncogene induces papillary thyroid carcinomas. *Endocrinology* 137, 375-378.
- Ji,J., Zhao,L., Wang,X., Zhou,C., Ding,F., Su,L., Zhang,C., Mao,X., Wu,M., and Liu,Z. (2004). Differential expression of S100 gene family in human esophageal squamous cell carcinoma. *J Cancer Res Clin Oncol* 130, 480-486.
- Jo,Y.S., Li,S., Song,J.H., Kwon,K.H., Lee,J.C., Rha,S.Y., Lee,H.J., Sul,J.Y., Kweon,G.R., Ro,H.K., Kim,J.M., and Shong,M. (2006). Influence of the BRAF V600E mutation on expression of vascular endothelial growth factor in papillary thyroid cancer. *J Clin Endocrinol. Metab* 91, 3667-3670.
- Kallio,J.P., Hopkins-Donaldson,S., Baker,A.H., and Kahari,V.M. (2011). TIMP-3 promotes apoptosis in nonadherent small cell lung carcinoma cells lacking functional death receptor pathway. *Int J Cancer* 128, 991-996.
- Kanamori,T., Takakura,K., Mandai,M., Kariya,M., Fukuhara,K., Sakaguchi,M., Huh,N.H., Saito,K., Sakurai,T., Fujita,J., and Fujii,S. (2004). Increased expression of calcium-binding protein S100 in human uterine smooth muscle tumours. *Mol Hum. Reprod.* 10, 735-742.
- Kanemitsu,N., Kato,M.V., Miki,T., Komatsu,S., Okazaki,Y., Hayashizaki,Y., and Sakai,T. (2000). Characterization of the promoter of the murine mac25 gene. *Biochem. Biophys. Res Commun.* 279, 251-257.
- Katoh,R., Bray,C.E., Suzuki,K., Komiyama,A., Hemmi,A., Kawaoi,A., Oyama,T., Sugai,T., and Sasou,S. (1995). Growth activity in hyperplastic and neoplastic human thyroid determined by an immunohistochemical staining procedure using monoclonal antibody MIB-1. *Hum. Pathol* 26, 139-146.
- Kebebew,E., Peng,M., Reiff,E., Duh,Q.Y., Clark,O.H., and McMillan,A. (2005a). Diagnostic and prognostic value of angiogenesis-modulating genes in malignant thyroid neoplasms. *Surgery* 138, 1102-1109.
- Kebebew,E., Peng,M., Reiff,E., Duh,Q.Y., Clark,O.H., and McMillan,A. (2005b). ECM1 and TMRSS4 are diagnostic markers of malignant thyroid neoplasms and improve the accuracy of fine needle aspiration biopsy. *Ann. Surg.* 242, 353-361.
- Khoo,M.L., Ezzat,S., Freeman,J.L., and Asa,S.L. (2002). Cyclin D1 protein expression predicts metastatic behavior in thyroid papillary microcarcinomas but is not associated with gene amplification. *J Clin Endocrinol. Metab* 87, 1810-1813.
- Khoshnoodi,J., Pedchenko,V., and Hudson,B.G. (2008). Mammalian collagen IV. *Microsc. Res Tech.* 71, 357-370.
- Kim,T.Y., Kim,W.B., Rhee,Y.S., Song,J.Y., Kim,J.M., Gong,G., Lee,S., Kim,S.Y., Kim,S.C., Hong,S.J., and Shong,Y.K. (2006). The BRAF mutation is useful for prediction of clinical recurrence in low-risk patients with conventional papillary thyroid carcinoma. *Clin Endocrinol. (Oxf)*. 65, 364-368.

- Kitahara,C.M., Platz,E.A., Freeman,L.E., Hsing,A.W., Linet,M.S., Park,Y., Schairer,C., Schatzkin,A., Shikany,J.M., and Berrington de,G.A. (2011). Obesity and thyroid cancer risk among U.S. men and women: a pooled analysis of five prospective studies. *Cancer Epidemiol. Biomarkers Prev.* 20, 464-472.
- Kitamura,Y., Shimizu,K., Ito,K., Tanaka,S., and Emi,M. (2001). Allelotyping of follicular thyroid carcinoma: frequent allelic losses in chromosome arms 7q, 11p, and 22q. *J Clin Endocrinol. Metab* 86, 4268-4272.
- Kjellman,P., Lagercrantz,S., Hoog,A., Wallin,G., Larsson,C., and Zedenius,J. (2001). Gain of 1q and loss of 9q21.3-q32 are associated with a less favorable prognosis in papillary thyroid carcinoma. *Genes Chromosomes Cancer* 32, 43-49.
- Kjellman,P., Wallin,G., Hoog,A., Auer,G., Larsson,C., and Zedenius,J. (2003). MIB-1 index in thyroid tumors: a predictor of the clinical course in papillary thyroid carcinoma. *Thyroid* 13, 371-380.
- Klein,M., Vignaud,J.M., Hennequin,V., Toussaint,B., Bresler,L., Plenat,F., Leclere,J., Duprez,A., and Weryha,G. (2001). Increased expression of the vascular endothelial growth factor is a pejorative prognosis marker in papillary thyroid carcinoma. *J Clin Endocrinol. Metab* 86, 656-658.
- Klugbauer,S., Demidchik,E.P., Lengfelder,E., and Rabes,H.M. (1998). Detection of a novel type of RET rearrangement (PTC5) in thyroid carcinomas after Chernobyl and analysis of the involved RET-fused gene RFG5. *Cancer Research* 58, 198-203.
- Klugbauer,S., Jauch,A., Lengfelder,E., Demidchik,E., and Rabes,H.M. (2000). A novel type of RET rearrangement (PTC8) in childhood papillary thyroid carcinomas and characterization of the involved gene (RFG8). *Cancer Res* 60, 7028-7032.
- Knauf,J.A., Ma,X., Smith,E.P., Zhang,L., Mitsutake,N., Liao,X.H., Refetoff,S., Nikiforov,Y.E., and Fagin,J.A. (2005). Targeted expression of BRAFV600E in thyroid cells of transgenic mice results in papillary thyroid cancers that undergo dedifferentiation. *Cancer Res* 65, 4238-4245.
- Kondo,A., Sakaguchi,M., Makino,E., Namba,M., Okada,S., and Huh,N.H. (2002). Localization of S100C immunoreactivity in various human tissues. *Acta Med. Okayama* 56, 31-34.
- Kondo,T., Ezzat,S., and Asa,S.L. (2006). Pathogenetic mechanisms in thyroid follicular-cell neoplasia. *Nat Rev Cancer*. 6, 292-306.
- Kornfeld,J.W., Meder,S., Wohlberg,M., Friedrich,R.E., Rau,T., Riethdorf,L., Loning,T., Pantel,K., and Riethdorf,S. (2011). Overexpression of TACE and TIMP3 mRNA in head and neck cancer: association with tumour development and progression. *Br. J Cancer* 104, 138-145.
- Kremenevskaja,N., von,W.R., Rao,A.S., Schofl,C., Andersson,T., and Brabant,G. (2005). Wnt-5a has tumor suppressor activity in thyroid carcinoma. *Oncogene*. 24, 2144-2154.
- Kremser,R., Obrist,P., Spizzo,G., Erler,H., Kendler,D., Kemmler,G., Mikuz,G., and Ensinger,C. (2003). Her2/neu overexpression in differentiated thyroid carcinomas predicts metastatic disease. *Virchows Arch* 442, 322-328.

- Kroll,T.G., Sarraf,P., Chen,C.J., Mueller,E., Spiegelman,B.M., and Fletcher,J.A. (2000). PAX8-PPARgamma1 fusion oncogene in human thyroid carcinoma. *Science* 289, 1357-1360.
- La,V.C., Bosetti,C., Lucchini,F., Bertuccio,P., Negri,E., Boyle,P., and Levi,F. (2010). Cancer mortality in Europe, 2000-2004, and an overview of trends since 1975. *Ann. Oncol* 21, 1323-1360.
- Lacroix,L., Lazar,V., Michiels,S., Ripoche,H., Dessen,P., Talbot,M., Caillou,B., Levillain,J.P., Schlumberger,M., and Bidart,J.M. (2005). Follicular thyroid tumors with the PAX8-PPARgamma1 rearrangement display characteristic genetic alterations. *Am. J Pathol.* 167, 223-231.
- Latini,F.R., Hemerly,J.P., Oler,G., Riggins,G.J., and Cerutti,J.M. (2008). Re-expression of ABI3-binding protein suppresses thyroid tumor growth by promoting senescence and inhibiting invasion. *Endocr. Relat Cancer.* 15, 787-799.
- Lazzereschi,D., Sambuco,L., Carnovale,S.C., Ranieri,A., Mincione,G., Nardi,F., and Colletta,G. (1998). Cyclin D1 and Cyclin E expression in malignant thyroid cells and in human thyroid carcinomas. *Int J Cancer* 76, 806-811.
- Lin,J., Lai,M., Huang,Q., Ma,Y., Cui,J., and Ruan,W. (2007). Methylation patterns of IGFBP7 in colon cancer cell lines are associated with levels of gene expression. *J Pathol.* 212, 83-90.
- Lind,P., Langsteger,W., Molnar,M., Gallowitsch,H.J., Mikosch,P., and Gomez,I. (1998). Epidemiology of thyroid diseases in iodine sufficiency. *Thyroid* 8, 1179-1183.
- Lovvorn,H.N., Westrup,J., Opperman,S., Boyle,S., Shi,G., Anderson,J., Perlman,E.J., Perantoni,A.O., Wills,M., and de,C.M. (2007). CITED1 expression in Wilms' tumor and embryonic kidney. *Neoplasia* 9, 589-600.
- Lu,Y., Roy,S., Nuovo,G., Ramaswamy,B., Miller,T., Shapiro,C., Jacob,S.T., and Majumder,S. (2011). Anti-microRNA-222 (anti-miR-222) and -181B suppress growth of tamoxifen-resistant xenografts in mouse by targeting TIMP3 protein and modulating mitogenic signal. *J Biol Chem* 286, 42292-42302.
- Lui,W.O., Foukakis,T., Liden,J., Thoppe,S.R., Dwight,T., Hoog,A., Zedenius,J., Wallin,G., Reimers,M., and Larsson,C. (2005). Expression profiling reveals a distinct transcription signature in follicular thyroid carcinomas with a PAX8-PPAR(gamma) fusion oncogene. *Oncogene* 24, 1467-1476.
- Lui,W.O., Zeng,L., Rehrmann,V., Deshpande,S., Tretiakova,M., Kaplan,E.L., Leibiger,I., Leibiger,B., Enberg,U., Hoog,A., Larsson,C., and Kroll,T.G. (2008). CREB3L2-PPARgamma fusion mutation identifies a thyroid signaling pathway regulated by intramembrane proteolysis. *Cancer Res.* 68, 7156-7164.
- Mahller,Y.Y., Vaikunth,S.S., Ripberger,M.C., Baird,W.H., Saeki,Y., Cancelas,J.A., Crombleholme,T.M., and Cripe,T.P. (2008). Tissue inhibitor of metalloproteinase-3 via oncolytic herpesvirus inhibits tumor growth and vascular progenitors. *Cancer Res.* 68, 1170-1179.
- Makino,E., Sakaguchi,M., Iwatsuki,K., and Huh,N.H. (2004). Introduction of an N-terminal peptide of S100C/A11 into human cells induces apoptotic cell death. *J Mol Med. (Berl)* 82, 612-620.

- Margineanu,E., Cotrutz,C.E., and Cotrutz,C. (2008). Correlation between E-cadherin abnormal expressions in different types of cancer and the process of metastasis. *Rev. Med. Chir Soc Med. Nat. Iasi. 112(2)*, 432-436.
- Masson,D., Rioux-Leclercq,N., Fergelot,P., Jouan,F., Mottier,S., Theoleyre,S., Bach-Ngohou,K., Patard,J.J., and Denis,M.G. (2010). Loss of expression of TIMP3 in clear cell renal cell carcinoma. *Eur J Cancer 46*, 1430-1437.
- Maximo,V., Botelho,T., Capela,J., Soares,P., Lima,J., Taveira,A., Amaro,T., Barbosa,A.P., Preto,A., Harach,H.R., Williams,D., and Sobrinho-Simoes,M. (2005). Somatic and germline mutation in GRIM-19, a dual function gene involved in mitochondrial metabolism and cell death, is linked to mitochondrion-rich (Hurthle cell) tumours of the thyroid. *Br. J Cancer. 92*, 1892-1898.
- Mazzanti,C., Zeiger,M.A., Costouros,N.G., Umbricht,C., Westra,W.H., Smith,D., Somervell,H., Bevilacqua,G., Alexander,H.R., and Libutti,S.K. (2004). Using gene expression profiling to differentiate benign versus malignant thyroid tumors. *Cancer Res 64*, 2898-2903.
- Melillo,R.M., Castellone,M.D., Guarino,V., De,F., V, Cirafici,A.M., Salvatore,G., Caiazzo,F., Basolo,F., Giannini,R., Kruhoffer,M., Orntoft,T., Fusco,A., and Santoro,M. (2005). The RET/PTC-RAS-BRAF linear signaling cascade mediates the motile and mitogenic phenotype of thyroid cancer cells. *J Clin Invest 115*, 1068-1081.
- Melillo,R.M., Guarino,V., Avilla,E., Galdiero,M.R., Liotti,F., Prevete,N., Rossi,F.W., Basolo,F., Ugolini,C., de,P.A., Santoro,M., and Marone,G. (2010). Mast cells have a protumorigenic role in human thyroid cancer. *Oncogene 29*, 6203-6215.
- Memon,A.A., Sorensen,B.S., Meldgaard,P., Fokdal,L., Thykjaer,T., and Nexø,E. (2005). Down-regulation of S100C is associated with bladder cancer progression and poor survival. *Clin Cancer Res 11*, 606-611.
- Mettler,F.A., Jr., Bhargavan,M., Faulkner,K., Gilley,D.B., Gray,J.E., Ibbott,G.S., Lipoti,J.A., Mahesh,M., McCrohan,J.L., Stabin,M.G., Thomadsen,B.R., and Yoshizumi,T.T. (2009). Radiologic and nuclear medicine studies in the United States and worldwide: frequency, radiation dose, and comparison with other radiation sources--1950-2007. *Radiology 253*, 520-531.
- Mineo,R., Costantino,A., Frasca,F., Sciacca,L., Russo,S., Vigneri,R., and Belfiore,A. (2004). Activation of the hepatocyte growth factor (HGF)-Met system in papillary thyroid cancer: biological effects of HGF in thyroid cancer cells depend on Met expression levels. *Endocrinology 145*, 4355-4365.
- Mitomo,S., Maesawa,C., Ogasawara,S., Iwaya,T., Shibasaki,M., Yashima-Abo,A., Kotani,K., Oikawa,H., Sakurai,E., Izutsu,N., Kato,K., Komatsu,H., Ikeda,K., Wakabayashi,G., and Masuda,T. (2008). Downregulation of miR-138 is associated with overexpression of human telomerase reverse transcriptase protein in human anaplastic thyroid carcinoma cell lines. *Cancer Sci 99*, 280-286.
- Mohammed,F.F., Smookler,D.S., Taylor,S.E., Fingleton,B., Kassiri,Z., Sanchez,O.H., English,J.L., Matrisian,L.M., Au,B., Yeh,W.C., and Khokha,R. (2004). Abnormal TNF activity in Timp3-/- mice leads to chronic hepatic inflammation and failure of liver regeneration. *Nat. Genet. 36*, 969-977.



- Montero-Conde,C., Martin-Campos,J.M., Lerma,E., Gimenez,G., Martinez-Guitarte,J.L., Combalia,N., Montaner,D., Matias-Guiu,X., Dopazo,J., de,L.A., Robledo,M., and Mauricio,D. (2008). Molecular profiling related to poor prognosis in thyroid carcinoma. Combining gene expression data and biological information. *Oncogene* 27, 1554-1561.
- Moore,B.W. (1965). A soluble protein characteristic of the nervous system. *Biochem. Biophys. Res Commun.* 19, 739-744.
- Moretti,F., Farsetti,A., Soddu,S., Misiti,S., Crescenzi,M., Filetti,S., Andreoli,M., Sacchi,A., and Pontecorvi,A. (1997). p53 re-expression inhibits proliferation and restores differentiation of human thyroid anaplastic carcinoma cells. *Oncogene* 14, 729-740.
- Mori,M., Shimada,H., Gunji,Y., Matsubara,H., Hayashi,H., Nimura,Y., Kato,M., Takiguchi,M., Ochiai,T., and Seki,N. (2004). S100A11 gene identified by in-house cDNA microarray as an accurate predictor of lymph node metastases of gastric cancer. *Oncol Rep.* 11, 1287-1293.
- Motoi,N., Sakamoto,A., Yamochi,T., Horiuchi,H., Motoi,T., and Machinami,R. (2000). Role of ras mutation in the progression of thyroid carcinoma of follicular epithelial origin. *Pathol Res Pract.* 196, 1-7.
- Murzik,U., Hemmerich,P., Weidtkamp-Peters,S., Ulbricht,T., Bussen,W., Hentschel,J., von,E.F., and Melle,C. (2008). Rad54B targeting to DNA double-strand break repair sites requires complex formation with S100A11. *Mol Biol Cell* 19, 2926-2935.
- Nagao,Y., Hisaoka,M., Matsuyama,A., Kanemitsu,S., Hamada,T., Fukuyama,T., Nakano,R., Uchiyama,A., Kawamoto,M., Yamaguchi,K., and Hashimoto,H. (2012). Association of microRNA-21 expression with its targets, PDCD4 and TIMP3, in pancreatic ductal adenocarcinoma. *Mod. Pathol* 25, 112-121.
- Nakamura,M., Ishida,E., Shimada,K., Kishi,M., Nakase,H., Sakaki,T., and Konishi,N. (2005). Frequent LOH on 22q12.3 and TIMP-3 inactivation occur in the progression to secondary glioblastomas. *Lab Invest* 85, 165-175.
- Namba,H., Rubin,S., and Fagin,J.A. (1990). Point mutations of ras oncogenes are an early event in thyroid tumorigenesis. *Molec. Endocrinol.* 4, 1474-1479.
- Nappi,T.C., Salerno,P., Zitzelsberger,H., Carlomagno,F., Salvatore,G., and Santoro,M. (2009). Identification of Polo-like kinase 1 as a potential therapeutic target in anaplastic thyroid carcinoma. *Cancer Res* 69, 1916-1923.
- Nardone,H.C., Ziober,A.F., LiVolsi,V.A., Mandel,S.J., Baloch,Z.W., Weber,R.S., Mick,R., and Ziober,B.L. (2003). c-Met expression in tall cell variant papillary carcinoma of the thyroid. *Cancer* 98, 1386-1393.
- Nikiforov,Y.E. (2006). Radiation-induced thyroid cancer: what we have learned from chernobyl. *Endocr. Pathol.* 17, 307-317.
- Nikiforov,Y.E. and Nikiforova,M.N. (2011). Molecular genetics and diagnosis of thyroid cancer. *Nat. Rev. Endocrinol.* 7, 569-580.
- Nikiforova,M.N., Kimura,E.T., Gandhi,M., Biddinger,P.W., Knauf,J.A., Basolo,F., Zhu,Z., Giannini,R., Salvatore,G., Fusco,A., Santoro,M., Fagin,J.A., and Nikiforov,Y.E. (2003a). BRAF mutations in thyroid tumors are restricted to papillary carcinomas and anaplastic or

poorly differentiated carcinomas arising from papillary carcinomas. *J Clin Endocrinol Metab* 88, 5399-5404.

Nikiforova,M.N., Lynch,R.A., Biddinger,P.W., Alexander,E.K., Dorn,G.W., Tallini,G., Kroll,T.G., and Nikiforov,Y.E. (2003b). RAS point mutations and PAX8-PPAR gamma rearrangement in thyroid tumors: evidence for distinct molecular pathways in thyroid follicular carcinoma. *J Clin Endocrinol. Metab.* 88, 2318-2326.

Nikiforova,M.N. and Nikiforov,Y.E. (2008). Molecular genetics of thyroid cancer: implications for diagnosis, treatment and prognosis. *Expert Rev. Mol. Diagn.* 8, 83-95.

Nikiforova,M.N., Stringer,J.R., Blough,R., Medvedovic,M., Fagin,J.A., and Nikiforov,Y.E. (2000). Proximity of chromosomal loci that participate in radiation-induced rearrangements in human cells. *Science* 290, 138-141.

Nikiforova,M.N., Tseng,G.C., Steward,D., Diorio,D., and Nikiforov,Y.E. (2008). MicroRNA expression profiling of thyroid tumors: biological significance and diagnostic utility. *J Clin Endocrinol. Metab.* 93, 1600-1608.

Nikolova,D.N., Zembutsu,H., Sechanov,T., Vidinov,K., Kee,L.S., Ivanova,R., Becheva,E., Kocova,M., Toncheva,D., and Nakamura,Y. (2008). Genome-wide gene expression profiles of thyroid carcinoma: Identification of molecular targets for treatment of thyroid carcinoma. *Oncol Rep.* 20, 105-121.

Ohuchida,K., Mizumoto,K., Ohhashi,S., Yamaguchi,H., Konomi,H., Nagai,E., Yamaguchi,K., Tsuneyoshi,M., and Tanaka,M. (2006). S100A11, a putative tumor suppressor gene, is overexpressed in pancreatic carcinogenesis. *Clin Cancer Res* 12, 5417-5422.

Oler,G., Camacho,C.P., Hojaij,F.C., Michaluart,P., Jr., Riggins,G.J., and Cerutti,J.M. (2008). Gene expression profiling of papillary thyroid carcinoma identifies transcripts correlated with BRAF mutational status and lymph node metastasis. *Clin Cancer Res* 14, 4735-4742.

Onda,M., Nagai,H., Yoshida,A., Miyamoto,S., Asaka,S., Akaishi,J., Takatsu,K., Nagahama,M., Ito,K., Shimizu,K., and Emi,M. (2004). Up-regulation of transcriptional factor E2F1 in papillary and anaplastic thyroid cancers. *J Hum. Genet.* 49, 312-318.

Paes,J.E. and Ringel,M.D. (2008). Dysregulation of the phosphatidylinositol 3-kinase pathway in thyroid neoplasia. *Endocrinol. Metab Clin North Am.* 37, 375-3ix.

Pallante,P., Federico,A., Berlingieri,M.T., Bianco,M., Ferraro,A., Forzati,F., Iaccarino,A., Russo,M., Pierantoni,G.M., Leone,V., Sacchetti,S., Troncone,G., Santoro,M., and Fusco,A. (2008). Loss of the CBX7 gene expression correlates with a highly malignant phenotype in thyroid cancer. *Cancer Res.* 68, 6770-6778.

Pallante,P., Visone,R., Croce,C.M., and Fusco,A. (2010). Deregulation of microRNA expression in follicular cell-derived human thyroid carcinomas. *Endocr. Relat Cancer.* 17, F91-104.

Pallante,P., Visone,R., Ferracin,M., Ferraro,A., Berlingieri,M.T., Troncone,G., Chiappetta,G., Liu,C.G., Santoro,M., Negrini,M., Croce,C.M., and Fusco,A. (2006). MicroRNA deregulation in human thyroid papillary carcinomas. *Endocr. Relat Cancer.* 13, 497-508.

Parkin,D.M., Bray,F., Ferlay,J., and Pisani,P. (2005). Global cancer statistics, 2002. *CA Cancer J Clin* 55, 74-108.

Patel,K.N., Maghami,E., Wreesmann,V.B., Shaha,A.R., Shah,J.P., Ghossein,R., and Singh,B. (2005). MUC1 plays a role in tumor maintenance in aggressive thyroid carcinomas. *Surgery* 138, 994-1001.

Pellegriti,G., De,V.F., Scollo,C., Attard,M., Giordano,C., Arena,S., Dardanoni,G., Frasca,F., Malandrino,P., Vermiglio,F., Previtera,D.M., D'Azzo,G., Trimarchi,F., and Vigneri,R. (2009). Papillary thyroid cancer incidence in the volcanic area of Sicily. *J Natl Cancer Inst* 101, 1575-1583.

Pickett,C.A., Agoff,S.N., Widman,T.J., and Bronner,M.P. (2005). Altered expression of cyclins and cell cycle inhibitors in papillary thyroid cancer: prognostic implications. *Thyroid* 15, 461-473.

Pierotti,M.A. and Greco,A. (2006). Oncogenic rearrangements of the NTRK1/NGF receptor. *Cancer Lett.* 232, 90-98.

Pilli,T., Prasad,K.V., Jayarama,S., Pacini,F., and Prabhakar,B.S. (2009). Potential utility and limitations of thyroid cancer cell lines as models for studying thyroid cancer. *Thyroid* 19, 1333-1342.

Pilotti,S., Collini,P., Mariani,L., placucci,m., Bongarzone,I., Vigneri,P., cipriani,s., falcetta,f., Miceli,R., Pierotti,M.A., and Rilke,F. (1997). Insular carcinoma. A distinct de novo entity among follicular carcinomas of the thyroid gland. *Am. J. Surg. Pathol.* 21, 1466-1473.

Placzkowski,K.A., Reddi,H.V., Grebe,S.K., Eberhardt,N.L., and McIver,B. (2008). The Role of the PAX8/PPARgamma Fusion Oncogene in Thyroid Cancer. *PPAR. Res.* 2008:672829. *Epub,%2008 Oct 29,* 672829.

Port,M., Boltze,C., Wang,Y., Roper,B., Meineke,V., and Abend,M. (2007). A radiation-induced gene signature distinguishes post-Chernobyl from sporadic papillary thyroid cancers. *Radiat. Res.* 168, 639-649.

Prasad,M.L., Pellegata,N.S., Huang,Y., Nagaraja,H.N., de la,C.A., and Kloos,R.T. (2005). Galectin-3, fibronectin-1, CITED-1, HBME1 and cytokeratin-19 immunohistochemistry is useful for the differential diagnosis of thyroid tumors. *Mod. Pathol.* 18, 48-57.

Prasad,M.L., Pellegata,N.S., Kloos,R.T., Barbacioru,C., Huang,Y., and de la,C.A. (2004). CITED1 protein expression suggests Papillary Thyroid Carcinoma in high throughput tissue microarray-based study. *Thyroid.* 14, 169-175.

Puxeddu,E., Zhao,G., Stringer,J.R., Medvedovic,M., Moretti,S., and Fagin,J.A. (2005). Characterization of novel non-clonal intrachromosomal rearrangements between the H4 and PTEN genes (H4/PTEN) in human thyroid cell lines and papillary thyroid cancer specimens. *Mutat. Res* 570, 17-32.

Qi,J.H., Ebrahim,Q., Moore,N., Murphy,G., Claesson-Welsh,L., Bond,M., Baker,A., and Anand-Apte,B. (2003). A novel function for tissue inhibitor of metalloproteinases-3 (TIMP3): inhibition of angiogenesis by blockage of VEGF binding to VEGF receptor-2. *Nat Med.* 9, 407-415.

- Rabes,H.M., Demidchik,E.P., Sidorow,J.D., Lengfelder,E., Beimfohr,C., Hoelzel,D., and Klugbauer,S. (2000). Pattern of radiation-induced RET and NTRK1 rearrangements in 191 post-Chernobyl papillary thyroid carcinomas: biological, phenotypic, and clinical implications. *Clin. Cancer Res.* 6, 1093-1103.
- Rehman,I., Azzouzi,A.R., Cross,S.S., Deloulme,J.C., Catto,J.W., Wylde,N., Larre,S., Champigneulle,J., and Hamdy,F.C. (2004). Dysregulated expression of S100A11 (calgizzarin) in prostate cancer and precursor lesions. *Hum Pathol.* 35, 1385-1391.
- Richards,R.I. (2001). Fragile and unstable chromosomes in cancer: causes and consequences. *Trends Genet.* 17, 339-345.
- Riesco-Eizaguirre,G., Gutierrez-Martinez,P., Garcia-Cabezas,M.A., Nistal,M., and Santisteban,P. (2006). The oncogene BRAF V600E is associated with a high risk of recurrence and less differentiated papillary thyroid carcinoma due to the impairment of Na<sup>+</sup>/I<sup>-</sup> targeting to the membrane. *Endocr. Relat Cancer.* 13, 257-269.
- Ringel,M.D., Hayre,N., Saito,J., Saunier,B., Schuppert,F., Burch,H., Bernet,V., Burman,K.D., Kohn,L.D., and Saji,M. (2001). Overexpression and overactivation of Akt in thyroid carcinoma. *Cancer Res.* 61, 6105-6111.
- Rintala-Dempsey,A.C., Santamaria-Kisiel,L., Liao,Y., Lajoie,G., and Shaw,G.S. (2006). Insights into S100 target specificity examined by a new interaction between S100A11 and annexin A2. *Biochemistry* 45, 14695-14705.
- Roccatto,E., Bressan,P., Sabatella,G., Rumio,C., Vizzotto,L., Pierotti,M.A., and Greco,A. (2005). Proximity of TPR and NTRK1 rearranging loci in human thyrocytes. *Cancer Res* 65, 2572-2576.
- Roccatto,E., Pagliardini,S., Cleris,L., Canevari,S., Formelli,F., Pierotti,M.A., and Greco,A. (2003). Role of TFG sequences outside the coiled-coil domain in TRK-T3 oncogenic activation. *Oncogene* 22, 807-818.
- Rocha,A.S., Soares,P., Fonseca,E., Cameselle-Teijeiro,J., Oliveira,M.C., and Sobrinho-Simoes,M. (2003). E-cadherin loss rather than beta-catenin alterations is a common feature of poorly differentiated thyroid carcinomas. *Histopathology* 42, 580-587.
- Rodrigues,R., Roque,L., Espadinha,C., Pinto,A., Domingues,R., Dinis,J., Catarino,A., Pereira,T., and Leite,V. (2007a). Comparative genomic hybridization, BRAF, RAS, RET, and oligo-array analysis in aneuploid papillary thyroid carcinomas. *Oncol Rep.* 18, 917-926.
- Rodrigues,R.F., Roque,L., Krug,T., and Leite,V. (2007b). Poorly differentiated and anaplastic thyroid carcinomas: chromosomal and oligo-array profile of five new cell lines. *Br. J Cancer* 96, 1237-1245.
- Roland,C.L., Dineen,S.P., Lynn,K.D., Sullivan,L.A., Dellinger,M.T., Sadegh,L., Sullivan,J.P., Shames,D.S., and Brekken,R.A. (2009). Inhibition of vascular endothelial growth factor reduces angiogenesis and modulates immune cell infiltration of orthotopic breast cancer xenografts. *Mol Cancer Ther.* 8, 1761-1771.
- Rosso,O., Piazza,T., Bongarzone,I., Rossello,A., Mezzanzanica,D., Canevari,S., Orengo,A.M., Puppo,A., Ferrini,S., and Fabbi,M. (2007). The ALCAM shedding by the metalloprotease ADAM17/TACE is involved in motility of ovarian carcinoma cells. *Mol. Cancer Res.* 5, 1246-1253.

- Ruan,D.T., Warren,R.S., Moalem,J., Chung,K.W., Griffin,A.C., Shen,W., Duh,Q.Y., Nakakura,E., Donner,D.B., Khanafshar,E., Weng,J., Clark,O.H., and Kebebew,E. (2008). Mitogen-inducible gene-6 expression correlates with survival and is an independent predictor of recurrence in BRAF(V600E) positive papillary thyroid cancers. *Surgery* 144, 908-913.
- Ruan,W.J., Lin,J., Xu,E.P., Xu,F.Y., Ma,Y., Deng,H., Huang,Q., Lv,B.J., Hu,H., Cui,J., Di,M.J., Dong,J.K., and Lai,M.D. (2006). IGFBP7 plays a potential tumor suppressor role against colorectal carcinogenesis with its expression associated with DNA hypomethylation of exon 1. *J Zhejiang. Univ Sci B.* 7, 929-932.
- Ruco,L.P., Stoppacciaro,A., Ballarini,F., Prat,M., and Scarpino,S. (2001). Met protein and hepatocyte growth factor (HGF) in papillary carcinoma of the thyroid: evidence for a pathogenetic role in tumorigenesis. *J Pathol* 194, 4-8.
- Russell,J.P., Powell,D.J., Cunnane,M., Greco,A., Portella,G., Santoro,M., Fusco,A., and Rothstein,J. (2000). The *TRK-T1* fusion protein induces neoplastic transformation of thyroid epithelium. *Oncogene* 19, 5729-5735.
- Russell,J.P., Shinohara,S., Melillo,R.M., Castellone,M.D., Santoro,M., and Rothstein,J.L. (2003). Tyrosine kinase oncoprotein, RET/PTC3, induces the secretion of myeloid growth and chemotactic factors. *Oncogene* 22, 4569-4577.
- Rust,R., Visser,L., van der,L.J., Harms,G., Blokzijl,T., Deloulme,J.C., van,d., V, Kamps,W., Kok,K., Lim,M., Poppema,S., and van den,B.A. (2005). High expression of calcium-binding proteins, S100A10, S100A11 and CALM2 in anaplastic large cell lymphoma. *Br J Haematol.* 131, 596-608.
- Ryder,M., Ghossein,R.A., Ricarte-Filho,J.C., Knauf,J.A., and Fagin,J.A. (2008). Increased density of tumor-associated macrophages is associated with decreased survival in advanced thyroid cancer. *Endocr. Relat Cancer.* 15, 1069-1074.
- Saavedra,H.I., Knauf,J.A., Shirokawa,J.M., Wang,J., Ouyang,B., Elisei,R., Stambrook,P.J., and Fagin,J.A. (2000). The RAS oncogene induces genomic instability in thyroid PCCL3 cells via the MAPK pathway. *Oncogene.* 19, 3948-3954.
- Sakaguchi,M. and Huh,N.H. (2011). S100A11, a dual growth regulator of epidermal keratinocytes. *Amino. Acids* 41, 797-807.
- Sakaguchi,M., Miyazaki,M., Inoue,Y., Tsuji,T., Kouchi,H., Tanaka,T., Yamada,H., and Namba,M. (2000). Relationship between contact inhibition and intranuclear S100C of normal human fibroblasts. *J Cell Biol* 149, 1193-1206.
- Sakaguchi,M., Miyazaki,M., Sonegawa,H., Kashiwagi,M., Ohba,M., Kuroki,T., Namba,M., and Huh,N.H. (2004). PKCalpha mediates TGFbeta-induced growth inhibition of human keratinocytes via phosphorylation of S100C/A11. *J Cell Biol.* 164, 979-984.
- Sakaguchi,M., Murata,H., Sonegawa,H., Sakaguchi,Y., Futami,J., Kitazoe,M., Yamada,H., and Huh,N.H. (2007). Truncation of annexin A1 is a regulatory lever for linking epidermal growth factor signaling with cytosolic phospholipase A2 in normal and malignant squamous epithelial cells. *J Biol Chem* 282, 35679-35686.
- Sakaguchi,M., Sonegawa,H., Murata,H., Kitazoe,M., Futami,J., Kataoka,K., Yamada,H., and Huh,N.H. (2008). S100A11, an dual mediator for growth regulation of human keratinocytes. *Mol Biol Cell* 19, 78-85.

- Salerno,P., Garcia-Rostan,G., Piccinin,S., Bencivenga,T.C., Di,M.G., Doglioni,C., Basolo,F., Maestro,R., Fusco,A., Santoro,M., and Salvatore,G. (2011). TWIST1 plays a pleiotropic role in determining the anaplastic thyroid cancer phenotype. *J Clin Endocrinol. Metab* 96, E772-E781.
- Salvatore,G., Nappi,T.C., Salerno,P., Jiang,Y., Garbi,C., Ugolini,C., Miccoli,P., Basolo,F., Castellone,M.D., Cirafici,A.M., Melillo,R.M., Fusco,A., Bittner,M.L., and Santoro,M. (2007). A cell proliferation and chromosomal instability signature in anaplastic thyroid carcinoma. *Cancer Res.* 67(21), 10148-10158.
- Sancho,M., Vieira,J.M., Casalou,C., Mesquita,M., Pereira,T., Cavaco,B.M., Dias,S., and Leite,V. (2006). Expression and function of the chemokine receptor CCR7 in thyroid carcinomas. *J Endocrinol.* 191, 229-238.
- Santoro,M., Carlomagno,F., Hay,I.D., Herrmann,M.A., Grieco,M., Melillo,R., Pierotti,M.A., Bongarzone,I., Della Porta,G., Berger,N., Peix,J.L., Paulin,C., Fabien,N., Vecchio,G., Jenkins,R.B., and Fusco,A. (1992). Ret oncogene activation in human thyroid neoplasms is restricted to the papillary cancer subtype. *J. Clin. Invest.* 89, 1517-1522.
- Santoro,M., Dathan,N.A., Berlingieri,M.T., Bongarzone,I., Paulin,C., Grieco,M., Pierotti,M.A., Vecchio,G., and Fusco,A. (1994). Molecular characterization of *RET/PTC3*; a novel rearranged version of the *RET* proto-oncogene in a human thyroid papillary carcinoma. *Oncogene* 9 (2), 509-516.
- Sassa,M., Hayashi,Y., Watanabe,R., Kikumori,T., Imai,T., Kurebayashi,J., Kiuchi,T., and Murata,Y. (2011). Aberrant promoter methylation in overexpression of *CITED1* in papillary thyroid cancer. *Thyroid* 21, 511-517.
- Sato,Y., Chen,Z., and Miyazaki,K. (2007). Strong suppression of tumor growth by insulin-like growth factor-binding protein-related protein 1/tumor-derived cell adhesion factor/mac25. *Cancer Sci.* 98, 1055-1063.
- Schenk,S., Hintermann,E., Bilban,M., Koshikawa,N., Hojilla,C., Khokha,R., and Quaranta,V. (2003). Binding to EGF receptor of a laminin-5 EGF-like fragment liberated during MMP-dependent mammary gland involution. *J Cell Biol* 161, 197-209.
- Schiff,B.A., McMurphy,A.B., Jasser,S.A., Younes,M.N., Doan,D., Yigitbasi,O.G., Kim,S., Zhou,G., Mandal,M., Bekele,B.N., Holsinger,F.C., Sherman,S.I., Yeung,S.C., El-Naggar,A.K., and Myers,J.N. (2004). Epidermal growth factor receptor (EGFR) is overexpressed in anaplastic thyroid cancer, and the EGFR inhibitor gefitinib inhibits the growth of anaplastic thyroid cancer. *Clin Cancer Res* 10, 8594-8602.
- Schweppe,R.E., Kloppe,J.P., Korch,C., Pugazhenti,U., Benezra,M., Knauf,J.A., Fagin,J.A., Marlow,L.A., Copland,J.A., Smallridge,R.C., and Haugen,B.R. (2008). Deoxyribonucleic acid profiling analysis of 40 human thyroid cancer cell lines reveals cross-contamination resulting in cell line redundancy and misidentification. *J Clin. Endocrinol. Metab.* 93, 4331-4341.
- Sedghizadeh,P.P., Williams,J.D., Allen,C.M., and Prasad,M.L. (2005). MSG-1 expression in benign and malignant melanocytic lesions of cutaneous and mucosal epithelium. *Med Sci Monit.* 11, BR189-BR194.
- Seemann,J., Weber,K., and Gerke,V. (1997). Annexin I targets S100C to early endosomes. *FEBS Lett.* 413, 185-190.

- Segev,D.L., Saji,M., Phillips,G.S., Westra,W.H., Takiyama,Y., Piantadosi,S., Smallridge,R.C., Nishiyama,R.H., Udelsman,R., and Zeiger,M.A. (1998). Polymerase chain reaction-based microsatellite polymorphism analysis of follicular and Hurthle cell neoplasms of the thyroid. *J Clin Endocrinol. Metab* 83, 2036-2042.
- Shankar,J., Messenberg,A., Chan,J., Underhill,T.M., Foster,L.J., and Nabi,I.R. (2010). Pseudopodial actin dynamics control epithelial-mesenchymal transition in metastatic cancer cells. *Cancer Res* 70, 3780-3790.
- Sheils,O. (2005). Molecular classification and biomarker discovery in papillary thyroid carcinoma. *Expert Rev. Mol Diagn.* 5(6), 927-946.
- Shi,G., Boyle,S.C., Sparrow,D.B., Dunwoodie,S.L., Shioda,T., and de Caestecker,M.P. (2006). The transcriptional activity of CITED1 is regulated by phosphorylation in a cell cycle-dependent manner. *J Biol Chem.* 281, 27426-27435.
- Smallridge,R.C., Marlow,L.A., and Copland,J.A. (2009). Anaplastic thyroid cancer: molecular pathogenesis and emerging therapies. *Endocr. Relat Cancer.* 16, 17-44.
- Smida,J., Salassidis,K., Hieber,L., Zitzelsberger,H., Kellerer,A.M., Demidchik,E.P., Negele,T., Spelsberg,F., Lengfelder,E., Werner,M., and Bauchinger,M. (1999). Distinct frequency of ret rearrangements in papillary thyroid carcinomas of children and adults from Belarus. *International Journal of Cancer* 80, 32-38.
- Smith,J.A., Fan,C.Y., Zou,C., Bodenner,D., and Kokoska,M.S. (2007). Methylation status of genes in papillary thyroid carcinoma. *Arch Otolaryngol. Head Neck Surg.* 133, 1006-1011.
- Soares,P., Berx,G., van,R.F., and Sobrinho-Simoes,M. (1997). E-cadherin gene alterations are rare events in thyroid tumors. *Int J Cancer* 70, 32-38.
- Sobrinho-Simoes,M., Preto,A., Rocha,A.S., Castro,P., Maximo,V., Fonseca,E., and Soares,P. (2005). Molecular pathology of well-differentiated thyroid carcinomas. *Virchows Arch* 447, 787-793.
- Sobrinho-Simoes,M., Sambade,C., Fonseca,E., and Soares,P. (2002). Poorly differentiated carcinomas of the thyroid gland: a review of the clinicopathologic features of a series of 28 cases of a heterogeneous, clinically aggressive group of thyroid tumors. *Int J Surg. Pathol* 10, 123-131.
- Sonegawa,H., Nukui,T., Li,D.W., Takaishi,M., Sakaguchi,M., and Huh,N.H. (2007). Involvement of deterioration in S100C/A11-mediated pathway in resistance of human squamous cancer cell lines to TGFbeta-induced growth suppression. *J Mol Med. (Berl)* 85, 753-762.
- Sprenger,C.C., Damon,S.E., Hwa,V., Rosenfeld,R.G., and Plymate,S.R. (1999). Insulin-like growth factor binding protein-related protein 1 (IGFBP-rP1) is a potential tumor suppressor protein for prostate cancer. *Cancer Res.* 59, 2370-2375.
- Spurbeck,W.W., Ng,C.Y., Strom,T.S., Vanin,E.F., and Davidoff,A.M. (2002). Enforced expression of tissue inhibitor of matrix metalloproteinase-3 affects functional capillary morphogenesis and inhibits tumor growth in a murine tumor model. *Blood.* 100(9), 3361-3368.

- Stein,L., Rothschild,J., Luce,J., Cowell,J.K., Thomas,G., Bogdanova,T.I., Tronko,M.D., and Hawthorn,L. (2010). Copy number and gene expression alterations in radiation-induced papillary thyroid carcinoma from chernobyl pediatric patients. *Thyroid* 20, 475-487.
- Stolf,B.S., Abreu,C.M., Mahler-Araujo,M.B., Dellamano,M., Martins,W.K., de Carvalho,M.B., Curado,M.P., Diaz,J.P., Fabri,A., Brentani,H., Carvalho,A.F., Soares,F.A., Kowalski,L.P., Hirata,R., Jr., and Reis,L.F. (2005). Expression profile of malignant and non-malignant diseases of the thyroid gland reveals altered expression of a common set of genes in goiter and papillary carcinomas. *Cancer Lett.* 227, 59-73.
- Suarez,H.G., du Villard,J.A., Severino,M., Caillou,B., Schlumberger,M., Tubiana,M., Parmentier,C., and Monier,R. (1990). Presence of mutations in all three *ras* genes in human thyroid tumors. *Oncogene* 5, 565-570.
- Tallini,G., Carcangiu,M.L., and Rosai,J. (1992). Oncocytic neoplasms of the thyroid gland. *Acta Pathol. Jpn.* 42, 305-315.
- Tanaka,M., Adzuma,K., Iwami,M., Yoshimoto,K., Monden,Y., and Itakura,M. (1995). Human calgizzarin; one colorectal cancer-related gene selected by a large scale random cDNA sequencing and northern blot analysis. *Cancer Lett.* 89, 195-200.
- Tian,T., Hao,J., Xu,A., Hao,J., Luo,C., Liu,C., Huang,L., Xiao,X., and He,D. (2007). Determination of metastasis-associated proteins in non-small cell lung cancer by comparative proteomic analysis. *Cancer Sci* 98, 1265-1274.
- Tohyama,K., Yoshida,Y., Ohashi,K., Sano,E., Kobayashi,H., Endo,K., Naruto,M., and Nakamura,T. (1992). Production of multiple growth factors by a newly established human thyroid carcinoma cell line. *Jpn. J Cancer Res* 83, 153-158.
- Torres-Cabala,C., Bibbo,M., Panizo-Santos,A., Barazi,H., Krutzsch,H., Roberts,D.D., and Merino,M.J. (2006). Proteomic identification of new biomarkers and application in thyroid cytology. *Acta Cytol.* 50, 518-528.
- Torres-Cabala,C., Panizo-Santos,A., Krutzsch,H.C., Barazi,H., Namba,M., Sakaguchi,M., Roberts,D.D., and Merino,M.J. (2004). Differential expression of S100C in thyroid lesions. *Int J Surg. Pathol.* 12, 107-115.
- Trovisco,V., Vieira,d.C., I, Soares,P., Maximo,V., Silva,P., Magalhaes,J., Abrosimov,A., Guiu,X.M., and Sobrinho-Simoes,M. (2004). BRAF mutations are associated with some histological types of papillary thyroid carcinoma. *J Pathol.* 202, 247-251.
- Tung,W.S., Shevlin,D.W., Bartsch,D., Norton,J.A., Wells,S.A., Jr., and Goodfellow,P.J. (1996). Infrequent CDKN2 mutation in human differentiated thyroid cancers. *Mol Carcinog.* 15, 5-10.
- U.K.Coordinating Committee on Cancer Research (1988). UKCCCR guide lines for the welfare of animals in experimental neoplasia. *Br. J. Cancer* 58, 109-113.
- Ueki,T., Toyota,M., Sohn,T., Yeo,C.J., Issa,J.P., Hruban,R.H., and Goggins,M. (2000). Hypermethylation of multiple genes in pancreatic adenocarcinoma. *Cancer Res* 60, 1835-1839.



- Van Ginkel,P.R., Gee,R.L., Walker,T.M., Hu,D.N., Heizmann,C.W., and Polans,A.S. (1998). The identification and differential expression of calcium-binding proteins associated with ocular melanoma. *Biochim. Biophys. Acta* 1448, 290-297.
- Vasko,V., Espinosa,A.V., Scouten,W., He,H., Auer,H., Liyanarachchi,S., Larin,A., Savchenko,V., Francis,G.L., de la,C.A., Saji,M., and Ringel,M.D. (2007). Gene expression and functional evidence of epithelial-to-mesenchymal transition in papillary thyroid carcinoma invasion. *Proc. Natl Acad. Sci U. S. A.* 104, 2803-2808.
- Vasko,V., Saji,M., Hardy,E., Kruhlak,M., Larin,A., Savchenko,V., Miyakawa,M., Isozaki,O., Murakami,H., Tsushima,T., Burman,K.D., De,M.C., and Ringel,M.D. (2004). Akt activation and localisation correlate with tumour invasion and oncogene expression in thyroid cancer. *J Med. Genet.* 41, 161-170.
- Viglietto,G., Chiappetta,G., Martinez-Tello,F.J., Fukunaga,F.H., Tallini,G., Rigopoulou,D., Visconti,R., Mastro,A., Santoro,M., and Fusco,A. (1995). RET/PTC oncogene activation is an early event in thyroid carcinogenesis. *Oncogene* 11, 1207-1210.
- Visconti,R., Federico,A., Coppola,V., Pentimalli,F., Berlingieri,M.T., Pallante,P., Kruhoffer,M., Orntoft,T.F., and Fusco,A. (2007). Transcriptional profile of Ki-Ras-induced transformation of thyroid cells. *Cancer Invest* 25, 256-266.
- Visone,R., Pallante,P., Vecchione,A., Cirombella,R., Ferracin,M., Ferraro,A., Volinia,S., Coluzzi,S., Leone,V., Borbone,E., Liu,C.G., Petrocca,F., Troncone,G., Calin,G.A., Scarpa,A., Colato,C., Tallini,G., Santoro,M., Croce,C.M., and Fusco,A. (2007a). Specific microRNAs are downregulated in human thyroid anaplastic carcinomas. *Oncogene*. 26, 7590-7595.
- Visone,R., Russo,L., Pallante,P., De,M., I, Ferraro,A., Leone,V., Borbone,E., Petrocca,F., Alder,H., Croce,C.M., and Fusco,A. (2007b). MicroRNAs (miR)-221 and miR-222, both overexpressed in human thyroid papillary carcinomas, regulate p27Kip1 protein levels and cell cycle. *Endocr. Relat Cancer*. 14, 791-798.
- Vizioli,M.G., Sensi,M., Miranda,C., Cleris,L., Formelli,F., Anania,M.C., Pierotti,M.A., and Greco,A. (2010). IGFBP7: an oncosuppressor gene in thyroid carcinogenesis. *Oncogene*.
- Volante,M., Croce,S., Pecchioni,C., and Papotti,M. (2002). E2F-1 transcription factor is overexpressed in oxyphilic thyroid tumors. *Mod. Pathol* 15, 1038-1043.
- von,W.R., Rhein,A., Werner,M., Scheumann,G.F., Dralle,H., Potter,E., Brabant,G., and Georgii,A. (1997). Immunohistochemical detection of E-cadherin in differentiated thyroid carcinomas correlates with clinical outcome. *Cancer Res* 57, 2501-2507.
- Vriens,M.R., Weng,J., Suh,I., Huynh,N., Guerrero,M.A., Shen,W.T., Duh,Q.Y., Clark,O.H., and Kebebew,E. (2012). MicroRNA expression profiling is a potential diagnostic tool for thyroid cancer. *Cancer* 118, 3426-3432.
- Wagner,P.L., Moo,T.A., Arora,N., Liu,Y.F., Zarnegar,R., Scognamiglio,T., and Fahey,T.J., III (2008). The chemokine receptors CXCR4 and CCR7 are associated with tumor size and pathologic indicators of tumor aggressiveness in papillary thyroid carcinoma. *Ann. Surg. Oncol* 15, 2833-2841.

Wajapeyee,N., Serra,R.W., Zhu,X., Mahalingam,M., and Green,M.R. (2008). Oncogenic BRAF induces senescence and apoptosis through pathways mediated by the secreted protein IGFBP7. *Cell.* 132, 363-374.

Wan,P.T., Garnett,M.J., Roe,S.M., Lee,S., Niculescu-Duvaz,D., Good,V.M., Jones,C.M., Marshall,C.J., Springer,C.J., Barford,D., and Marais,R. (2004). Mechanism of activation of the RAF-ERK signaling pathway by oncogenic mutations of B-RAF. *Cell.* %19;116, 855-867.

Wang,B., Hsu,S.H., Majumder,S., Kutay,H., Huang,W., Jacob,S.T., and Ghoshal,K. (2010). TGFbeta-mediated upregulation of hepatic miR-181b promotes hepatocarcinogenesis by targeting TIMP3. *Oncogene* 29, 1787-1797.

Wang,G., Wang,X., Wang,S., Song,H., Sun,H., Yuan,W., Cao,B., Bai,J., and Fu,S. (2008). Colorectal cancer progression correlates with upregulation of S100A11 expression in tumor tissues. *Int J Colorectal Dis.* 23, 675-682.

Wang,S., Lloyd,R.V., Hutzler,M.J., Safran,M.S., Patwardhan,N.A., and Khan,A. (2000). The role of cell cycle regulatory protein, cyclin D1, in the progression of thyroid cancer. *Mod. Pathol* 13, 882-887.

Wang,Y., Hou,P., Yu,H., Wang,W., Ji,M., Zhao,S., Yan,S., Sun,X., Liu,D., Shi,B., Zhu,G., Condouris,S., and Xing,M. (2007). High prevalence and mutual exclusivity of genetic alterations in the phosphatidylinositol-3-kinase/akt pathway in thyroid tumors. *J Clin Endocrinol. Metab.* 92, 2387-2390.

Ward,L.S., Brenta,G., Medvedovic,M., and Fagin,J.A. (1998). Studies of allelic loss in thyroid tumors reveal major differences in chromosomal instability between papillary and follicular carcinomas. *J Clin Endocrinol. Metab.* 83, 525-530.

Weber,F., Shen,L., Aldred,M.A., Morrison,C.D., Frilling,A., Saji,M., Schuppert,F., Broelsch,C.E., Ringel,M.D., and Eng,C. (2005). Genetic classification of benign and malignant thyroid follicular neoplasia based on a three-gene combination. *J Clin Endocrinol. Metab.* 90, 2512-2521.

Weber,F., Teresi,R.E., Broelsch,C.E., Frilling,A., and Eng,C. (2006). A limited set of human MicroRNA is deregulated in follicular thyroid carcinoma. *J Clin Endocrinol Metab.* 91, 3584-3591.

Wilson,H.M., Birnbaum,R.S., Poot,M., Quinn,L.S., and Swisshelm,K. (2002). Insulin-like growth factor binding protein-related protein 1 inhibits proliferation of MCF-7 breast cancer cells via a senescence-like mechanism. *Cell Growth Differ.* 13, 205-213.

Wiseman,S.M., Griffith,O.L., Deen,S., Rajput,A., Masoudi,H., Gilks,B., Goldstein,L., Gown,A., and Jones,S.J. (2007). Identification of molecular markers altered during transformation of differentiated into anaplastic thyroid carcinoma. *Arch Surg.* 142, 717-727.

Wiseman,S.M., Melck,A., Masoudi,H., Ghaidi,F., Goldstein,L., Gown,A., Jones,S.J., and Griffith,O.L. (2008). Molecular phenotyping of thyroid tumors identifies a marker panel for differentiated thyroid cancer diagnosis. *Ann. Surg. Oncol* 15, 2811-2826.

Wreesmann,V.B., Siczka,E.M., Socci,N.D., Hezel,M., Belbin,T.J., Childs,G., Patel,S.G., Patel,K.N., Tallini,G., Prystowsky,M., Shaha,A.R., Kraus,D., Shah,J.P., Rao,P.H.,

Ghossein,R., and Singh,B. (2004). Genome-wide profiling of papillary thyroid cancer identifies MUC1 as an independent prognostic marker. *Cancer Res* 64, 3780-3789.

Wu,G., Mambo,E., Guo,Z., Hu,S., Huang,X., Gollin,S.M., Trink,B., Ladenson,P.W., Sidransky,D., and Xing,M. (2005). Uncommon mutation, but common amplifications, of the PIK3CA gene in thyroid tumors. *J Clin Endocrinol. Metab.* 90, 4688-4693.

Xing,M. (2007a). BRAF mutation in papillary thyroid cancer: pathogenic role, molecular bases, and clinical implications. *Endocr. Rev.* 28, 742-762.

Xing,M. (2007b). Gene methylation in thyroid tumorigenesis. *Endocrinology* 148, 948-953.

Xing,M. (2007c). Gene methylation in thyroid tumorigenesis. *Endocrinology.* 148, 948-953.

Xing,M., Westra,W.H., Tufano,R.P., Cohen,Y., Rosenbaum,E., Rhoden,K.J., Carson,K.A., Vasko,V., Larin,A., Tallini,G., Tolaney,S., Holt,E.H., Hui,P., Umbricht,C.B., Basaria,S., Ewertz,M., Tufaro,A.P., Califano,J.A., Ringel,M.D., Zeiger,M.A., Sidransky,D., and Ladenson,P.W. (2005). BRAF mutation predicts a poorer clinical prognosis for papillary thyroid cancer. *J Clin Endocrinol. Metab.* 90, 6373-6379.

Yahata,T., de Caestecker,M.P., Lechleider,R.J., Andriole,S., Roberts,A.B., Isselbacher,K.J., and Shioda,T. (2000). The MSG1 non-DNA-binding transactivator binds to the p300/CBP coactivators, enhancing their functional link to the Smad transcription factors. *J Biol Chem.* 275, 8825-8834.

Yahata,T., Shao,W., Endoh,H., Hur,J., Coser,K.R., Sun,H., Ueda,Y., Kato,S., Isselbacher,K.J., Brown,M., and Shioda,T. (2001). Selective coactivation of estrogen-dependent transcription by CITED1 CBP/p300-binding protein. *Genes Dev.* 15, 2598-2612.

Yamanaka,Y., Wilson,E.M., Rosenfeld,R.G., and Oh,Y. (1997). Inhibition of insulin receptor activation by insulin-like growth factor binding proteins. *J Biol Chem.* 272, 30729-30734.

Yane,K., Konishi,N., Kitahori,Y., Naito,H., Okaichi,K., Ohnishi,T., Miyahara,H., Matsunaga,T., and Hiasa,Y. (1996). Lack of p16/CDKN2 alterations in thyroid carcinomas. *Cancer Lett.* 101, 85-92.

Yeh,J.J., Marsh,D.J., Zedenius,J., Dwight,T., Delbridge,L., Robinson,B.G., and Eng,C. (1999). Fine-structure deletion mapping of 10q22-24 identifies regions of loss of heterozygosity and suggests that sporadic follicular thyroid adenomas and follicular thyroid carcinomas develop along distinct neoplastic pathways. *Genes Chromosomes Cancer* 26, 322-328.

Yeow,K.M., Kishnani,N.S., Hutton,M., Hawkes,S.P., Murphy,G., and Edwards,D.R. (2002). Sorsby's fundus dystrophy tissue inhibitor of metalloproteinases-3 (TIMP-3) mutants have unimpaired matrix metalloproteinase inhibitory activities, but affect cell adhesion to the extracellular matrix. *Matrix Biol.* 21, 75-88.

Yip,L., Kelly,L., Shuai,Y., Armstrong,M.J., Nikiforov,Y.E., Carty,S.E., and Nikiforova,M.N. (2011). MicroRNA signature distinguishes the degree of aggressiveness of papillary thyroid carcinoma. *Ann. Surg. Oncol* 18, 2035-2041.

- Yuan,Y., Wang,J., Li,J., Wang,L., Li,M., Yang,Z., Zhang,C., and Dai,J.L. (2006). Frequent epigenetic inactivation of spleen tyrosine kinase gene in human hepatocellular carcinoma. *Clin Cancer Res* 12, 6687-6695.
- Zedenius,J., Wallin,G., Svensson,A., Grimelius,L., Hoog,A., Lundell,G., Backdahl,M., and Larsson,C. (1995). Allelotyping of follicular thyroid tumors. *Hum. Genet.* 96, 27-32.
- Zeki,K., Nakano,Y., Inokuchi,N., Watanabe,K., Morimoto,I., Yamashita,U., and Eto,S. (1993). Autocrine stimulation of interleukin-1 in the growth of human thyroid carcinoma cell line NIM 1. *J Clin Endocrinol. Metab.* 76, 127-133.
- Zhao,X.Q., Naka,M., Muneyuki,M., and Tanaka,T. (2000). Ca(2+)-dependent inhibition of actin-activated myosin ATPase activity by S100C (S100A11), a novel member of the S100 protein family. *Biochem. Biophys. Res Commun.* 267, 77-79.
- Zhu,H., Wu,H., Liu,X., Li,B., Chen,Y., Ren,X., Liu,C.G., and Yang,J.M. (2009). Regulation of autophagy by a beclin 1-targeted microRNA, miR-30a, in cancer cells. *Autophagy.* 5, 816-823.
- Zhu,Z., Gandhi,M., Nikiforova,M.N., Fischer,A.H., and Nikiforov,Y.E. (2003). Molecular profile and clinical-pathologic features of the follicular variant of papillary thyroid carcinoma. An unusually high prevalence of ras mutations. *Am J Clin Pathol* 120, 71-77.
- Zochbauer-Muller,S., Fong,K.M., Virmani,A.K., Geradts,J., Gazdar,A.F., and Minna,J.D. (2001). Aberrant promoter methylation of multiple genes in non-small cell lung cancers. *Cancer Res* 61, 249-255.
- Zou,M., Al Baradie,R.S., Al Hindi,H., Farid,N.R., and Shi,Y. (2005). S100A4 (Mts1) gene overexpression is associated with invasion and metastasis of papillary thyroid carcinoma. *Br J Cancer.* 93, 1277-1284.
- Zou,M., Famulski,K.S., Parhar,R.S., Baitei,E., Al Mohanna,F.A., Farid,N.R., and Shi,Y. (2004). Microarray analysis of metastasis-associated gene expression profiling in a murine model of thyroid carcinoma pulmonary metastasis: identification of S100A4 (Mts1) gene overexpression as a poor prognostic marker for thyroid carcinoma. *J Clin Endocrinol Metab* 89, 6146-6154.

### List of abbreviations

ADC	Adenocarcinoma
AJCC	American Joint Committee on Cancer
ATC	Anaplastic Thyroid Cancer
BRAF	v-Raf murine sarcoma viral oncogene homolog B1
CITED1	Cbp/p300-interacting transactivator 1
CM	Conditioned medium
DSBs	Double-strand breaks
DTC	Differentiated thyroid cancers
ECM	Extracellular matrix
EGF	Epidermal growth factor
EGFR	Epidermal growth factor receptor
EMT	Epithelial to mesenchymal transition
EV	Empty vector
FA	Follicular adenoma
FCS	Fetal calf serum
FMTC	Familial medullary thyroid carcinoma
FNA	Fine-needle aspiration
FNAB	Fine-needle aspiration biopsy
FTC	Follicular thyroid cancer
GDNF	Glial cell line-derived neurotrophic factor
HCC	Hürthle cell carcinoma
HGF	Hepatocyte growth factor
HIF-1	Hypoxia-inducible factor-1
HIMF	hypoxia-induced mitogenic factor
HNSCC	Head and neck squamous cell carcinoma
IGFBP7	Insulin-like growth factor-binding protein 7
LOH	Loss of heterozygosity
MAPK	Mitogen-activated protein kinase
MEN	Multiple endocrine neoplasia
MET	Mesenchymal-epithelial transition
MIG-6	Mitogen-inducible gene 6
MMP	Metalloprotease
MPNST	Malignant peripheral nerve sheath tumours
MSG1	Melanocyte-specific gene 1
MTC	Medullary thyroid cancer
NGF	Nerve growth factor
NHK	Normal human keratinocytes
NIS	Sodium iodide symporter
NSCLC	Non small cell lung cancer
NTRK1	Neurotrophin tyrosine kinase receptor
OS	Overall survival
PAX8	Paired box gene 8
PDTC	Poorly differentiated thyroid carcinoma
PFS	Progression free survival
PI3K	Phosphatidylinositol 3-kinase
PPAR $\gamma$	Peroxisome proliferator-activated receptor gamma
PTC	Papillary thyroid cancer
PTEN	Phosphatase and tensin homolog
PTMC	Papillary thyroid microcarcinoma
RAGE	Receptor for advanced glycation end products

RAI	Radioactive iodine
RET	Rearranged during transfection
RRTC	RAI resistant thyroid carcinomas
SCC	Squamous cell carcinoma
SCLC	Small cell lung cancers
TC	Thyroid cancer
TFG	TRK Fused Gene
TGFA	Transforming growth factor alpha
TGF-beta	Transforming growth factor beta
TIMP3	Tissue inhibitor of metalloproteinase-3
TKI	Tyrosine kinase inhibitor
TNF	Tumor necrosis factor
TPM3	Non-muscle tropomyosin
TPO	Thyroid peroxidase
TPR	Translocated Promoter Region
TSH	Thyroid-stimulating hormone
TTF-1	Thyroid transcription factor-1
VEGF	Vascular endothelial growth factor

### **List of Figures**

Figure 1.1 Scheme of development of follicular cell-derived thyroid cancer

Figure 1.2 Model of multistep carcinogenesis of thyroid neoplasia.

Figure 1.3 Molecular pathways involved in thyroid tumourigenesis and molecular targets for new drugs

Figure 4.1 Mechanisms involved in TIMP3 effects on apoptosis, angiogenesis, cell proliferation and migration.

Figure 4.2 Meta-analysis of *TIMP3* gene expression levels in PTC in five different data sets.

Figure 4.3 TIMP3 mRNA expression by RT-PCR

Figure 4.4 Restoration of TIMP3 expression in NIM1 cell line.

Figure 4.5 Detection of TNF- $\alpha$  protein in the conditioned media of NIM1-EV and NIM1-T clones.

Figure 4.6. Cell proliferation analysis of NIM1 treated with conditioned media.

Figure 4.7 Effect of TIMP3 re-expression on NIM1 cell cycle and apoptosis

Figure 4.8 Effect of TIMP3 expression on NIM1 cell adhesion.

Figure 4.9 Effect of TIMP3 expression on wound healing.

Figure 4.10 Effect of TIMP3 expression on migration, invasion and anchorage-independent growth.

Figure 4.11 Anchorage-independent growth in TIMP3 transfected and control cells.

Figure 4.12 Modulation of adhesion molecules by TIMP3 expression

Figure 4.13 Analysis of cell cultures established from tumours induced in nude mice by NIM1 and NIM1-T clones.

Figure 4.14 Microscopic and immunohistochemical analysis of NIM1-TIMP3 and NIM1 induced tumours

Figure 4.15 *In vitro* and *in vivo* effects of TIMP3 restoration in thyroid tumour cells.

Figure 5.1 Mechanism of S100A11-mediated growth inhibition in NHK cells.

Figure 5.2 Alternative mechanism of S100A11-mediated growth inhibition in NHK cells

Figure 5.3 Mechanism of S100A11-mediated growth promotion in NHK cells.

Figure 5.4 cDNA array expression of S100A11 gene.

Figure 5.5 Metanalysis of S100A11 gene expression levels in PTC in four different data sets.

Figure 5.6 S100A11 mRNA expression by RT-PCR.

Figure 5.7 Analysis of S100A11 localization after Ca<sup>2+</sup> stimulation.

Figure 5.8 Analysis of S100A11 localization after TGF- $\beta$  stimulation.

Figure 5.9 Analysis of interaction between S100A11 and EGF/EGFR pathway

Figure 5.10 Transient silencing of S100A11 in K1 cells.

Figure 5.11 Effect of transient S100A11 silencing on growth rate.

Figure 5.12 Analysis of the effect of S100A11 on growth rate by colony forming assay.

Figure 5.13 Knockdown of S100A11 expression in K1 cells.

Figure 5.14 Analysis of stable S100A11 silencing on growth rate.

Figure 5.15 Anchorage-independent growth of stable S100A11-silenced K1 cells.

Figure 5.16 In vivo tumourigenicity assay.

Figure 5.17 Transforming activity of S100A11 and TRK-T3 proteins.

Figure 5.18 Biochemical analysis of T3/S100 foci.

Figure 5.19 Analysis of cell proliferation of T3/S100 foci.

Figure 5.20 Invasion analysis of 2F and 6F cells

Figure 5.21 Anchorage-independent growth of 2F and 6F foci.

Figure 5.22 Analysis of 2F and 6F cells before injection in nude mice.

Figure 5.23 Tumour xenografts analysis.

Figure 6.1 cDNA array expression of CITED1 gene.

Figure 6.2 CITED1 mRNA expression by RT-PCR.

Figure 6.3 Expression of CITED1-myc protein in HEK293T cells.

**List of Tables**

Table 1.1 Fusion oncogenes in thyroid tumours

Table 1.2 Tyrosin kinase inhibitors in current trials and their targets

Table 2.1 Gene expression profiles in PTC compared with normal thyroid tissues

Table 2.2 Gene expression profiles in PTC compared with FTC

Table 2.3 Gene expression profiles in FTC compared with normal thyroid tissues

Table 2.4 Gene expression profiles in ATC compared with normal thyroid tissues

Table 2.5 Overview of the most relevant gene expression studies of malignant thyroid tumours

Table 3.1 Details of RT-PCR conditions for TIMP3, S100A11, CITED1 and GAPDH genes

Table 3.2 Mutational status and in vivo tumourigenecity of thyroid cell lines

Table 3.3 List of antibodies used for western and dot blot analysis

Table 4.1 In vivo tumour growth of NIM1 cells and NIM1-TIMP3 clonesa

Table 5.1 In vivo tumour growth of K1-sh1, -sh2 and –sh scr cells

Table 5.2 In vivo tumour growth of T3/S100 foci

## ***Publications***

Specifically related to PhD project:

1. **MC Anania**, M. Sensi, MG Vizioli, C Miranda, S Pagliardini, E Favini, L Cleris, R Supino, F Formelli, MG Borrello, M A Pierotti, and A Greco (2011) "*TIMP3 regulates migration, invasion and in vivo tumorigenicity of thyroid tumor cells*" Oncogene Jul 7;30(27):3011-23;
2. MG Vizioli, M Sensi, C Miranda, L Cleris , F Formelli , **MC Anania** , Pierotti MA, A Greco (2010) "*IGFBP7: an oncosuppressor gene in thyroid carcinogenesis*" Oncogene 29(26), 3835-44;

Other than PhD project:

1. C Miranda, M Nucifora, F Molinari, E Conca, **MC Anania** , A Bordoni, P Saletti, L Mazzucchelli, S Pilotti, MA Pierotti, E Tamborini, A Greco , M Frattini (2011) "*KRAS and BRAF mutations predict primary resistance to Imatinib in Gastrointestinal Stromal Tumors (GIST)*" Clin Cancer Res. 2012 Jan 26;
2. MG Vizioli, PA Possik, E Tarantino, K Meissl, MG Borrello, C Miranda, **MC Anania**, S Pagliardini, E Seregni, MA Pierotti, S Pilotti, DS Peeper, A Greco (2011) "*Evidence of oncogene-induced senescence in thyroid carcinogenesis*" Endocr Relat Cancer, Dec 1; 18(6):743-757;
3. C Miranda, T Fumagalli, **MC Anania**, MG Vizioli, S Pagliardini, MA Pierotti, A Greco (2010) "*Role of STAT3 in vitro transformation triggered by TRK oncogenes*" PLoSOne 5(3), e9446.